AD-A044 198 ENVIRO CONTROL INC ROCKVILLE MD F/G 13/2
A CRITICAL TECHNICAL REVIEW OF SIX ADDITIONAL HAZARD ASSESSMENT--ETC(U)
MAR 77 A H RAUSCH, R M. /KUMAR, C J LYNCH DOT-CG-33377-A
UNCLASSIFIED USCG-D-54-77 NL

1 OF 3
AD A044 198

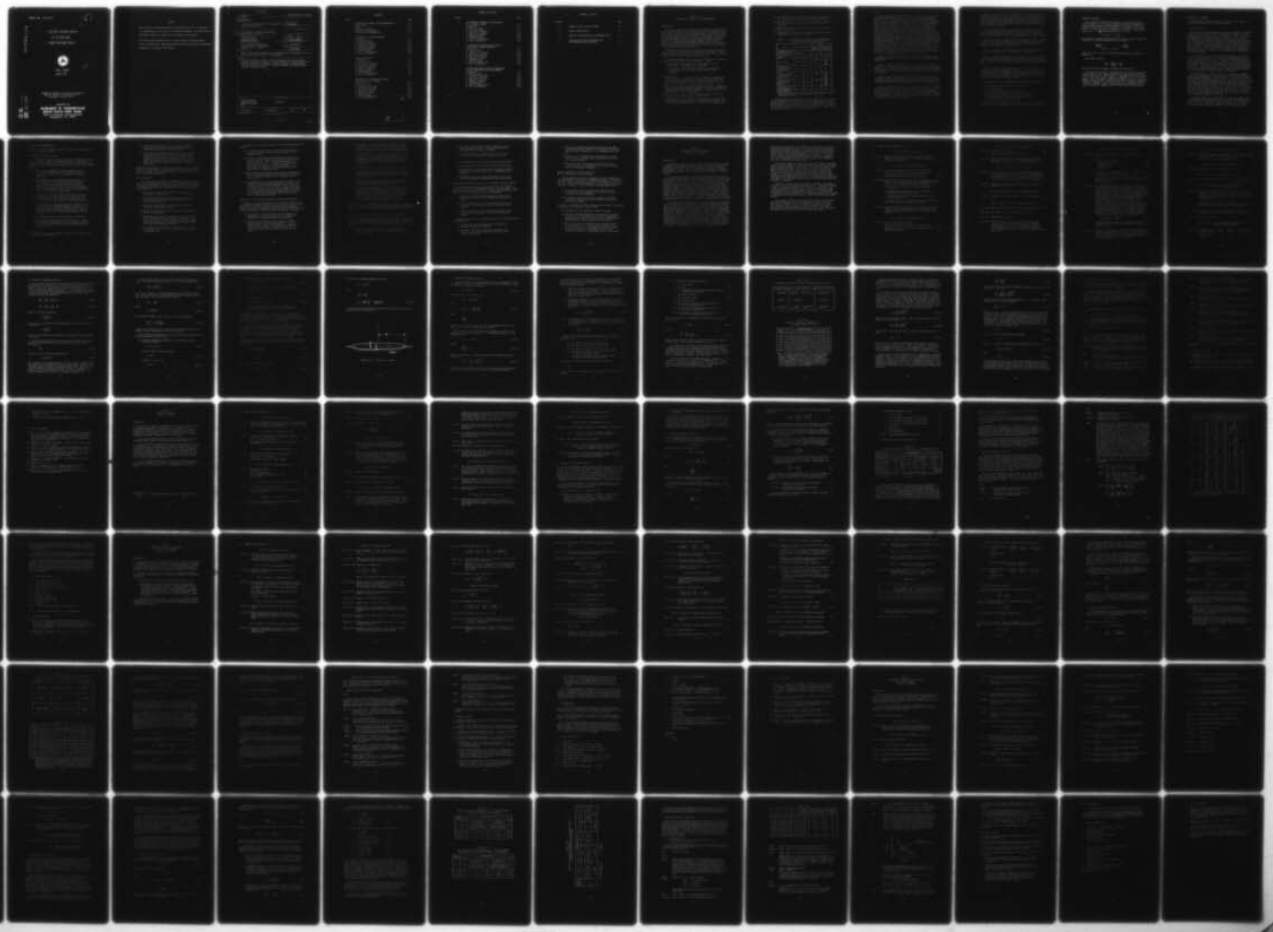

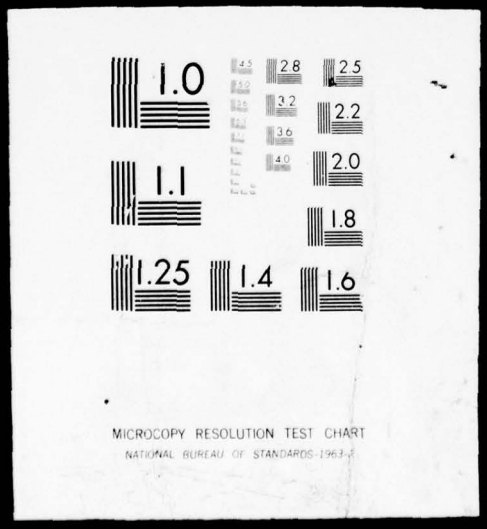

Report No. CG-D-54-77

A CRITICAL TECHNICAL REVIEW OF SIX ADDITIONAL HAZARD ASSESSMENT MODELS

FINAL REPORT

MARCH 1977

Prepared for

DEPARTMENT OF TRANSPORTATION
UNITED STATES COAST GUARD
Office of Research and Development
Washington, D.C. 20590

NOTICE

This document is disseminated under the sponsorship of the U. S. Department of Transportation in the interest of information exchange. The United States Government assumes no liability for the contents or use thereof.

The United States Government does not endorse products or manufacturers. Trade or manufacturers' names appear herein solely because they are considered essential to the object of this report.

Technical Report Documentation Page

1. Report No.	2. Government Accession No.	3. Recipient's Catalog No.
CG-D-54-77		

4. Title and Subtitle

A Critical Technical Review of Six Additional Hazard Assessment Models.

5. Report Date: March 1977

6. Performing Organization Code

8. Performing Organization Report No.

7. Author(s)

A. H. Rausch, R. M. Kumar, G. J. Lynch

9. Performing Organization Name and Address

Enviro Control, Inc.
One Central Plaza
11300 Rockville Pike
Rockville, Maryland

10. Work Unit No. (TRAIS)

3142

11. Contract or Grant No.

DOT-CG-33377-A

13. Type of Report and Period Covered

Final Report.

12. Sponsoring Agency Name and Address

U. S. Coast Guard Headquarters
Office of Research and Development
Washington, D. C. 20590

14. Sponsoring Agency Code

G-DSA-1/TP44

15. Supplementary Notes

The U. S. Coast Guard's Research and Development Technical Representative for the work performed herein was Dr. M. C. Parnarouskis.

16. Abstract

This report presents a critical, technical review of six simulation models currently being used in connection with the following U. S. Coast Guard research programs: the Vulnerability Model, a simulation system for assessing damage resulting from spills of hazardous chemicals; and CHRIS, the Chemical Hazards Response Information System.

17. Key Words	18. Distribution Statement
Hazard Assessment Vulnerability Model Hazardous Chemicals CHRIS	Unlimited

19. Security Classif. (of this report)	20. Security Classif. (of this page)	21. No. of Pages	22. Price
Unclassified	Unclassified	202	

Form DOT F 1700.7 (8-72) Reproduction of completed page authorized

CONTENTS

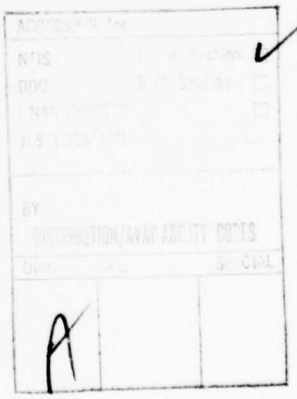

CONTENTS (continued)

CONTENTS (continued)

Chapter 1

INTRODUCTION, SUMMARY, AND RECOMMENDATIONS

INTRODUCTION

This report presents a critical technical review of six simulation models currently being used in connection with the following U.S. Coast Guard research programs: the Vulnerability Model, a simulation system for assessing damage resulting from spills of hazardous materials [1]; the Chemical Hazards Response Information System (CHRIS), as described in *Assessment Models in Support of the Hazard Assessment Handbook* (AMSHAH) [2]; and the Hazard Assessment Computer System (HACS) [3]. These research programs are concerned with describing, in a predictive manner, the behavior of maritime spills of hazardous materials and the damages that may result from such spills.

AMSHAH describes 12 models that are among those used in the above research programs; six of these are addressed in this report. The remaining models have been reviewed in an earlier report [4]. The models addressed in this report are listed in Table 1-1.

The primary objective of this review is to evaluate the validity of the models. This evaluation was carried out as follows.

(1) Assumptions stated explicitly or made implicit in the derivation of each model were documented.

(2) The errors introduced by the departure from underlying assumptions in actual situations were defined, where applicable.

---

[1] Eisenberg, N. A., C. J. Lynch, and R. J. Breeding, *Vulnerability Model: A Simulation System for Assessing Damage Resulting from Marine Spills*, CG-D-136-75, NTIS AD-A015245, prepared for Department of Transportation, U.S. Coast Guard, June 1975.

[2] Raj, P. P. K., and A. S. Kalelkar, *Assessment Models in Support of the Hazard Assessment Handbook* (CG-446-3), CG-D-65-74, prepared by Arthur D. Little, Inc. for Department of Transportation, U.S. Coast Guard, NTIS AD-776617, January 1974.

[3] Arthur D. Little, Inc., *Hazard Assessment Computer System, User Manual* (HACS), Cambridge, Mass., December 1974.

[4] Eisenberg, N. A., C. J. Lynch, et al., *A Critical Technical Review of Six Hazard Assessment Models*, prepared by Enviro Control, Inc. for Department of Transportation, U.S. Coast Guard, December 1975.

(3) The sensitivity of the results of each model to estimates of input variables and input parameters were determined.

(4) The errors introduced by sequential simulation of processes that actually occur simultaneously were defined, where applicable.

(5) Errors in analysis, documentation, and computer coding were defined and rectified.

(6) Inconsistencies between written documentation and computer programming were defined and resolved.

TABLE 1-1. ORGANIZATION OF THIS REPORT AND CORRESPONDING ENTITIES IN AMSHAH [2] AND HACS [3]

Title	This Report	AMSHAH	HACS	
			Executive Subroutine[a]	Computational Subroutine
Introduction, Summary, and Recommendations	Chapter 1	--	--	--
Spreading of A Liquid on Water	Chapter 2	Chapter 3	MODT	RLJSP
Vapor Dispersion	Chapter 3	Chapter 5	MODC1 MODC2	VAPC TOXIC IVAPC ITOX
Spreading of A Low-Viscosity Liquid on A High-Viscosity Liquid	Chapter 4	Chapter 8	MODT	RLJSP
Simultaneous Spreading and Evaporation of A Cryogen on Water	Chapter 5	Chapter 9	MODD	CRYSP COMPQ CRIT GRSPD
Simultaneous Spreading and Cooling of A High Vapor Pressure Chemical	Chapter 6	Chapter 10	MODV	COMPD PKRHI HMTC PKRRK
Boiling Rate Model for Heavy Liquids with Boiling Temperatures Less Than Ambient	Chapter 7	Chapter 12	MODI	EVDRP

[a] These subroutines acquire the necessary data and call the required computational subroutines.

Table 1-1 shows the correspondence between chapters in this report, those in AMSHAH, and the subroutines in HACS. Each chapter in this report treats one of the models described in AMSHAH; however, one model may correspond to several computer programs or subroutines. Because of the self-contained nature of the material covered, each chapter contains its own list of symbols and list of references.

SCOPE

The ultimate purpose of this effort is to provide the information required to plan further research efforts in the area of hazardous material spills. Of primary interest is the determination of areas in which research would yield the greatest benefits in terms of improving model accuracy. Although the models analyzed describe physical occurrences resulting from spills of hazardous materials, the immediate objective is not to improve the description of spill development, but rather to determine which areas of research will yield the greatest improvements in the capability of the models to estimate damages to people, property, and the environment. Improvements to damage assessment techniques may be achieved by further research in two distinct but related areas, namely: parameter estimation and model development. For example, if it is determined that changing a particular parameter by 10% does not substantially affect the hazard assessment, the research effort to establish a precise value of that parameter is unnecessary. Similarly, if it is determined that one model gives estimates good to, say, 10% of experimental or field values, while another model yields estimates which are good only to one order of magnitude, the direction for further research is clear. As stated above, the models that are analyzed are those documented in AMSHAH and used in several USCG efforts including the Vulnerability Model (VM), HACS, and CHRIS.

In order to obtain a quantitative evaluation of the damage assessment model, the scope of work includes the following nine tasks summarized below.

Task 1. Document the assumptions and approximations inherent in each model. For each model, document the assumptions and approximations inherent in it. Identify the parametric estimations made in each model and identify frequently estimated chemical property values that are used by each model.

Task 2. Assess the errors introduced when the assumptions of the model are violated. Quantitatively assess the ability of each model to represent accurately the physical phenomena being modeled under a range of conditions expected to be encountered in actual spill situations.

Task 3. Determine the sensitivity of computed results to estimated model parameters and chemical property estimates. Determine the sensitivity of each model's output to changes in the estimated parametric values identified in Task 1. This includes placing maximum error bounds on model parameters and chemical property data. The possible variance of the computed results should then be determined for a range of parametric inputs within the error bounds.

Task 4. Assess the errors introduced by sequentially simulating physical processes that occur simultaneously. For those models whose inputs are computed by preceding models, determine the limitations on the accuracy of their results based on the possible errors of the inputs. Determine the possible degree of error of those sequentially executed groups of hazard assessment models representing simultaneously occurring physical phenomena.

Task 5. Document coding errors and make necessary corrections. For the computerized version of each submodel, document any coding errors and the suggested correction; upon approval of the USCG, the corrections will be made and the corrected programs used for Tasks 3 and 4.

Task 6. Document inconsistencies between AMSHAH and HACS. Document any discrepancies between AMSHAH and HACS, indicate which version is judged to be preferable, and, upon approval of the USCG, change either AMSHAH or HACS or both to reconcile the two.

Task 7. Document implicit assumptions. Document any assumptions implicit in HACS that are not stated explicitly in AMSHAH.

Task 8. Document and correct errors in analysis. Document any suspected errors in AMSHAH manifested as formulas not following from the stated assumptions. Upon approval of the Project Officer, change AMSHAH, HACS, or both to correspond to the physically and mathematically correct form.

Task 9. Perform a sensitivity analysis only on those models for which such an analysis is deemed worthwhile. In the event that the assumptions stated in AMSHAH appear to be unrealistic, the USCG will determine whether it is worthwhile to perform Tasks 3 and 4 on the model, as is, or whether it is feasible to modify the model to a more correct form with the time and resources available.

The models chosen to be analyzed in depth are (also see Table 1-1):

- Spreading of High-Viscosity Liquid on Water
- Vapor Dispersion
- Spreading of Low-Viscosity Liquid on Water
- Spreading and Evaporation of a Cryogen on Water
- Spreading and Cooling of High Vapor Pressure Liquid
- Boiling Rate Model for Heavy Liquids

The nine tasks listed above were performed on each of these six models, and the results of the analyses are reported in the chapters that follow.

SENSITIVITY ANALYSIS

The sensitivity analysis that we employ on the analytical models reviewed computes the fractional change in a dependent variable for a given fractional change in a given independent variable, holding all remaining independent variables constant. For example, if the concentration, C, of an effluent is expressed as a function of several variables, $x,y,z,\ldots$, and parameters such as a_1, a_2, etc.:

$$C = C(x,y,z,\ldots, a_1,a_2,\ldots)$$

we calculate the logarithmic derivative of C with respect to one of the variables or parameters, holding the rest constant:

$$\left.\frac{\partial \ln C}{\partial \ln a_1}\right|_{x,y,z,\ldots,a_2,a_3,\ldots} = \frac{\delta C/C}{\delta a_1/a_1}$$

where $\delta C/C$ and $\delta a_1/a_1$ are the fractional changes in C and a_1, respectively.

As a result, we have

$$\frac{\delta C}{C} = \frac{\partial \ln C}{\partial \ln a_1} \cdot \frac{\delta a_1}{a_1}$$

and $(\partial \ln C)/(\partial \ln a_1)$ becomes the sensitivity coefficient.

The sensitivity analysis is performed over all variables and parameters appearing in the models reviewed, where applicable, and is displayed in matrix form. More details of the method are given in Chapters 2, 3, 4, and 5 which treat, respectively, Chapters 3, 5, 8, and 9 of AMSHAH. Should the models reviewed be numerical algorithms, a different procedure is called for. This is the case for the models of Chapters 10 and 12 of AMSHAH. Since the procedure used is a numerical one, we refer the reader to Chapters 6 and 7 of this report for more details.

ORGANIZATION OF MATERIAL

The material contained in Chapters 2 through 7 of this report is organized according to the format detailed below.

A. Review of Text

In this review Roman numerals denote chapters of AMSHAH, followed by a comma and then by the same Arabic number used in AMSHAH to delineate sections, with the notation enclosed in parentheses. Thus, Section 3.3 of AMSHAH appears as Section (III,3) in Chapter 2 of this review. A brief summary of the results appears in each of the sections cited in the review outline, along with a check (√) to indicate that the material in the corresponding section of AMSHAH has been reviewed and that the text is correctly stated and appropriate for the context in which it is set down. Thus, a check beside any section means that that section has been reviewed and that, unless otherwise indicated, all numbers and formulas are correct. *In addition, a check means that the assumptions are correctly stated.*

In the case of errors in equations and/or formulas, the error is generally noted by a cross (X). In order to note explicitly the corrections or modifications, the review sections have been divided still further by appending a letter, e.g., (III,3,a). The specific item may be followed by asterisks. Items without asterisks are concerned merely with a report on and summary of the review of some particular aspect of the section. Items with a single asterisk (*) are statements relating to incorrect or unclear assumptions, etc. Items with double asterisks (**) are corrections to errors in numbers and formulas.

As an illustration, consider Section 3.7 of Chapter 3 in AMSHAH (pp. 20-23), "Spreading of a Liquid on Water." This section describes a specific numerical example. Our review (Ch. 2, p. 2-4) refers to sections with four statements marked (III,7,a), (III,7,b)**, (III,7,c), and (III,7,d)*. (III,7,a) is a statement of the fact that all of the data used in AMSHAH describing the calculations of Section 3.7 are correct, except for the viscosity of water. This is followed by a check (√). (III,7,b)** gives the correct viscosity of water. (III,7,c) is a statement of the fact that all of the calculations in Section 3.7 of AMSHAH have been reviewed, numbers and formulas, and found to be correct. (III,7,d)* is a statement concerning some of the data used in relation to the underlying assumptions of the model.

Tables and figures are also reviewed. As explained above, corresponding Roman numerals replace the Arabic numerals used in AMSHAH to denote chapters. In addition, literal designations for tables are preceded by a T, while those for figures are preceded by an F. Thus, T(III,1) refers to a section of Chapter III in the review outline

describing the results of the review of Table 3.1 in AMSHAH. Similarly, F(III,2) refers to the results of a review of Figure 3.2 in AMSHAH. The sections dealing with reviews of tables and figures in the review outline are further subdivided and marked off with single or double asterisks, as are the reviews of the sections.

Note: Tables, figures, and equations in the review outline do not necessarily have any relation to corresponding items in AMSHAH, e.g., Table (III,1) in the review is not related to Table 3.1 in AMSHAH.

Coding Legend Used in Review of Text

Symbol	*Denotation*	*Example*
Roman numeral	Chapter in AMSHAH under review	(III,3), review of Chapter 3, Section 3 in AMSHAH
✓	Section in AMSHAH reviewed and found correct	(III,3) ✓
X	Statement or section in AMSHAH reviewed and found in error	(III,2,a) X
*	Statements relating to *incorrect* and/or unclear assumptions	(III,5,b)*
**	Corrections to errors in number or formula	(III,7,b)**
T	Table in AMSHAH under review	T(III,1) reviews Table 3.1 in AMSHAH
F	Figure in AMSHAH under review	F(III,2) reviews Figure 3.2 in AMSHAH

B. Critique of the Model

Section B of each chapter of this review is a brief theoretical statement related to the specific model with which each chapter is concerned.

C. Sensitivity Analysis

Section C in each chapter of the review outline is concerned with the Sensitivity Study pertaining to the model with which the chapter is concerned. Since the models generally yield analytic formulas, it is possible to obtain sensitivity coefficients explicitly in terms of logarithmic derivatives. In these studies, numerical examples were constructed to determine whether the assumptions of the model are compatible with the numerical relations among the parameters. In the cases where difficulties were encountered, the basic formulas of the model were reformulated and, using results of dimensional analysis, different forms were developed to permit proper scaling of the observed results.

D. HACS Error Analysis

All errors in logic and particular statement errors are outlined in this section.

E. Summary of Results

A brief statement of the major findings of the review of the model is presented.

F. Recommendations

Recommendations for further investigation and study are presented.

G. Table of Symbols Used

H. List of References

RESULTS AND RECOMMENDATIONS

The results and recommendations of the review of each of the six models are summarized below.

Spreading of a Liquid on Water

"Spreading of a Liquid on Water" is Chapter 3 of AMSHAH and Chapter 2 of this report. There are several minor errors in the text of Chapter 3 involving numerical data and formulas. Several questionable assumptions in the analysis and modeling have been noted and are stated below.

(a) The viscosity and surface tension parameters used in Chapter 3 of AMSHAH may not be valid and may have to be determined empirically as suggested by Fannelop and Waldman [5].

(b) The AMSHAH models on spreading are predicated on the notion that a low-viscosity liquid will continue to spread regardless of the character of the inertial momentum term. Since Chapter 3 is not concerned with low-viscosity liquids, we merely note that the dynamical basis for distinguishing high-viscosity liquids from low-viscosity ones is highly questionable.

(c) The liquid pool will not spread indefinitely as assumed in Chapter 3. The model gives us no insight into the ultimate extent of the pool. Also, the description of the late stages of pool growth may be highly unrealistic.

(d) The boundary conditions assumed are questionable, in view of the fact that one assumes asymptotic solutions in the modeling. Also, the Fannelop-Waldman constants used in the AMSHAH model are semiempirical and may not scale up properly, particularly if the boundary conditions are not suitable.

It is recommended that the following actions be considered.

(1) A review of the underlying assumptions involved in viscous spread ought to be undertaken for the purpose of drawing up a rigorous distinction between high-viscosity and low-viscosity flows.

---

[5] Fannelop, T. K., and G. D. Waldman, Dynamics of oil slicks, *AIAA Journal 10*:506-510, 1972.

(2) A more careful analysis of the spread rate involving surface forces is needed, particularly with respect to determining ultimate limits of pool growth.

(3) In the case where parameters entering the model are not well defined, a more careful distinction should be made between data and observed results. Should there be an impasse on this point, one can always reformulate the model and propose an experimental design so that the model will scale up properly in spite of its theoretical limitations.

Remodeling liquid spread to overcome the deficiencies noted is both feasible and inexpensive, as is the experimental design required to verify the theory. Actual experimentation, on the other hand, can be both time consuming and costly.

Vapor Dispersion

"Vapor Dispersion" is Chapter 5 of AMSHAH and Chapter 3 of this report. There are several minor errors in the text involving formulas and numerical calculations. The most serious objections that can be raised against the model for vapor dispersion, as given in Chapter 5, are stated below.

(a) The model is invalid in regions close to spill and at times close to spill event.

(b) The model cannot handle spills whose duration lies in the span between instantaneous and continuous, i.e., a *"real world" incident*.

(c) The "puff" model predicts results that are physically invalid for events near the source.

(d) Equivalency of an area source to a point source displaced upwind is questionable.

(e) Dispersion coefficients, while appearing to be different for continuous sources as opposed to instantaneous, probably do not differ. Proper treatment of the spill process, along with recognition of wind-created turbulence, might well resolve the apparent differences.

(f) As the HACS review indicates, extrapolation of coefficients of dispersion, σ_x, σ_y, σ_z, on a linear basis can lead to considerable error.

On the basis of the above objections, the following recommendations are made.

(1) An attempt should be made to include transient effects in the dispersion model that will calculate effect of time-dependent sources.

(2) A review of turbulence-caused fluctuations should be made in order that their impact on concentration fluctuations can be determined. This is especially important for regions near the source. If successful peak-to-average concentration ratios can be reliably estimated for a given stability condition, this knowledge might change areal extent of flammability zone.

(3) Source behavior for cryogen spills should be reworked to include transient behavior of heat transfer on a spreading pool. No dispersion model will be any better than its source term.

(4) A formal analysis of scale effects should be made, so that considerably large-scale extrapolations can be made with confidence based on dispersion models. We do not know at the present state of the art whether a spill of the order of 10^6 gallons will scale up, as per the model, or whether a significant change of behavior might result because of, say, a fundamental weather effect alteration caused by a spill of that large a magnitude.

Spreading of a Low-Viscosity Liquid On a High-Viscosity Liquid

"Spreading of a Low Viscosity Liquid On a High-Viscosity Liquid" is Chapter 8 of AMSHAH and Chapter 4 of this report. There are many minor errors in the text involving numerical data and formulas. Several questionable assumptions in the analysis and modeling have been noted and are similar to those discovered in Chapter 3 of AMSHAH.

(a) The parameter of surface tension used in Chapter 8 of AMSHAH may not be valid and may have to be determined empirically as suggested by Fannelop and Waldman.

(b) Boundary layer theory as used in Chapter 3 of AMSHAH would have given a better spread law ($t^{1/4}$) in the gravity-viscous regime, and in addition its application would require no artificial dynamical basis for distinguishing high-viscosity liquids from low-viscosity ones.

(c) The liquid pool will not spread indefinitely as assumed in Chapter 8. The model gives us no insight into the ultimate extent of the pool. Also, the description of the late stages of pool growth may be highly unrealistic.

(d) The boundary conditions assumed are questionable in view of the fact that one assumes asymptotic solutions in the modeling. Also, the Fannelop-Waldman constants used in the AMSHAH model are semiempirical and may not scale up properly, particularly if the boundary conditions are not suitable.

It is recommended that the following actions be considered.

(1) A review of the underlying assumptions involved in viscous spread ought to be undertaken for the purpose of drawing up a rigorous distinction between high-viscosity and low-viscosity flows.

(2) A more careful analysis of the spread rate involving surface forces is needed, particularly with regard to determining ultimate limits of pool growth.

(3) In the case where parameters entering the model are not well defined, a more careful distinction should be made betweeen data and observed results. Should there be an impasse on this point, one can always reformulate the model and propose an experimental design as has been done in Section C (Sensitivity Analysis) in Chapter 4 of this report, so that the model will scale up properly in spite of its limitations.

Essentially, the recommendations that apply to Chapter 3 of AMSHAH also apply to Chapter 8, since the only real physical difference between the two models involved is the magnitude of the respective liquid viscosities.

Simultaneous Spreading and Evaporation of a Cryogen on Water

"Simultaneous Spreading and Evaporation of a Cryogen on Water" is Chapter 9 of AMSHAH and Chapter 5 of this report. There are many minor errors in the text involving numerical data and formulas. The most questionable aspects of the modeling of Chapter 9, however, are outlined below.

(a) The model is phenomenological, a method that finally appeals to empiricism for its justification rather than to first principles.

(b) The spread law establishing radial dependence as the one-eighth power of time is erroneous and contrary to properly applied boundary layer theory.

(c) Ice formation, which is claimed to be a factor, will not occur unless the water is bounded on all sides.

It is recommended that the following actions should be taken.

(1) Time dependence of heat transfer should be investigated.

(2) Hydrodynamic field modeling should be attempted, utilizing boundary layer theory rather than the phenomenological approach.

(3) Experiments should be designed and carried out so as to fit the hydrodynamic field models and thus confirm them.

Simultaneous Spreading and Cooling of a High Vapor Pressure Chemical

"Simultaneous Spreading and Cooling of a High Vapor Pressure Chemical" is Chapter 10 in AMSHAH and Chapter 6 of this report. There are several minor errors in the text involving numerical data and formulas. The most serious objections are listed below.

(a) The method of calculating mean heat flux from water to liquid is in error; it grossly underestimates mean heat flux.

(b) It has been found that HACS gives erroneous results for the values of time greater than time for complete evaporation.

(c) There is a lack of internal consistency among the values of the specific evaporation rate obtained by different methods.

Because of these specific findings and others, the following actions are recommended.

(1) The method of calculating mean heat flux should be replaced (Equation 10.5, AMSHAH).

(2) As noted in (a) and (b) above, the appropriate subroutines in HACS should be modified in order to get intelligible results.

(3) Since it is possible to incorporate easily the variation of the mass-transfer coefficient in the course of spreading and simultaneous evaporation, it is recommended that it be done.

(4) Equation (10.2) of AMSHAH should be replaced by equation (X-10) of this report, and this change should be included in the subroutine HMTC.

(5) This model should be expanded to include the situation of the occurrence of ice formation in the course of simultaneous spreading and evaporation.

Boiling Rate Model for Heavy Liquids with Boiling Temperatures Less Than Ambient

"Boiling Rate Model for Heavy Liquids with Boiling Temperatures Less Than Ambient" is Chapter 12 of AMSHAH and Chapter 7 of this report. The text contains several minor errors involving numerical data and formulas. Several incorrect assumptions in the analysis and modeling are noted in Chapter 7. The most salient of these appear below.

(a) If the time to reach the terminal settling velocity is not exceedingly small compared to the life of the drop, the model will not be applicable.

(b) An incorrect value of the surface tension of the system liquid-air is being used for the interfacial tension of the liquid with water.

In addition, the numerical results obtained from this model could easily be off by a factor of three to four or more.

The following work is recommended to improve the model.

(1) Because the results obtained from this model will probably be far from the actual values in view of the simplifying assumptions made, more work ought to be done--experimentally and otherwise--to obtain results that are realistic.

(2) Very little data are available on the interfacial tension of various liquids. If the interfacial tension for the liquid in question is not available, the use of the model is highly questionable. Experimental work to obtain interfacial tensions of the concerned liquids is necessary.

Chapter 2

"SPREADING OF A LIQUID ON WATER"
(Chapter 3 of AMSHAH)

INTRODUCTION

The spreading model of a highly viscous liquid such as oil on water is designed to determine the extent of spread and mean thickness of the resulting film as a function of time after the spill of a fixed and given amount of liquid. The liquid undergoing spreading is assumed to be immiscible with water and, of course, must be less dense to prevent sinking.

It is well known that the spreading phenomenon manifests itself in three different hydrodynamic regimes or temporal stages. The first stage is marked by the fact that the strong tendency of gravity head to cause acceleration of all portions of the slick is dynamically resisted by the reactive inertial force of the spreading mass. This regime is most generally referred to by authors working in the field as the "gravity-inertial" regime. It is analytically treated by neglecting the viscous term in the Navier-Stokes equation and retaining the nonlinear velocity gradient terms as well as the pressure gradient term. These are then treated on a similarity basis using such methods as those of characteristics. This is easily possible because the hydrodynamic flow is conservative requiring that important properties of the system are constants of the motion, thus allowing for convenient interpretation of the results.

On the other hand, when sufficient time has elapsed after the spill such that the slick has become long or widespread compared to its thickness, the velocity gradient and acceleration terms in the Navier-Stokes equation can be neglected and the viscous term brought into the picture. The pressure gradient term is retained, of course, since it represents the gravity "head" effect. This regime is known as the "gravity-viscous" regime and is analytically handled by equating the gravity pressure term with the viscous term. Because the motion is now not conservative, characteristics are no longer convenient; however, since the nonlinear acceleration terms are absent, the solution remains tractable. What the resulting solution ultimately depends on, however, is the precise form of the viscous force law, i.e., what kind of "drag law" takes place in this regime. There probably have been as many assumptions as authors

treating the problem, but it can generally be said that the two principal avenues one can follow are: solve the matched slick layer-water boundary layer equation in detail, or assume a drag law based on existing solutions such as classical boundary layer theory. The first approach is beset with enormous mathematical difficulties. The second gives tractable results which should then be matched with experiment. It is the second approach which has evidently been used in Chapter 3 which will be explained in detail later.

At very late times or for very thin slicks, the dominant spreading force is the net difference of the respective surface tensions of three pairwise surface tensions. The first is oil to air, the second oil to water, and the third water to air. The net effect of these is the driving force which is still resisted by viscosity, hence the name "surface tension-viscous" regime. Because an exact analysis of the problem in this regime is very difficult, most authors follow simple engineering-type approximations that will allow experimental correlations to be made. At the present state of the art, this is the most that can reasonably be expected.

Chapter 3 is based principally on work by Fannelop and Waldman [5] as given in their classic paper published in 1972. The model of Chapter 3 does not include the effects of heat transfer to cause vapor loss or dissolution of the liquid in water. The spill is assumed to take place quickly which, for mathematical purposes, can be described as instantaneous. The hydrodynamic and thermodynamic parameters are assumed to remain constant during the spread, as are the total mass and volume spilled.

A few errors in the text have been identified and questions have been raised regarding some of the assumptions employed in the late stages of pool spread. An analytic sensitivity study has revealed error variance involving numerical relations assumed in the model. When questions regarding the formulations have been found, alternative suggestions have been given where possible and practicable.

A. *REVIEW OF TEXT (Chapter 3)* (1)

(III,1) *Section 3.1, Aim (p.19)*

(III,1,a) The aim of the model is that of obtaining the extent of spread and mean thickness of the film at any time after the spill of a liquid. (√)

(III,2) *Section 3.2, Introduction (p.19)*

(III,2,a) Basic forces involved in the process of pool spread:

Initial spread results from hydrostatic pressure. (√)

Later spread controlled by surface tension. (√)

(III,2,b)* As the authors point out later, the actual sequence of pool growth is more complicated than that described in (III,2,a). There are three recognizable stages of pool growth:

(a) gravity-inertia stage controlled by hydrostatic pressure;

(b) gravity-viscous stage controlled by hydrostatic pressure and viscous forces; and

(c) viscous-surface tension stage controlled by viscous and surface forces.

In addition, there is a final stage where pool growth ceases. This is not, however, described by the model.

(III,2,c) After a review of previous work on the subject, the authors state that they are describing the spread of a very high-viscosity liquid over water assuming no heat loss or mass boiloff. (√)

(III,3) *Section 3.3, Assumptions (p.19)*

(III,3,a) Liquid spilled instantaneously. (√)

Properties and mass of liquid are assumed constant. (√)

Derivations are based on balance of spreading forces with resisting forces. (√)

(III,4) *Section 3.4, Data Required (p.19)*

(III,4,a) Quantity of liquid spilled. (√)

Physical properties of liquid and water. (√)

(III,4,b)* Data on surface tension should be obtained from dynamic experimental measurements since equilibrium values are expected to deviate from these by a fair amount.

(III,5) *Section 3.5, Model (pp.19-20)*

(III,5,a) Results taken from Fannelop and Waldman[2] are summarized in Tables 3.1 and 3.2 (pp. 26 and 27), along with ranges of (dimensionless) viscous and surface tension parameters ranging through a 10,000-ton maximum spill. Figure 3.1 is a plot of the spread relations for the radial case. (√)

(III,5,b)* The authors do not include formulas on mean thickness as stated in Section 3.1.

(III,6) *Section 3.6, Algorithm for Computation (p.20)*

(III,6,a) A flow chart is shown in Figure 3.2 for the calculations. (√)

(III,7) *Section 3.7, Specific Example (pp.20-21)*

(III,7,a) Data. All data correct except for viscosity of water. (√)

(III,7,b)** The correct viscosity of water[3] 10^{-3} $N\ s/m^2$.

(III,7,c) Calculations all correct. (√)

(III,7,d)* The authors do not state explicitly what the formulas assert, that in their calculations they are using the viscosity of water (not oil) and the surface tension of oil (presumably oil in water). This could cause some serious misunderstanding in interpreting and understanding the results.

(III,8) *Section 3.8, Discussions (pp.23-24)*

(III,8,a) Scaling - late spread rate is not sensitive to spill volume. (√)

Limitations of the model:

- assumption of calm water (√)
- no wind effects (√)
- no tidal current (√)
- no waves (√)

The authors note that the slick ceases to spread after some time. They quote the Fay model:

$$\text{Maximum area} = 10^5[\text{spill volume in } m^3]^{3/4} \qquad \text{(III-1)}$$

based on presumed changes in composition resulting from fractional boiloff. (√)

(III,8,b)* The most severe limitation of the model is that of failure to account properly for the limiting effects of surface forces on the late stages of pool growth. The authors have assumed that the surface viscous parameter responsible for the outward drag is that of oil in water. However, this is a static limit of a surface force of a more complex nature, a point emphasized by Fannelop and Waldman when they asserted that the σ to be used in their models is to be determined empirically. The surface tension utilized in Chapter 3 of AMSHAH is an inward force and is not the outward drag force postulated by Fannelop and Waldman. One can thus conceive of two limiting cases. The one used by Fannelop and Waldman is based on a dynamic outward surface drag which is balanced by an inward viscous force and leads to the prediction of indefinite pool growth. However, this dynamic force is not constant in time and ultimately merges into the static limit where[4]

$$\text{Maximum area} \sim V\left[\frac{\rho G}{\sigma}\right]^{1/2} \qquad \text{(III-2)}$$

The Fay model which predicts a $V^{3/4}$-dependence is an attempt to account for the time-dependence of σ during the growth interval.

(III,8,c)* The Fannelop-Waldman model is based on boundary conditions involving liquid flow past flat plates. These are the boundary conditions used in the AMSHAH models on pool spread. It is not clear how this limitation affects the validity of the predicted results. (See Appendix A.)

(III,9) *Section 3.9, Conclusions (p.24)*

(III,9,a) Theoretical formulas for spreading have been developed and discussed along with an illustrative example. (√)

Limitations of the model have been cited. (√)

(III,10) *Section 3.10, References (p.24)*

(III,10,a) References used in the report are listed. (√)

(III,11) *Section 3.11, Nomenclature (pp.24-25)*

(III,11,a) A list of symbols along with their meanings is presented. (√)

F(III,1) *Figure 3.1 (p.21), Radial Spreading of High Viscous Liquid on Water*

F(III,1,a)* The curves showing radial spreading on water are ambiguous and some of the numerical values questionable. The scaling scheme is also poorly developed. We have recalculated the spread rate using the formulas of Table 3.2, along with the following values of Γ_w:

$$\Gamma_w = 1.5 \times 10^4,\ 4.6 \times 10^3,\ 1.5 \times 10^3$$

Numerical values (rounded off to two digits) are listed in Table (III,1) and curves are shown in Figure (III,1).

F(III,2) *Figure 3.2 (p.22), Flow Chart for the Calculation of the Extent of Spread of a High Viscosity Liquid on Water*

F(III,2,a) Flow chart is shown. (√)

T(III,1) *Table 3.1 (p.26), Dimensional Equations of Spread With High Viscosity*

T(III,1,a)

Spread Regimes → / Geometry of Spread ↓	Gravity-Inertia	Gravity-Viscous	Viscous-Surface Tension
One-Dimensional	√	√	√
Radial	√	√	√

T(III,2) *Table 3.2 (p.27), Non-Dimensional Equations of Spread With High Viscosity*

T(III,2,a) Regimes of Spread → / Geometry ↓	Gravity-Inertia	Gravity-Viscous	Viscous-Surface Tension
One-Dimensional	✓	✓	X
Radial	✓	✓	✓

T(III,2,b)** In Table 3.2 there is an error in the formula for one-dimensional pool radius in the viscous-surface tension regime. The correct formula is:

$$\chi = 1.43 \left(\frac{\Sigma}{\Gamma}\right)^{1/2} \tau^{3/4}$$

TABLE (III,1)

NUMERICAL CALCULATIONS ON RADIAL SPREADING OF A HIGH-VISCOSITY LIQUID ON WATER

Γ_w	V	L	Σ_w	Σ_w/Γ_w	τ_1	τ_2	χ_1	χ_2
1.5×10^4	16×10^4	56	5.8	4×10^{-4}	300	2.4×10^4	20	61
4.6×10^3	10^3	10	14	3×10^{-3}	150	2×10^3	14	27
1.5×10^3	16	2.4	28	2×10^{-2}	70	230	10	13

V is in m^3.

L is in m.

τ_1 is time (dimensionless) for first changeover -- from gravity-inertia stage to gravity-viscous stage.

τ_2 is time (dimensionless) for second changeover -- from gravity-viscous to gravity-surface tension stage.

χ_1 and χ_2 are the (dimensionless) pool radii at τ_1 and τ_2, respectively.

$G = g(1 - \rho_L/\rho_w) = .49\ m/s^2$

$\mu_w = 10^{-3}\ Ns/m^3$

$\rho_w = 1000\ kg/m^3$

$\rho_L = 950\ kg/m^3$

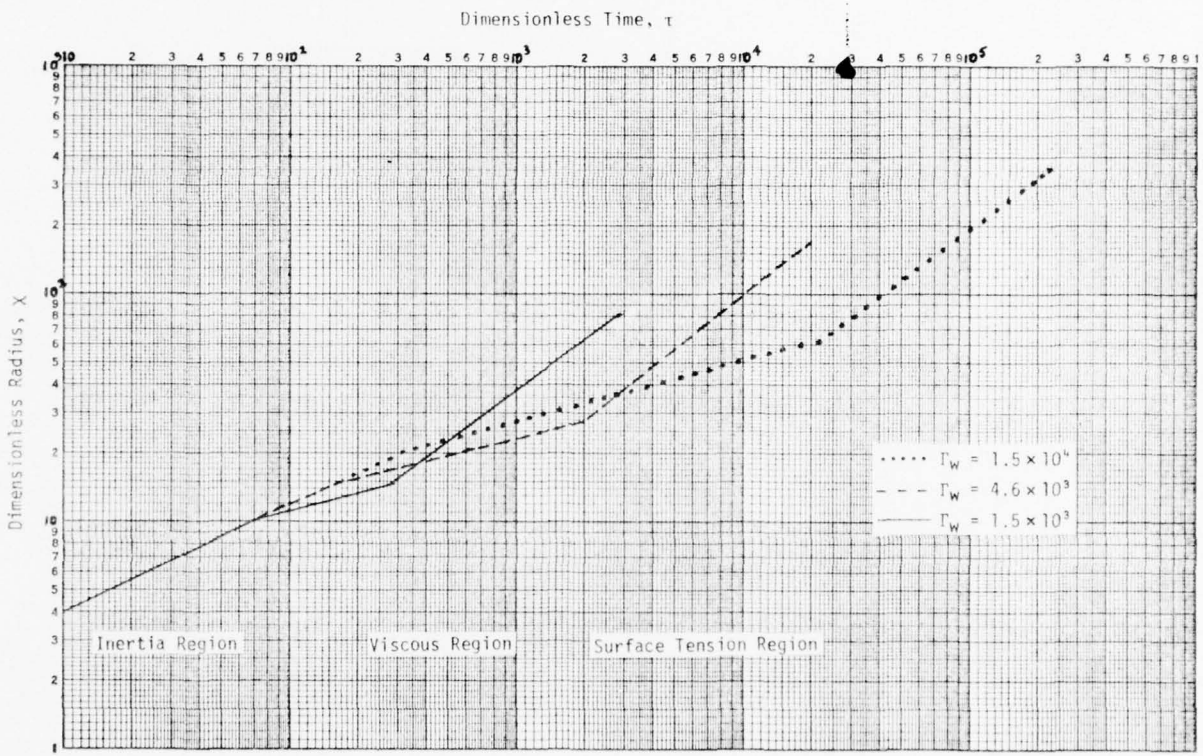

FIGURE (III,1). Radial Spreading of a High-Viscosity Liquid

B. CRITIQUE OF THE MODEL (Chapter 3)

Apart from the limitations of the model that have already been cited (see discussions on Section 3.8), we note that the complexity of the problem is such that one attempts to describe the major features of the flow in terms of the essential singularities. The separate stages of flow are dominated by these singularities. The Fannelop-Waldman approach is based on the Karman-Pohlhausen representation of the basic hydrodynamic relations (see Appendix A):

$$\frac{\partial \delta}{\partial t} + u \frac{\partial \delta}{\partial x} + \frac{\delta}{x} \frac{\partial}{\partial x} (xu) = 0 \qquad \text{(III-3a)}$$

$$\frac{\partial u}{\partial t} + u \frac{\partial u}{\partial x} + G \frac{\partial \delta}{\partial x} = \frac{\Lambda}{\rho \delta} \qquad \text{(III-3b)}$$

where δ is the local thickness

$$G = \left(\frac{\rho_w - \rho_L}{\rho_L} \right) g \qquad \text{(III-3c)}$$

is an effective gravitational force density and Λ the viscous force -- in this case

$$\Lambda = \mu \frac{\partial u}{\partial z} \Bigg|_{Z_1}^{Z_2}$$

where Z_1 and Z_2 denote the coordinates of the upper and lower boundaries of the pool.

(a) Initially the viscous force is not very important. The flow is determined by singularities of the characteristic velocity which, in this case, is

$$\sqrt{G\delta} \qquad \text{(III-4)}$$

One can use this to show quite readily that

$$R = C[GV]^{1/4} t^{1/2} \qquad \text{(III-5)}$$

The constant C can be estimated using a specific "model." However, this will involve use of boundary conditions of questionable validity. Any reasonable model will show C to be approximately unity. The value 1.14 given by Fannelop and Waldman and used in Chapter 3 of AMSHAH is a presumed value, and the observed constant may differ from this. (The formal development of the theory is presented in Appendix A.)

(b) The gravity-viscous stage involves essentially the balance of viscous force with hydrostatic pressure. Thus one can require that

$$G \frac{\partial \delta}{\partial x} \approx \frac{\mu}{\rho \delta} \frac{\partial v}{\partial z} \Bigg|_{z_1}^{z_2} \tag{III-6}$$

in (III-3b). However, the inertial momentum term might also be important. To allow for this, we may model the pool as a boundary layer in the later stage. This is achieved by letting[5,6]

$$\frac{\delta}{X - x} \sim \frac{1}{\sqrt{Re}} \tag{III-7}$$

where

$$Re = \frac{u(X - x)}{\nu} \tag{III-7a}$$

is the Reynolds number. This, in turn, yields (see Appendix B):

$$\frac{\partial v}{\partial z} \Bigg|_{z_1}^{z_2} \sim \frac{v^{3/2}}{\sqrt{\nu}\ \sqrt{(X - x)}} \tag{III-8}$$

so that one is assured that the inertial momentum density will be comparable in order of magnitude to the viscous stress.

There are then two viewpoints that can be adopted in discussing the flow for the gravity-viscous stage:

(i) Following Fannelop and Waldman, we can attempt to satisfy (III-6) by letting

$$\delta^2 = \delta_0{}^2 (X - x)^{1/2} \tag{III-9}$$

We then satisfy (III-3b) by setting

$$\delta_0 = At^n \tag{III-10}$$

and find $n = -5/8$ and

$$R \sim t^{1/4} \tag{III-11}$$

(ii) We may attempt to satisfy (III-3b) by setting

$$\delta = \delta_0 \ (X - x)^{1/3} \tag{III-12}$$

assuming that the velocity at the pool edge is finite. Then set

$$X = At^n \qquad \delta_0 = \delta_{00} t^{n'} \tag{III-13}$$

This will yield

$$n = 1/8 \quad \text{and} \quad n' = -7/24 \tag{III-14}$$

These represent the results for pool spreading used in Chapter 8 of AMSHAH for the case of spreading of low-viscosity liquids.

Evidently the two models -- low-viscosity vs. high-viscosity -- differ only to the extent to which they account for inertial effects. At no point in the AMSHAH treatment of pool spreading models is any attempt made to justify this distinction -- namely, why one can completely ignore the inertial terms in the "low-viscosity" case alone.

(c) The viscous-surface tension regime will automatically yield a $t^{3/4}$-dependence for radial spread if one uses (III-8). Since this is the Fannelop-Waldman result, this behavior is predicted in AMSHAH in Chapter 3 under the heading "high-viscosity case." However, if we equate the viscous force to the surface force using (III-12) we obtain an $R \sim t^{1/4}$-dependence, as is the case for the viscous-surface tension regime for the "low-viscosity case" used in AMSHAH.

There is also a problem of flat plate boundary conditions assumed in all the AMSHAH models. The actual geometry is closer to the one shown in Figure (III,2):

$$\delta_1 = - \frac{\rho_L}{\rho_W - \rho_L} \delta_2 \tag{III-15a}$$

or

$$\delta_1 = - \frac{\rho_L}{\rho_W} \delta \tag{III-15b}$$

If we now assume similarity conditions

$$\dot{\delta}_1 = - \frac{\rho_L}{\rho_W} \dot{\delta} \tag{III-15c}$$

Then using the standard boundary layer result

$$v_Z = - \frac{\delta}{X - x} \dot{\delta}$$

with

$$\frac{\delta}{X - x} = \frac{1}{\sqrt{Re^*}}$$

$$v_{Z_1} \sim \frac{1}{\sqrt{Re^*}} \frac{\rho_L}{\rho_w} \dot{\delta} \approx \frac{1}{\sqrt{Re^* Re}} \frac{\rho_L}{\rho_w} v \qquad \text{(III-15d)}$$

We could develop such a model in greater detail; however, there is still a question of how to define Re^*.

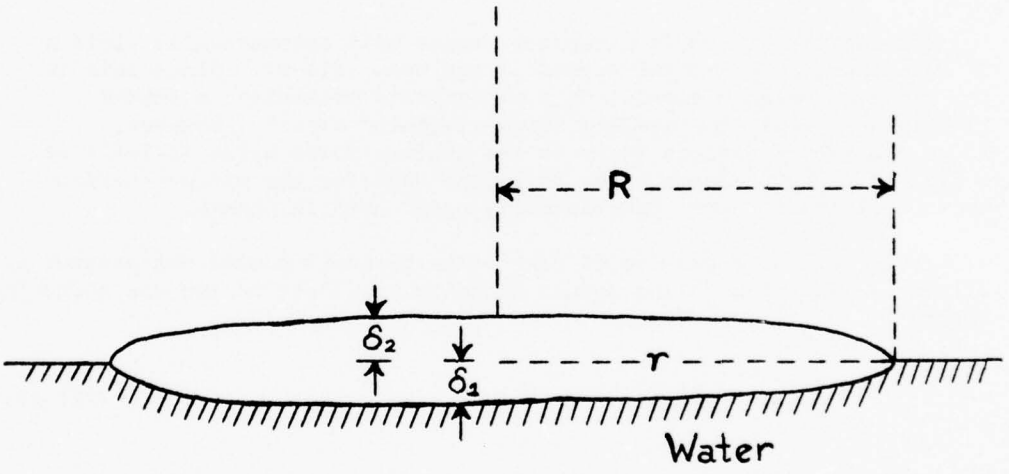

FIGURE (III,2). Model for Pool Spread

C. SENSITIVITY ANALYSIS (Chapter 3)

A standard approach that is suitable for these relationships is that of assuming that one has a dependent variable f which is defined in terms of a field of independent variables

$$f_i = \phi_i(X_j) \tag{III-16}$$

More explicitly, it is better to set

$$\ell n f_i = \ell n \phi_i(\ell n X_j)$$

with

$$\frac{1}{f_i} df_i = \sum_j \frac{\partial \ell n \phi_i}{\partial \ell n X_j} \frac{dX_j}{X_j} \tag{III-17}$$

Then

$$\frac{\partial \ell n \phi_i}{\partial \ell n X_j}$$

represents a matrix connecting the field of dependent fractions increments df_i/f_i with the independent ones dX_i/X_i.

What makes our results most amenable to simple calculation is the fact that the dependent variables f_i are expressed as products of the independent ones

$$f_i = \phi_i = \prod_j X_j^{n_{ij}} \tag{III-18}$$

so that

$$\frac{\partial \ell n \phi_i}{\partial \ell n X_j} = n_{ij} \tag{III-19}$$

Then one could obtain a composite estimate of the overall sensitivity by setting[7]

$$\left| \frac{df_i}{f_i} \right| = \left[\sum_j \left(n_{ij} \frac{dX_j}{X_j} \right)^2 \right]^{1/2} \tag{III-20}$$

There is also the problem of errors introduced by varying the exponents. This is best handled using the techniques of regression analysis.

In the absence of any noteworthy singularities in the equations themselves (such as vanishing denominators or exponents containing independent variables), we can consider the following salient features of any sensitivity analysis.

(i) There are discrete discontinuities in the logarithmic derivatives at the points of inflection t_1 and t_2 as defined in T(III,1). A detailed investigation of these singularities is unwarranted, since these are precisely the regions where the model is no longer valid.

(ii) An unbiased indicator of the relative effect of each of the independent variables can best be obtained by assuming all the $\delta X_j/X_j$ in (III-20) are equal. Then the relative effect of each variable, say the y^{th} variable on the i^{th} dependent factor would be

$$S_{ij} = \frac{n_{ij}}{[\sum_j n_{ij}^2]^{1/2}} \qquad \text{(III-21)}$$

(iii) It may turn out that one independent variable is more likely to be unmeasurable or undefined than others. Then if we assume all other independent variables to be determined with reasonable precision,

$$\frac{df_i}{f_i} \approx n_{ij} \frac{dX_j}{X_j} \qquad \text{(III-22)}$$

As an example, consider the formulas in Table 3.1 of Chapter 3 in AMSHAH. There are five dependent variables [we discuss the radial case only]:

R_{IG}	the radius in the inertia-gravity regime	- f_1
R_{GV}	the radius in the gravity-viscous regime	- f_2
R_{VT}	the radius in the viscous-surface tension regime	- f_3
t_1	the time for changeover from the gravity-inertia to the gravity-viscous regime	- f_4
t_2	the time for changeover from the gravity-viscous to the viscous-surface tension regime	- f_5

In addition, we might have two other dependent variables

R_1	- f_6
R_2	- f_7

where R_1 and R_2 are the respective crossover radii for the separate regimes.

For our independent variables, we choose:

V	the spill volume	$- x_1$
t	the time	$- x_2$
$J = \rho_w G$	an effective gravitational constant (normalized to the density of water)	$- x_3$
ρ_w	the density of water	$- x_4$
μ_w	the viscosity of water	$- x_5$
σ	the surface tension	$- x_6$
C_{IG}	the constant 1.14 appearing in the equation for r in the inertia-gravity case	$- x_7$
C_{GV}	the constant 0.98 appearing in the equation for r in the gravity-viscous case	$- x_8$
C_{VT}	the constant 1.6 appearing in the equation for r in the viscous-surface tension case	$- x_9$

The choice of V and t as independent variables is self-explanatory. Note also that

$$J = (\rho_w - \rho_L) g \qquad \text{(III-23a)}$$

so that

$$\frac{\delta J}{J} = \frac{-\delta \rho_L}{\rho_L} \frac{\rho_L}{\rho_w - \rho_L} \qquad \text{(III-23b)}$$

and small errors in the estimate of liquid density may be magnified several times in the resulting formulas if $\rho_w \simeq \rho_L$.

At the same time, the values of viscosity and surface tension used in these formulas are not necessarily the static published values (presumably determined with reasonably good precision) but dynamical quantities which may not even be constant in time. We thus include them among the independent variables. The last three independent variables are the semiempirical constants used in the model.

In order to proceed with our analysis, we must rewrite the formulas that appear in Table 3.1 in Chapter 3 of AMSHAH in terms of these variables. This is shown in Table (III,2). One can then construct a matrix of the sensitivity parameters n_{ij} as in Table (III,3). One can draw several general conclusions from these results.

TABLE (III,2)

DIMENSIONAL EQUATIONS FOR RADIAL SPREAD WITH HIGH VISCOSITY

Gravity-Inertia Regime	Gravity-Viscous Regime	Viscous-Surface Tension Regime
$0 < t < \left(\frac{C_{GV}}{C_{IG}}\right)^4 \left(\frac{V\rho_w^2}{J\mu_w}\right)^{1/3}$	$\left(\frac{C_{GV}}{C_{IG}}\right)^4 \left(\frac{V\rho_w^2}{J\mu_w}\right)^{1/3} < t < \left(\frac{C_{GV}}{C_{VT}}\right)^2 \frac{1}{\sigma} \left(\rho_w V^2 J\mu_w\right)^{1/3}$	$t > \left(\frac{C_{GV}}{C_{VT}}\right)^2 \frac{1}{\sigma} \left(\rho_w V^2 J\mu_w\right)^{1/3}$
$r = C_{IG} \left(\frac{JV}{\rho_w}\right)^{1/4} t^{1/2}$	$r = C_{GV} \left(\frac{J^2 V^4}{\rho_w \mu_w}\right)^{1/12} t^{1/4}$	$r = C_{VT} \left(\frac{\sigma^2}{\mu_w \rho_w}\right)^{1/4} t^{3/4}$
$0 < r < \frac{C_{GV}^2}{C_{IG}} \left(\frac{J\rho_w V^5}{\mu_w^2}\right)^{1/12}$	$\frac{C_{GV}^2}{C_{IG}} \left(\frac{J\rho_w V^5}{\mu_w^2}\right)^{1/12} < r < \left(\frac{C_{GV}^3}{C_{VT}}\right)^{1/2} \left(\frac{JV^2}{\sigma}\right)^{1/4}$	$r > \left(\frac{C_{GV}^3}{C_{VT}}\right)^{1/2} \left(\frac{JV^2}{\sigma}\right)^{1/4}$

TABLE (III,3)

MATRIX OF SENSITIVITY PARAMETERS (n_{ij})
FOR RADIAL SPREAD OF A POOL

Dependent Variable	Independent Variable									$\left[\sum_j n_{ij}^2\right]^{1/2}$
	V	t	J	ρ_w	μ_w	σ	C_{IG}	C_{GV}	C_{VT}	
R_{IG}	1/4	1/2	1/4	-1/4	0	0	1	0	0	1.20
R_{GV}	1/3	1/4	1/6	-1/12	-1/12	0	0	1	0	1.10
R_{VT}	0	3/4	0	-1/4	-1/4	1/2	0	0	1	1.39
t_1	1/3	0	-1/3	2/3	-1/3	0	-4	4	0	5.72
t_2	2/3	0	1/3	1/3	1/3	-1	0	2	-2	3.11
R_1	5/12	0	1/12	1/12	-1/6	0	-1	2	0	2.28
R_2	1/2	0	1/4	0	0	-1/4	0	3/2	-1/2	1.70

Note: To determine the percentage error in a given output or dependent variable, i, caused be a given error in an input or independent variable, j, multiply the matrix entry, n_{ij}, by the error in the independent variable, j. For example, if the error in R_{VT}, the radius of spread in the viscous-surface tension regime is sought due to error in C_{VT}, the spread constant pertaining therein, one looks to the entry in the third row (i=3) and ninth column (j=9). In this case n_{39}=1 and thus a 5 % error in C_{VT} will cause a 5% error in R_{VT}. The percentage of the total error caused by variance in C_{VT} is $(1/1.39)^2$ or 52%.

Thus by inspecting the first row of Table (III,3), one finds that the percentage error in pool radius is equally likely to result from errors in V, J, ρ_w respectively, but twice as likely from an equal error in t; that, if all errors are random, there is a 5% likelihood for it to arise from V, J, ρ_w, but a 70% likelihood for it to arise from C_{IG}, etc.

One should not draw too many far-reaching conclusions from these results, since we do not know that the errors are random. For example, the constants C_{IG}, C_{GV}, C_{VT} depend most certainly on size and geometry (though their ratios may be volume- and shape-independent). Then the parameters μ and σ may not be independent of each other, although the precise relation is not part of the model. The greatest practical difficulty is that of not knowing the initial condition of the spill. Thus, the radius in the gravity-inertia stage will start from a small value (presumably close to zero) and grow to a large value given by

$$R_1 = \frac{C_{GV}^2}{C_{IG}^2} \left(\frac{J \rho_w V^5}{\mu_w^2} \right)^{1/12} \qquad \text{(III-24a)}$$

where a point of inflection occurs. Now, if we assume that the initial radius R_0 is of the order $V^{1/3}$

$$\frac{R_1}{R_0} \sim \frac{C_{GV}^2}{C_{IG}^2} \left(\frac{J \rho_w V}{\mu_w^2} \right)^{1/12} \qquad \text{(III-24b)}$$

For heavy oil, of density 950 kg/m^3, we find on inserting numerical values

$$\frac{R_1}{R_0} \sim 7 \; V^{1/12} \qquad \text{(III-24c)}$$

where V is in m^3. Thus, for this ratio to be of order 20, one must have a spill of volume 30,000 m^3. Hence, the result of (III-24b) will not be an asymptotic limit even for the largest spills. Ignoring the initial geometry of the spill is thus unfortunate, considering the inherent character of the model which is based on asymptotic solutions.

In the light of these circumstances, it is proposed that a completely different approach to the problem of scaling and experimental design be attempted. Since, as discussed earlier, the parameters μ and σ may not necessarily be inputs to the model, we can simplify the analysis of the sensitivity studies using some results of dimensional analysis.[8] Thus consider the parameters R_1, R_2, t_1, t_2. These are given in Table (III,2). Note, however, that they are not independent since they are connected by a relation

$$\frac{R_2}{R_1} = \left(\frac{t_2}{t_1}\right)^{1/4} \tag{III-25}$$

Thus, there will be six separate dependent variables, R_{IG}, R_{GV}, R_{VT} along with R_1, t_1, R_2/R_1 where

$$\frac{R_2}{R_1} = \frac{C_{IG}}{\sqrt{C_{GV}C_{VT}}} \left(\frac{J^2 V \mu_w^2}{\rho_w \sigma^3}\right)^{1/12} \tag{III-26}$$

Note that this ratio has a weak dependence on V. For example, using heavy oil of S.G. 0.95, one obtains

$$\frac{R_2}{R_1} = 1.5\ V^{1/12} \tag{III-27}$$

where V is in m^3. One thus notes that R_2/R_1 will range in values from 1.5 for very small spills (of order 1 m^3) to 4.5 for very large spills where $V \sim 5.3 \times 10^5$ m^3. Evidently this parameter is not very sensitive to spill volume. These parameters can be identified by observing the turning points in the logarithmic derivative of the pool growth rate. (According to the AMSHA model, there should be two such points.) Then from Table (III,2) we could propose the following dimensionless equations. For the gravity-inertia regime

$$\lambda = \tau^{1/2} \tag{III-28a}$$

for $0 < \tau < 1$; for the gravity-viscous regime

$$\lambda = \tau^{1/4} \tag{III-28b}$$

for $1 < \tau < (R_2/R_1)^4$; and for the viscous-surface tension case

$$\lambda = (R_1/R_2)^2 (t/t_1)^{3/4} \tag{III-28c}$$

Here

$$\lambda = R/R_1 \tag{III-28d}$$

Since we expect the model to be valid in the asymptotic limit, in spite of its shortcomings this seems to be the best procedure for verifying the model and checking out the scaling laws. An improvement, of course, would consist of taking initial conditions of the spill into account and incorporating them as parameters, but this is difficult if not impossible.

D. HACS ERROR ANALYSIS (Chapter 3)

In this section, we explicitly list each HACS Fortran statement at variance with its parent mathematical expression as stated in Chapter 3, "Spreading of a Liquid on Water," in AMSHAH.

MODT obtains data from the subroutines FRCL and IRCL and computes the spread of an immiscible liquid on the water surface at any time after the spill for a liquid with a boiling point greather than the ambient temperature. There is a provision to calculate the size of the spill for the channel spread as well as for the radial spread. It calls subroutines BEGPR, FRCL, IRCL, EPRNT, RLJSP, ENDPR. All these subroutines have been checked for errors.

MODT:

For obtaining surface tension of a liquid in seawater, MODT uses the relation:

$$\text{surface tension} = |72.8 - \text{surface tension of liquid}|$$

where 72.8 dynes/cm is taken as the surface tension of water against air. This value corresponds to the surface tension of water in air at 20°C. However, this value does vary with temperature. At 10°C, it is 74.22 and at 50°C it is 67.91.

There are no errors in this subroutine.

RLJSP:

If $\mu_L > 2\mu_W$, this subroutine uses the equations of Chapter 3 of AMSHAH for calculating the size of the spread of the spilled liquid at any time; and, if $\mu_L < 2\mu_W$, the equations given in Chapter 8 are used. However, in many cases, agreement between the equations used in this subroutine and those given in Chapters 3 or 8 is lacking.

LN0037 `45 IF(T-(.972*A**.75/SQRT(B))**2.66666)50,50,55`
RLJSP checks if $\tau \leq 0.927\ \Gamma_W^2/\Sigma_W^{4/3}$ for gravity-viscous regime while the corresponding equation in AMSHAH (p.27) is $\tau \leq 0.989\ \Gamma_W^2/\Sigma_W^{4/3}$.

LN0040 `55 S=1.43*SQRT(B/A)*T**.75`
RLJSP uses $\chi = 1.43\ \Sigma_L^{1/2}/\Gamma_L^{1/2} * \tau^{3/4}$ for viscous-surface tension regime while AMSHAH (p.111) gives $\chi = 1.2\ \Sigma_L^{1/3}\tau^{1/3}$.

LN0051, 0052 `C...START CALCULATIONS FOR THE CASE WHEN THE LIQUID VISCOSITY IS LESS THAN THE VISCOSITY OF WATER`

should be: `C...START CALCULATIONS FOR THE CASE WHEN THE LIQUID VISCOSITY IS LESS THAN TWICE THE VISCOSITY OF WATER`

LN0057 90 IF(T-(.81*A**.4)**(15./7.))40,40,100
RLJSP checks if $\tau \leq 0.6366\ \Gamma^{6/7}$ for gravity-inertia regime while the corresponding equation of AMSHAH (p.111) is $\tau < 0.644\ \Gamma^{3/4}$.

LN0058 100 IF(T-(.90*A**.4/B**.333333)**7.5)105,105,110
RLJSP checks if $\tau \leq 0.4537\ \Gamma_L^{3.0}/\Sigma_L^{5/2}$ for gravity-viscous regime while the corresponding equation of AMSHAH (p.111) is $\tau \leq 0.645\ \Gamma_L^{3/4}/\Sigma_L^{5/2}$.

LN0059 105 S=1.13*A**.4*T**.2
RLJSP uses $\chi = 1.13\ \Gamma_L^{2/5}\tau^{1/5}$ for gravity-viscous regime while AMSHAH (p.111) gives $\chi = 1.132\ \Gamma^{1/10}\tau^{1/5}$.

LN0061 110 S=1.26*(B*T)**.333333
RLJSP uses $\chi = 1.26\ \Sigma_L^{1/3}\tau^{1/3}$ for viscous-surface tension regime while AMSHAH (p.111) gives $\chi = 1.2\ \Sigma_L^{1/3}\tau^{1/3}$.

LN0064 115 IF(T-(.685*A**.25)**2.66666)65,65,125
RLJSP checks if $\tau \leq 0.3646\ \Gamma_L^{2/3}$ for gravity-inertia regime while the corresponding equation of AMSHAH (p.111) is $\tau < 0.4446\ \Gamma_L^{2/3}$.

LN0065 125 IF(T-(.735*(A/B)**.25)**8)130,130,135
RLJSP checks if $\tau \leq 0.08517\ \Gamma_L^2/\Sigma_L^2$ for gravity-viscous regime while the corresponding equation of AMSHAH (p.111) is $\tau \leq 0.1697\ \Gamma_L^2/\Sigma_L^2$.

LN0066 130 S=.78*A**.25*T**.125
RLJSP uses $\chi = 0.78\ \Gamma_L^{1/4}\tau^{1/8}$ for viscous-gravity regime while AMSHAH (p.111) gives $\chi = 0.8412\ \Gamma_L^{1/4}\tau^{1/8}$.

LN0068 135 S=1.062*(B*T)**.25
RLJSP uses $\chi = 1.062\ \Sigma_L^{1/4}\tau^{1/4}$ for viscous-surface tension regime while AMSHAH (p.111) gives $\chi = 1.05\ \Sigma_L^{1/4}\tau^{1/4}$.

There are no errors in the subroutines BEGPR, FRCL, IRCL, EPRNT, and ENDPR.

E. SUMMARY OF RESULTS

The model described in Chapter 3 of AMSHAH has been reviewed with the following conclusions.

(1) There are several minor errors in the text involving numerical data and formulas. These have been cited and the corrections indicated.

(2) Except for the erroneous cases noted in (1) above, all formulas and calculations have been checked and found to be correct.

(3) Several questionable assumptions in the analysis and modeling have been noted. Among these the most salient ones are:

(i) The parameters μ and σ used in Chapter 3 of AMSHAH may not be valid and may have to be determined empirically as suggested by Fannelop and Waldman.

(ii) The AMSHAH models on spreading are predicated on the notion that a low-viscosity liquid will continue to spread regardless of the character of the inertial momentum term. Since Chapter 3 is not concerned with low-viscosity liquids, we merely note that the dynamical basis for distinguishing high-viscosity liquids from low-viscosity ones is highly questionable.

(iii) The liquid pool will not spread indefinitely as assumed in Chapter 3. The model gives us no insight into the ultimate extent of the pool. Also, the description of the late stages of pool growth may be highly unrealistic.

(iv) The boundary conditions assumed are questionable in view of the fact that one assumes asymptotic solutions in the modeling. Also, the Fannelop-Waldman constants used in the AMSHAH model are semiempirical and may not scale up properly, particularly if the boundary conditions are not suitable.

(4) The AMSHAH model for high-viscosity liquids omits results on average thickness.

(5) A sensitivity study was undertaken, and it was concluded that in view of the limitations of the model noted in (3) above that it would be best to parameterize the pool growth at the identifiable points of inflection and scale the model accordingly. *The subsequent scaling factors would then be highly insensitive to spill volume.*

F. RECOMMENDATIONS

(1) A review of the underlying assumptions involved in viscous spread ought to be undertaken for the purpose of drawing up a rigorous distinction between high-viscosity and low-viscosity flows.

(2) A more careful analysis of the spread rate involving surface forces is needed, particularly with regard to determining ultimate limits of pool growth.

(3) In the case where parameters entering the model are not well defined, a more careful distinction should be made between data and observed results. Should there be an impasse on this point, one can always reformulate the model and propose an experimental design as has been done in Section C (Sensitivity Analysis), so that the model will scale up properly in spite of its limitations.

G. TABLE OF SYMBOLS USED

A = area of pool [In (III-10) A is coefficient]

f = dependent variable in sensitivity studies

g = gravitational constant

G = effective gravitational constant $G = g(\rho_W - \rho_L)/\rho_W$

J = force density used in sensitivity studies $J = G\rho_W$

L = length scale used in AMSHAH models $L = V^{1/3}$

R = radius of pool

T = time scale used in AMSHAH models $T = \sqrt{L/G}$

u = lateral velocity; for radial growth $u = \dot{r}$

v = velocity

V = volume

x = lateral spread variable; for radial growth $x \equiv r$; in sensitivity studies, x is the independent variable

X = leading edge variable; for radial growth $X = R$

Z = local film thickness

Γ = dimensionless coefficient of viscosity used in AMSHAH models $\Gamma = [L^3 G/V_W^2]^{1/4}$

λ = dimensionless radial extent of pool used in sensitivity studies $\lambda = r/R$

Λ = viscous force

μ = coefficient of viscosity

ρ = mass density

σ = surface tension

Σ = dimensionless surface tension used in AMSHAH models $\Sigma = \sigma/\mu_W\sqrt{GL}$

E. SUMMARY OF RESULTS

τ = dimensionless time; in AMSHAH models $\tau = t/T$; in sensitivity studies $\tau = t/t_1$

χ = dimensionless pool radius used in AMSHAH models $\chi = r/L$

H. *LIST OF REFERENCES*

(1) Raj, P. P. K., and A. S. Kalelkar. Spreading of a liquid on water, ch. 3, pp. 19-27. In *Assessment Models in Support of the Hazard Assessment Handbook* (CG-446-3), CG-D-65-74. Prepared by Arthur D. Little, Inc. for Department of Transportation, U.S. Coast Guard, NTIS AD-776617, January 1974.

(2) Fannelop, T. K., and G. D. Waldman. Dynamics of oil slicks, *AIAA Journal 10*(4):506-510, 1972.

(3) Weast, R. C. (ed.). *Handbook of Physics and Chemistry*, 53rd ed., p. F34. Chemical Rubber Publishing Co., Cleveland, Ohio, 1972-73.

(4) This result can be obtained from Laplace's equation. See, for example, Levich, V. G., *Physicochemical Hydrodynamics*, p. 378. Prentice-Hall, Englewood Cliffs, N.J., 1962.

(5) Landau, L. D., and E. M. Lifshitz. *Fluid Mechanics*, pp. 145-151. Pergamon Press, London, 1959.

(6) Reference (4), p. 16.

(7) Beers, Y. *Introduction to the Theory of Errors*, pp. 26-35. Addison Wesley Publishing Co., Reading, Mass., 1953.

(8) Duncan, W. J. *Physical Similarity and Dimension Analysis*, ch. V. Edward Arnold & Co., London, 1953.

This is especially important for regions near the source, if

Chapter 3

"VAPOR DISPERSION"
(Chapter 5 of AMSHAH)

INTRODUCTION

The purpose of Chapter 5 of AMSHAH is to describe a model for estimating vapor dispersion or concentration in air resulting from an evaporating marine spill. The model provides estimates as a function of position in space for any time after the hazardous vapor cloud is released into the atmosphere. Molecular diffusion caused by material concentration agents is the prime agent of dispersion.

Point sources and area sources, as well as continuous and instantantaneous vapor releases, are treated and considered separately.

Much of the theory and early experimental justification was carried out by Pasquill [6]. Essentially, the theory is involved with solving the diffusion equations for area and point sources whose strengths are, in general, functions of time. The result is the well-known Gaussian form expressing downwind concentration as a function of distance from source and atmospheric stability, the latter asserting itself through the existence of diffusion parameters which play the role of variance in the Gaussian exponential expression.

It is to be noted that the precision of the results emanating from the technique increases the farther one proceeds in time and distance from the spill event that gives rise to the formation of the vapor cloud.

---

[6] Pasquill, F., *Atmospheric Diffusion*, pp. 101-165, John Wiley, N.Y., 1974.

A. *REVIEW OF TEXT (Chapter 5)*[1]

(V,1) *Section 5.1, Aim (p.51)*

(V,1,a) The aim of the model is to obtain the vapor concentration at any position in space and at any time after a hazardous vapor cloud is released into the atmosphere. (√)

(V,2) *Section 5.2, Introduction (p.51)*

(V,2,a) Primary agent of dispersion is atmospheric turbulence. (√)

Neutral buoyancy is assumed. (√)

No changes in meteorological conditions during spill and dispersion. (√)

(V,3) *Section 5.3, Assumption (p.52)*

(V,3,a) Vapor that is diffusing is neutrally buoyant. (√)

Mixing with air is uniform. (√)

Concentration obtained is time-averaged. (√)

(V,4) *Section 5.4, Data Required (p.52)*

(V,4,a) Atmospheric condition. (√)
Wind velocity. (√)
Field point coordinates. (√)
Rate of release as a function of time. (√)
Area of source. (√)

(V,5) *Section 5.5, Details of the Model (pp.52-57)*

(V,5,a) Results taken from Pasquill and others. (√)

The x-direction is direction of wind, z is vertical and y lateral coordinates. (√)

Section 5.5.1, Point Source

(V,5,1,a) Point source equation (5.1) is correct under assumptions given, i.e., instantaneous spill. (√)

(V,5,1,b) Continuous source concentration equations (5.2a) and (5.2b) are correct under assumptions given. (√)

(V,5,1,c) Equation (5.3) in in error. (X)

(V,5,1,d)** Equation (5.3) should read

$$C_f = \frac{1}{1 + \frac{M_v}{M_a}\left(\frac{1 - C}{C}\right)}$$

Section 5.5.2, Area Sources

(V,5,2,a)* Equation (5.4) employs a highly questionable procedure and is valid only if windward dispersion is ignored. It is inapplicable for a highly variable source like a water spill.

(V,5,2,b)* Equation (5.5a) is highly questionable and could lead to serious underestimation of the concentration. In the limit of an instantaneous spill, (5.5a) becomes valid. However, in general, neither this equation nor the case for a continuous source is valid for a water spill where the diameter, d, is a strong function of time.

Section 5.5.3, Plume Width

(V,5,3,a) Equation (5.5b) is correct. (√)

(V,6) *Section 5.6, Algorithm for Computations (p.58)*

(V,6,a) The algorithm for computations is correct. (√)

(V,7) *Section 5.7, Specific Example (pp. 58-59)*

(V,7,a)** Position of observation point should read x = 1000 m.

(V,7,b)* The value for C_0 for the instantaneous spill for t = 400 seconds and x = 1000 meters if given as .81 kg/m^3 which is numerically correct but greater than the density of pure methane at 1 atmosphere pressure and 0°C. The density of methane at these conditions is .72 kg/m^3 .

Difficulties of this type reflect the inadequacy of Gaussian models that undergo "instantaneous spills," the latter being a required artifice in order to maintain closed form expression in the Gaussian model. As a result, it is possible to obtain results that are not physically valid.

(V,7,c)* The mole fraction C_f must be greater than unity for the problem given, instantaneous spill. This, of course, is impossible.

(V,7,d)* The plume width for a 5% mole fraction has no meaning in this context, where the results for concentration are not physically valid.

(V,7,e) Value for C_0 for continuous spill is correct and physically valid. (√)

(V,7,f)** Value for C_f should be .064 for continuous spill.

(V,7,g)* Note that, for a continuous spill of the same size as the instantaneous one, the concentration at about the same distance and time from the event of the spill is more than one order of magnitude lower.

(V,8) *Section 5.8, Discussion (pp.59-60)*

(V,8,a) Model uses two experimentally determined parameters, σ_y and σ_z , which are functions of downwind distance and meteorological stability. Curves shown in Figure 5.2 are valid for continuous spills. These curves give σ_y and σ_z as a function of distance for Pasquill's turbulence conditions A through F. (√)

(V,8,b)* Authors suggest use of data from Figures 5.2a and 5.2b to determine σ_y and σ_z for instantaneous spill corresponding to a puff model. This is a highly questionable procedure.

(V,8,c) Models do not take account of change of wind direction or plume buoyancy. (√)

(V,9) *Section 5.9, Conclusions (p.60)*

(V,9,a) Theoretical formulas for dispersion for continuous and instantaneous or puff sources have been presented, discussed, and illustrated with examples. Limitations of model have been cited. (√)

(V,10) *Section 5.10, References (pp.60-61)*

(V,10,a) References used in this section are listed. (√)

(V,11) *Section 5.11, Nomenclature (p.61)*

(V,11,a) A list of symbols along with their meanings is presented. (√)

F(V,1) *Figures 5.1a and 5.1b, Schematic Diagrams of Continous Point and Area Sources (p.53)*

F(V,1,a) Both figures are correct as shown. (√)

F(V,2) *Figures 5.2a and 5.2b, Lateral and Vertical Diffusion, σ_y and σ_z, Versus Downwind Distance From Source for Pasquill's Turbulence Types (pp.55-56)*

F(V,2,a)* See comments and calculations regarding Figures 5.2a and 5.2b of text in HACS ERROR ANALYSIS MOD JHHDC. They appear in Section D of this review of Chapter 5.

B. *CRITIQUE OF THE MODEL (Chapter 5)*

The entire development of the dispersion model in Chapter 5 is based on the Gaussian plume and puff model which is the asymptotic form of the solution of the diffusion equation.[2] However, the expressions given, (5.1), (5.2a), and (5.2b), are for special cases. The expression (5.4) is one that is valid for a source of constant strength. As a result, the most general case, the variable source over a finite area, is not considered. Also the simplified expression, (5.5a), in which the area is replaced by a point source displaced upwind, is highly questionable.

The Gaussian plume model is a suitable one which has been widely used with considerable empirical success far away from the source. It suffers from the following limitations.

(1) It is valid only in the asymptotic limit.

(2) Because it represents a composite solution of a more complex problem, one involving turbulence, it does not yield a true picture of the dispersion process. Among the missing ingredients are realistic estimates of buoyancy effects and fluctuations due to turbulence.

(3) The Gaussian plume model is valid only for a constant velocity windfield.

In spite of these qualifications, the Gaussian plume model is a good description of the dispersion process, provided one uses a proper time-dependent development of the equations and restricts the interpretation of the results to the appropriate limits. The development of the modeling in Chapter 5 might be improved with this in mind. Appendix D covering the use of Green's functions for the solution to the diffusion process will illustrate this point.

C. SENSITIVITY ANALYSIS (Chapter 5)

A standard approach that is suitable for these relationships is that of assuming that one has a dependent variable f which is defined in terms of a field of independent variables

$$f_i = \phi_i(X_j) \tag{V-1}$$

More explicitly, it is better to set

$$\ell n f_i = \ell n \phi_i(\ell n X_j)$$

with

$$\frac{1}{f_i} df_i = \sum_j \frac{\partial \ell n \phi_i}{\partial \ell n X_j} \frac{dX_j}{X_j} \tag{V-2}$$

Then

$$\frac{\partial \ell n \phi_i}{\partial \ell n X_j}$$

represents a matrix connecting the field of dependent fraction increments df_i/f_i with the independent ones dX_i/X_i .

What makes our results more amenable to simple calculation is the fact that the dependent variables f_i are expressed as products of the independent ones

$$f_i = \phi_i = \prod_j X_j^{n_{ij}} \tag{V-3}$$

so that

$$\frac{\partial \ell n \phi_i}{\partial \ell n X_j} = n_{ij} \tag{V-4}$$

Then one could obtain a composite estimate of the overall sensitivity by setting

$$\left|\frac{df_i}{f_i}\right| = \left[\sum_j \left(n_{ij}\ \frac{dX_j}{X_j}\right)^2\right]^{1/2} \qquad \text{(V-5)}$$

There is also the problem of errors introduced by varying the exponents. This is best handled using the techniques of regression analysis.

In the absence of any noteworthy singularities in the equations themselves (such as vanishing denominators or exponents containing independent variables), we can consider the following salient features of any sensitivity analysis.

(1) An unbiased indicator of the relative effect of each of the independent variables can best be obtained by assuming all the $\delta X_j/X_j$ in (V-5) are equal. Then the relative effect of each variable, say the jth variable on the ith dependent factor, would be

$$S_{ij} = \frac{n_{ij}}{\left(\sum_j n_{ij}{}^2\right)^{1/2}} \qquad \text{(V-6)}$$

(2) It may turn out that one independent variable is less likely to be measurable or defined than others. Then, if we assume all other independent variables to be determined with reasonable precision,

$$\frac{df_i}{f_i} \approx n_{ij}\ \frac{dX_j}{X_j} \qquad \text{(V-7)}$$

As an example, consider the formulas (5.1) and (5.2) of Chapter 5 in AMSHAH. There are two dependent variables, one each for the instantaneous and continuous spills. We will designate them as follows:

$C(x,y,z,t)$	concentration resulting from instantaneous release for point source	$- f_1$
$C(x,y,z,t)$	concentration resulting from continuous release for point source	$- f_2$

As a third dependent variable of interest we choose the plume width $W(C^*)$ of (5.5b) and let this be $- f_3$

For independent variables, we have:

m	the spill mass	x_1
σ_x	the dispersion coefficient for x-direction	x_2
σ_y	the dispersion coefficient for y-direction	x_3
σ_z	the dispersion coefficient for z-direction	x_4
U	wind speed	x_5
h	height of source	x_6
$\dot{m}$	mass release rate	x_7
$C_0(x,t)$	centerline concentration for y=z=0	x_8

The matrix of n_{ij} is shown in Table (V,1)

TABLE (V,1)

MATRIX OF SENSITIVITY PARAMETERS (n_{ij}) FOR VAPOR DISPERSION

Dependent Variable	Independent Variable							
	m	σ_x	σ_y	σ_z	U	h	$\dot{m}$	C_0
Instantaneous Spill $C(x,y,z,t)$	1	$-1+\frac{(X-Ut)^2}{\sigma_x^2}$	$-1+\frac{y^2}{\sigma_y^2}$	$-1+\frac{2}{\beta}\left[\alpha e^{-\alpha}+\gamma e^{-\gamma}\right]$	$\frac{(X-Ut)Ut}{\sigma_x^2}$	$\frac{h}{\beta}\left[e^{-\alpha\delta}-e^{-\gamma\xi}\right]$	0	0
Continuous Spill $C(x,y,z,t)$	0	0	$-1+\frac{y^2}{\sigma_y^2}$	$-1+\frac{2}{\beta}\left[\alpha e^{-\alpha}+\gamma e^{-\gamma}\right]$	-1	$\frac{h}{\beta}\left[e^{-\alpha\delta}+e^{-\gamma\xi}\right]$	1	0
Plume Width $W(C^*)$	0	0	1	0	0	0	0	$\frac{1}{2}\left[\ell n\left(\frac{C_0}{C^*}\right)\right]^{-1}$

$\beta = e^{-(z-h)^2/2\sigma_z^2} + e^{-(z+h)^2/2\sigma_z^2}$ $\quad \gamma = (z+h)^2/2\sigma_z^2$ $\quad \xi = (z+h)/\sigma_z^2$

$\alpha = (z-h)^2/2\sigma_z^2$ $\quad \delta = (z-h)/\sigma_z^2$

We observe first that most of the entries for n_{ij} of Table (V,1) that are nonzero are explicitly dependent on various independent position and time variables. For this reason, the sensitivity of say $C(x,y,z,t)$ to σ_X for an instantaneous spill depends on the magnitudes of the wind speed U, σ_X distance downwind X, and the time of observance t. Depending on the functional behavior of σ_X with X, we would always expect $(X-Ut)^2/\sigma_X^2$ to be of order unity or less, since for $X \ll Ut$ the absolute concentration $C(x,y,z,t)$ is virtually zero. On the other hand,

F(VIII,1) *Figure 8.1 (p.87), Details of the Spreading Model*

for $X = Ut$, the error induced in $C(x,y,z,t)$ by σ_x is the same and opposite to the error in σ_x itself.

In all cases, in the asymptotic limit of time and distance, the value of n_{ij} for $C(x,y,z,t)$ is of the order unity where meaningful nonzero concentrations exist. This holds for both instantaneous and continuous spills.

Plume width, on the contrary, is sensitive to error in C_0 for values of specified concentration C^* that are close to the centerline concentration. This is understandable, because the plume width in such a case would be expected to be small, smaller even than σ_y itself. This being so, the concept of width loses its meaning and becomes a rapidly varying function of centerline concentration C_0.

In any case, the sensitivity coefficients given here improve as x and t become large in accord with the precision behavior of the Gaussian model itself. For times and distances, i.e., events, near the source, they start to break down. But then this is the precise region where the model is invalid in the first instance.

D. HACS ERROR ANALYSIS (Chapter 5)

MODC1 and MODC2 obtain data from the subroutines FRCL and IRCL. MODC1 computes (i) vapor concentration at any point (x,y,z) as a function of time and (ii) maximum ground level concentrations as a function of distance (x). MODC2 (i) computes semi-width of the cloud of a given concentration at a given ground level position (i.e., given value of x), (ii) computes time of arrival of this cloud at the given value of x, (iii) checks if the point (x,y,o) is inside or outside this cloud (concentration zone), (iv) if it is inside, calculates the duration for which hazardous cloud remains at this point.

MODC1 calls the subroutines, namely, BEGPR, FRCL, IRCL, EPRNT, VAPC, TOXIC, OUTPR, ENDPR. MODC2 calls BEGPR, FRCL, IRCL, EPRNT, IVAPC, ITOX, OUTPR, ENDPR. Subroutine JHHDC is used by both VAPC and IVAPC to compute the dispersion coefficient. All these subroutines have been checked for errors.

MODC1:

```
LN 0095     100 FORMAT(1X,8HVAP CONC,6X,1H=,6X,E10.3,4X,
   0096         27HMOLE%≥,IS A COMPUTED VALUE./)

should be   100 FORMAT(1X,8HVAP CONC,6X,1H=,6X,E10.3,4X,
                 27HMOLE%,IS A COMPUTED VALUE./)
```

MODC2: No error was found.

VAPC:

LN 0044 `C=CO*EXP(-(X-UWIND*T)**2/(2.*SIGX**2))`
`*EXP(-Y**2/(2.*SIGY**2))`

should be `C=CO*EXP(-(X+FACT-UWIND*T)**2/(2.*SIGX**2))`
`*EXP(-Y**2/(2.*SIGY**2))`

JHHDC: In order to check the consistency between the values calculated by the subroutine JHHDC and the corresponding values obtained from Figures 5.2a and 5.2b in Chapter 5 of AMSHAH for the dispersion coefficients, this subroutine was run for various values of the "distance from source" under various atmospheric conditions. The results are shown in Table (V,2) on the next page. The values of σ_z which were beyond the range of the values given in Figure 5.2b have been left out. Realizing the limited accuracy with which these figures can be read, the agreement between the values calculated by the subroutine JHHDC and those obtained from AMSHAH is reasonable. There is one important point to be borne in mind about the values calculated by the subroutine JHHDC. For instance, consider the curve A of Figure 5.2b. For distance from source of 2000 m, the calculated value of σ_z by subroutine JHHDC is 1933 m. The corresponding value obtained by the extension of curve A is 36,000 m. In view of this, one can get completely erroneous values of σ_z if they are outside the range of values obtainable from Figure 5.2b.

TOXIC: TOXIC uses the following relation to obtain mole fraction of chemical,

$$XCONC = \frac{1}{\left[1 + \frac{AM}{28.9} * \frac{DENA}{C} * \left(1 - \frac{C}{DENV}\right)\right]}$$

where AM = molecular weight of chemical
28.9 = molecular weight of air
DENA = 0.012894 (density of air at standard conditions of 0°C and 1 atm, gm/cc)
DENV = AM/22414 (density of chemical (vapor) at standard conditions, gm/cc)

$$XCONC = \frac{1}{\left[1 + \frac{AM}{28.9} * \frac{DENA}{C} * \frac{(DENV - C)}{DENV}\right]}$$

$$= \frac{1}{\left[1 + \frac{AM}{28.9} * \frac{DENA}{DENV}\left(\frac{DENV}{C} - 1\right)\right]}$$

TABLE (V,2)

Atmospheric Conditions	Distance from Source (m)	σ_y, Horizontal Dispersion Coefficient (m)		σ_z, Vertical Dispersion Coefficient (m)	
		Calculated	Figure 5.2a	Calculated	Figure 5.2b
A	1,000	207	210	534	510
	2,000	372	380	1,933	
	4,000	681	660	8,787	
	8,000	1,247	1,200	43,980	
	16,000	2,283	2,100	242,368	
	32,000	4,177	3,500	1,470,552	
	64,000	7,643	6,000	9,823,530	
B	1,000	158	150	121	120
	2,000	295	280	233	
	4,000	550	500	496	
	8,000	1,027	940	1,059	
	16,000	1,849	1,800	2,263	
	32,000	3,264	3,100	4,842	
	64,000	5,744	5,000	10,375	
C	1,000	104	110	61	66
	2,000	196	205	115	130
	4,000	369	380	219	215
	8,000	694	710	413	400
	16,000	1,278	1,300	777	680
	32,000	2,323	2,200	1,452	1,050
	64,000	4,219	3,600	2,700	1,700
D	1,000	69	72	30	33
	2,000	130	135	50	51
	4,000	247	250	80	84
	8,000	466	460	122	125
	16,000	858	800	182	190
	32,000	1,557	1,400	261	290
	64,000	2,819	2,300	363	390
E	1,000	51	54	22	23
	2,000	96	100	35	37
	4,000	182	185	53	56
	8,000	345	340	76	80
	16,000	636	590	104	105
	32,000	1,159	1,050	135	140
	64,000	2,108	1,800	168	160
F	1,000	34	37	14	14
	2,000	64	66	22	21
	4,000	122	125	32	31
	8,000	230	220	45	42
	16,000	424	410	58	56
	32,000	772	770	72	70
	64,000	1,405	1,200	84	84

A: Extremely Unstable; B: Moderately Unstable; C: Slightly Unstable; D: Neutral; E: Slightly Stable; F: Moderately Stable

By Avogadro's law, equal volumes of gases at the same temperature and pressure contain equal number of molecules, i.e., at same temperature and pressure, molar densities of ideal gases are equal. Therefore

$$DENA/28.9 = DENV/AM$$

$$XCONC = \frac{C}{DENV} = \frac{C*V}{DENV*V}$$ where V is the volume of gas mixture in cc at T and P.

$$= \frac{C*V/AM}{DENV*V/AM}$$

By definition,

$$XCONC = \frac{\text{moles of chemical in V}}{\text{total moles in V}}$$

$$\frac{C*V}{AM} = \text{moles of chemical in V}$$

$$\frac{DENV*V}{AM} \neq \text{total moles in V unless the gas mixture is at standard conditions}$$

The correct relationship to obtain mole fraction of chemical follows:

$$XCONC = \frac{\text{moles of chemical in V}}{\text{total moles in V}}$$

$$= \frac{C*V/AM}{P*V/R*T} = \frac{C*R*T}{P*AM}$$ This reduces to the equation given on p. A-3.

ITOX: ITOX uses the following relation to obtain concentration C in gm/cc from the corresponding value in mole% or ppm:

$$C = \frac{1}{\left| \frac{1}{DENV} + \frac{(1 - CHAZ) * 28.9}{(CHAZ * AM * DENA)} \right|}$$ where CHAZ is mole fraction of chemical

By the same reasoning as given in the subroutine TOXIC, this expression is wrong. The correct relationship is

$$C = \frac{CHAZ * P * AM}{R * T}$$

No error was found in the subroutines BEGPR, FRCL, IRCL, EPRNT, ENDPR, OUTPR.

Although AMSHAH gives equations 5.2a and 5.2b for calculating the concentration at any position in the case of vapor released continuously at a constant rate, these have not been included in HACS.

E. *SUMMARY OF RESULTS*

The model described in Chapter 5 of AMSHAH has been reviewed with the following conclusions.

(1) There are several errors in the text involving formulas and numerical calculations. These have been cited and the corrections indicated.

(2) Except for the erroneous cases noted in (1) above, all formulas and calculations have been checked and found to be correct.

(3) The most serious objections that can be raised against the model of Chapter 5 are the following:

(a) Model is invalid in regions close to spill and times close to spill event.

(b) Model cannot handle spills whose duration lies in the span between instantaneous and continuous, i.e., a "real-world" incident.

(c) The "puff" model predicts results that are physically invalid for events near the source.

(d) Equivalency of an area source to a point source displaced *upwind is questionable.*

(e) Dispersion coefficients, while appearing to be different for continuous sources as opposed to instantaneous, probably do not differ. Proper treatment of the spill process, along with recognition of wind-created turbulence, might well resolve the apparent differences.

(4) As the HACS review indicates, extrapolation of coefficients of dispersion, σ_x, σ_y, σ_z, on a linear basis can lead to considerable error.

(5) Sensitivity analysis on the model would seem to indicate that all input parameters contribute about equally to output error. As said before, the real error-producing factor is the very form of the model itself.

F. *RECOMMENDATIONS*

(1) An attempt should be made to include transient effects in the dispersion model that will calculate effect of time-dependent sources.

(2) A review of turbulence-caused fluctuations should be made in order that its impact on concentration fluctuations can be determined.

This is especially important for regions near the source. If successful, peak-to-average concentration ratios can be reliably estimated for a given stability condition, this knowledge might change areal extent of flammability zone.

(3) Source behavior for cryogen spills should be reworked to include transient behavior of heat transfer on a spreading pool. No dispersion model is going to be any better than its source term.

(4) A formal analysis of scale effects should be made, so that considerably large-scale extrapolations can be made with confidence based on dispersion models. We do not know at the present state of the art whether a spill of the order of 10^6 gallons will scale up, as per the model, or whether a significant change of behavior might result because of, say, a fundamental weather effect alteration caused by a spill of that large magnitude.

G. *TABLE OF SYMBOLS USED*

C = vapor concentration in kg/m^3

C_0 = vapor concentration at $y=z=0$

C_f = mole fraction of vapor concentration

h = height of spill

m = mass of spill

$\dot{m}$ = mass rate of spill

M_a = molecular weight of air

M_v = molecular weight of vapor

U = wind speed

$W(C^*)$ = plume width corresponding to concentration C^*

$\sigma_{x,y,z}$ = dispersion coefficients in x-, y-, z-directions

H. *LIST OF REFERENCES*

(1) Raj, P. P. K., and A. S. Kalelkar. Vapor dispersion, ch. 5, pp. 51-61. In *Assessment Models in Support of the Hazard Assessment Handbook*, Report No. CG-D-65-74, prepared by Arthur D. Little, Inc. for the Department of Transportation, NTIS Document No. AD776617, January 1974.

(2) Pasquill, F. *Atmospheric Diffusion*, pp. 101-165. John Wiley, N.Y., 1974.

Chapter 4

"SPREADING OF A LOW-VISCOSITY LIQUID
ON A HIGH-VISCOSITY LIQUID"
(Chapter 8 of AMSHAH)

INTRODUCTION

The spreading model of a low-viscosity liquid on water is designed to determine the extent of spread as a function of time after the spill of a fixed and given amount of liquid. The liquid undergoing spreading is assumed to be immiscible with water and less dense. No changes in physical chemical properties are assumed in the duration of the spill.

The two principal differences between the treatment of Chapter 3 of AMSHAH [2], "Spreading of a Liquid on Water," and that of the present chapter are:

1) The viscosity of water exceeds that of the liquid, $\mu_w > \mu_\ell$.

2) The effect of viscosity on the spread law is not treated in this chapter as it was in Chapter 3, namely, boundary layer theory and the subsequent $V^{3/2}$ law are omitted [5]. Instead, the authors apparently utilized a modified Rayleigh treatment of the viscosity resulting in a $t^{1/8}$ rather than a $t^{1/4}$ time-dependence for the spill radius in the gravity-viscous regime. (See Appendix A.)

Because the material of Chapters 3 and 8 was so similar, the HACS computer program for each was integrated into one grand program. Hence, we repeat here in Section D the review of HACS presented for Chapter 3 which covers Chapter 8 also.

A. *REVIEW OF TEXT (Chapter 8)* (1)

(VIII,1) *Section 8.1, Aim (p.85)*

(VIII,1,a) The aim of the derivations given in this chapter is to obtain expressions for the extent of spread at any time after a sudden spill of a low-viscosity liquid on a high-viscosity liquid. (√)

(VIII,2) *Section 8.2, Introduction (p.85)*

(VIII,2,a) Model is described as being strictly correct in the limit, $\mu_\ell/\mu_s \to 0$. (√)

(VIII,3) *Section 8.3, Assumptions (p.85)*

(VIII,3,a) The total mass of the spilled liquid remains constant, no evaporation or dissolution, no chemical reactions. (√)

The physical properties of the liquid and water do not change. (√)

The liquid is less dense and viscous than water as well as immiscible. (√)

The spill is instantaneous. (√)

(VIII,4) *Section 8.4, Data Required (pp.85-86)*

(VIII,4,a) Physical properties of liquid, water, and size of spill. (√)

(VIII,4,b)* Data on surface tension should be obtained from dynamic experimental measurements, since equilibrium values are expected to deviate from these by a fair amount.

(VIII,5) *Section 8.5, Details of the Model (pp.86-101)*

(VIII,5,a) Results of spreading of both radial and one-dimensional spreading are summarized in Table 8.1 and Table 8.2 (dimensionless). (√)

Section 8.5.1, Radial Spreading

(VIII,5.1,a)* Would recommend $T = \sqrt{L/g}$ rather than $\sqrt{L/G}$. Recalling that $G = g(1 - \rho_\ell/\rho_w)$, this could become important for $\rho_\ell \approx \rho_w$.

(VIII,5.1,b) Equation (8.1a) and (8.1b) are standard results which will probably require modification for scaling. (√)

(VIII,5.1,c)** Equation (8.2) should read

$$\frac{1}{r}\frac{\partial}{\partial r}\int_{y=0}^{h}(ru)dy + \left(\frac{\partial h}{\partial t}\right)_r = 0$$

However, the results which depend on (8.2) are correct.

(VIII,5.1,d)* Equation (8.4a) is an approximation to the momentum equation based on the assumption of small v_y. The authors do not discuss range of values of the velocity or its gradient in this approximation.

(VIII,5.1,e)* Equation (8.7a) is highly questionable in view of the absence of equation (8.7e).

(VIII,5.1,f)** Equation (8.7d) should read $h(R,t) = 0$.

(VIII,5.1,g) Equation (8.7e) is entirely missing. (X)

(VIII,5.1,h) Equation (8.9) is in accord with assumptions regarding the smallness of terms ignored in equations (8.4a) and (8.4b). (√)

(VIII,5.1,i)** Equation (9.2) should read (8.2) in sentence preceding (8.11).

(VIII,5.1,j) Equation (8.11) is consistent with (8.2) if the latter is correctly written. (√)

(VIII,5.1,k)* Equations (8.12a) and (8.12b) make no sense, although it does not seem to affect the final result.

(VIII,5.1,l)** Equation (8.14) should read

$$\frac{1}{\chi_1^2 \xi}\left[\frac{\partial}{\partial \xi}\left(\xi \frac{\partial \delta_1^4}{\partial \xi}\right)\right]_{\tau_1} = \left(\frac{\partial \delta_1}{\partial \tau_1}\right)_{\xi} - \frac{\xi}{\chi_1}\left(\frac{d\chi_1}{d\tau_1}\right)\left(\frac{\partial \delta_1}{\partial \xi}\right)_{\tau_1}$$

(VIII,5.1,m) The word "globl" should read "global" on line 14, p.90, and Eq. (8.2) should be (8.3).

(VIII,5.1,n) Equation (8.19) is in accord with the nonboundary layer treatment of viscous spreading. It is not clear from this treatment that this is the case, i.e., follows from (8.4b). (√)

(VIII,5.1,o)** Equation (8.22c) should read

$$R(t) = .8412\left[\frac{GV^3}{\nu \ell}\right]^{1/8} t^{1/8}$$

Surface Tension-Viscous Regime

(VIII,5.1,p)** Equation (8.24) should read

$$F_\psi = 2\pi \int_0^R r\,\psi\, dr$$

(VIII,5.1,q)** Equation (8.26b) should read

$$\frac{2}{3}\,\frac{1}{\chi}\left[\frac{1}{\xi}\frac{\partial}{\partial \xi}\,\xi v \delta\right]_{\tau} + \left(\frac{\partial \delta}{\partial \tau}\right)_{\xi} - \frac{\xi}{\chi}\frac{d\chi}{d\tau}\left(\frac{\partial \delta}{\partial \xi}\right)_{\tau} = 0$$

(VIII,5.1,r)** F_χ should be F_ψ on line 2, p. 93.

(VIII,5.1,s)* Initial condition δ = a delta function at $\tau = 0$ and $\chi = 0$ at $\tau = 0$ depends on model of initial spill which is not clear from text.

(VIII,5.1,t)** Equation at bottom of p. 93 should have constant 3/2 instead of 2/3 preceding bracket; f in integral should read f'.

(VIII,5.1,u)** In equation (8.35) the factor $\frac{3}{8\pi\Sigma_\ell}$ should read $\frac{3}{8\pi\tau\Sigma_\ell}$.

(VIII,5.1,v)** Equation (8.36a) should have $f(\xi)$ preceding radical sign and τ under radical in denominator.

(VIII,5.1,w)** Equation (8.36b) should read

$$\chi^2(\tau) = \sqrt{\frac{2\tau\Sigma}{3\pi}} \left\{ \frac{1}{\left[\int_0^1 \xi \, f(\xi) d\xi \int_0^1 \frac{\xi^2 d\xi}{f(\xi)} \right]^{1/2}} \right\}$$

(VIII,5.1,x)** Integral $\int_0^1 f \, d\xi$ should read $\int_0^1 \xi \, f d\xi$.

(VIII,5.1,y)** Values of C for $p = 1/2$ and $p = 3/4$ should read, respectively, 0.87 and 0.60.

(VIII,5.1,z)** $R(t)$ should be $R(t) = 1.05 \left[\frac{\sigma V}{\mu_\ell}\right]^{1/4} t^{1/4}$

Section 8.5.2, One-Dimensional Spread

Gravity-Inertia Regime

(VIII,5.2,a)** "Intertia" in title should be "Inertia."

(VIII,5.2,b)* There is a problem in defining the characteristic length when one goes to dimensionless form. Equations (8.38a) and (8.38b) will work if $L = 2W$ or $L^2 = A$, i.e., for volume conservation to hold.

Gravity-Viscous Regime

(VIII,5.2,c)** Equation (8.41a) should read

$$\frac{\partial p}{\partial x} = \mu_\ell \frac{\partial^2 u}{\partial y^2}$$

(VIII,5.2,d)* Equations (8.41a,b) and (8.42) are subject to the same comments as equation (8.4b) in statement (VIII,5.1,d). Again, this is not a boundary layer theory.

(VIII,5.2,e)** Equation (8.39b) should read

$$\frac{1}{\chi^2}\frac{\partial}{\partial\xi}\left(\frac{\partial\delta^4}{\partial\xi}\right)_{\tau_1} = \left(\frac{\partial\delta}{\partial\tau_1}\right)_{\xi} - \frac{\xi}{\chi}\frac{\partial\chi}{\partial\tau_1}\left(\frac{\partial\delta}{\partial\xi}\right)_{\tau_1}$$

(VIII,5.2,f)** Equation for C on bottom of p. 97 should have 0.2 rather than 0.6 for exponent.

(VIII,5.2,g)* In equation (8.46a) and beyond Γ_ℓ seems to be $L^3\ G/\nu_\ell{}^2$ for one-dimensional spread.

(VIII,5.2,h)* In equation (8.46c) there is a problem interpreting L. Here L^2 is A or $V/2W$.

Surface Tension-Viscous Regime

(VIII,5.2,i)* In the expression for ψ, we have the same problem interpreting the approximation for the momentum equation as in the radial case. See statement (VIII,5.1,d)*.

(VIII,5.2,j)** Equation (8.50b) should read

$$\frac{2}{3}\ \frac{1}{\chi}\left[\frac{\partial}{\partial\xi}(v\delta)\right]_{\tau} + \left(\frac{\partial\delta}{\partial\tau}\right)_{\xi} - \frac{\xi}{\chi}\ \frac{\partial\chi}{\partial\tau}\left(\frac{\partial\delta}{\partial\xi}\right)_{\tau} = 0$$

(VIII,5.2,k)* Again, there is difficulty in the initial condition δ = a delta function at $\tau = 0$. It does not affect result in any case.

(VIII,5.2,l)** For C in the case of $p = 1/4$, the value should be 1.45.

(VIII,6) *Section 8.6, Computational Algorithm (p.101)*

(VIII,6,a) A flow chart is shown in Figure 8.4 for the calculations. (√)

(VIII,7) *Section 8.7, Specific Example (pp.101-104)*

(VIII,7,a) Data all correct. (√)

(VIII,7,b)** Second crossover time should be $t_2 = 41.06$ hrs.

(VIII,8) *Section 8.8, Discussions (pp.104-105)*

(VIII,8,a) Derivations in chapter are rigorously true for spread of liquid on solid. (✓)

For small spills, the solution tends toward the solution where $\mu_\ell/\mu_w > 1$ as in Chapter 3. This is because surface tension and gravity tend to dominate the force picture. (✓)

Variations in viscosity and surface tension affect crossover times more than spread radius. (✓)

Solutions do not depend on water properties. (✓)

(VIII,8,b)* The most severe limitations of the model are threefold:

1) Failure to account for limiting effects of surface forces. For details, refer to (III,8,b)*.

2) Failure to use most sophisticated drag law available to evaluate viscous term, i.e., they omit boundary layer theory.

3) Does not conform to known liquid.

(VIII,9) *Section 8.9, Conclusions (p.105)*

(VIII,9,a) Theoretical formulas for spreading have been developed and discussed along with an illustrative example. (✓)

(VIII,9,b) Limitations of model have been cited. (✓)

(VIII,10) *Section 8.10, Reference (p.105)*

(VIII,10,a) The reference used in the chapter is listed. (✓)

(VIII,11) *Section 8.11, List of Symbols (pp.105-108)*

(VIII,11,a) A list of symbols and their meanings is presented. (✓)

(VIII,11,b)**For one-dimensional regime, Γ should be $L^3 G/\nu^2$.

(VIII,12) *Section 8.12, Appendices (pp.108-109)*

(VIII,12,a) Solutions to nonlinear differential equation (Appendix A) and to differential equation (Appendix B) are given. (✓)

F(VIII,1) *Figure 8.1 (p.87), Details of the Spreading Model*

F(VIII,1,a) Figure 8.1 gives details of the hydrodynamic picture of the spreading model. (√)

F(VIII,2) *Figure 8.2 (p.87), Control Volume*

F(VIII,2,a) Figure 8.2 gives details of the control volume depicting mass and momentum conservation during spill spread. (√)

F(VIII,3) *Figure 8.3 (p.102), Dimensionless Spread Radius for Various Regions*

F(VIII,3,a)** The following Table (VIII,1) is a listing of the calculated values of τ_1, τ_2, X_1, and X_2 versus their values as given in Figure 8.3 of AMSHAH.

TABLE (VIII,1)

	τ_1		τ_2		X_1		X_2	
	Calculated	From Figure 8.3	Calculated	From Figure 8.3	Calculated	From Figure 8.3	Calculated	From Figure 8.3
$\Gamma_\ell = 1 \times 10^3$; $\Sigma_\ell = 10$	44.46	46	1.697×10^3	1,700	7.60	7.5	11.98	12
$\Gamma_\ell = 5 \times 10^3$; $\Sigma_\ell = 50$	130.07	150	1.697×10^3	2.250	13.00	13.5	17.92	17
$\Gamma_\ell = 10 \times 10^3$; $\Sigma_\ell = 100$	206.52	220	1.697×10^3	2,150	16.38	18	21.31	20.5

F(VIII,4) *Figure 8.4 (p.103), Flow Chart for the Calculation of Extent of Spread of a Low-Viscosity Liquid on Water*

F(VIII,4,a) Flow chart is shown. (√)

T(VIII,1) *Table 8.1 (p.110), Dimensional Equations of Spread*

T(VIII,1,a) Regimes of Spread→ / Geometry ↓	Gravity-Inertia	Gravity-Viscous	Viscous-Surface Tension
One-Dimensional	✓	✓	✓
Radial	✓	✓	✓

T(VIII,2) *Table 8.2 (p.111), Nondimensional Equations of Spread*

T(VIII,2,a) Regimes of Spread→ / Geometry ↓	Gravity-Inertia	Gravity-Viscous	Viscous-Surface Tension
One-Dimensional	✓	✓	✓
Radial	✓	✓	✓

B. CRITIQUE OF THE MODEL (Chapter 8)

The crucial aspect of the model for a "low-viscosity" liquid is contained in equation (8.8)

$$G \frac{\partial \delta}{\partial r} = \nu_\ell \frac{\partial^2 v}{\partial y^2} \qquad \text{(VIII-1)}$$

which is the Navier-Stokes equation without the inertial term. This leads to a thickness profile

$$\delta^2 \left(1 - \frac{r^2}{R^2}\right)^{1/3} \qquad \text{(VIII-2)}$$

as in equation (8.21) and a radial spread rate of

$$R \sim t^{1/8} \qquad \text{(VIII-3)}$$

as in (8.22c) and (8.22d). This is in contrast to the Fannelop-Waldman model[2] used in Chapter 3--ostensibly for high-viscosity liquids--where

$$\delta^2 \left(1 - \frac{r^2}{R^2}\right)^{1/2} \qquad \text{(VIII-4)}$$

and

$$R \sim t^{1/4} \qquad \text{(VIII-5)}$$

The Fannelop-Waldman model is based on boundary layer theory where one considers the effect of the inertial terms in the Navier-Stokes equation. AMSHAH does not make clear why relations (VIII-1) to (VIII-3) should be preferable to (VIII-4) and (VIII-5) for a low-viscosity liquid.

The final stage of pool spread, as described in both the models (Chapters 3 and 8), is predicated on the fact that the pool will continue to grow indefinitely. This occurs because of the use of a surface tension-viscous dynamical balance which neglects the effect of gravity. However, even in the Fannelop-Waldman treatment, it is recognized that the problem is not simple and that empirical verification is necessary.

They do not, however, consider the case where a limiting pool radius is possible. Nevertheless, there is ample evidence that such a limit will occur, on purely experimental grounds. Theoretically one would predict a limiting pool radius of the order[3]

$$\sqrt{\frac{V}{2\pi\delta}}$$

with δ given by

$$\sqrt{\frac{4\sigma}{g\rho}}$$

The effect of such a limiting radius will be enhanced if one has a pool which evaporates at a relatively substantial rate. In any case, it is unlikely that in a realistic situation the pool will grow indefinitely and that a criterion for a limiting radius is a desirable feature of any complete model.

C. *SENSITIVITY ANALYSIS (Chapter 8)*

A standard approach[4] that is suitable for these relationships is that of assuming that one has a dependent variable f which is defined in terms of a field of independent variables

$$f_i = \phi_i(X_j) \qquad \text{(VIII-6)}$$

More explicitly, it is better to set

$$\ln f_i = \ln \phi_i (\ln X_j)$$

with

$$\frac{1}{f_i} df_i = \Sigma \frac{\partial \ln \phi_i}{\partial \ln X_j} \frac{dX_j}{X_j} \qquad \text{(VIII-7)}$$

Then

$$\frac{\partial \ell n \phi_i}{\partial \ell n X_j}$$

represents a matrix connecting the field of dependent fraction increments df_i/f_i with the independent ones dX_i/X_i .

What makes our results most amenable to simple calculation is the fact that the dependent variables f_i are expressed as products of the independent ones

$$f_i = \phi_i = \prod_j X_j^{n_{ij}} \qquad \text{(VIII-8)}$$

so that

$$\frac{\partial \ell n \phi_i}{\partial \ell n X_j} = n_{ij} \qquad \text{(VIII-9)}$$

Then one could obtain a composite estimate of the overall sensitivity by setting[4]

$$\left|\frac{df_i}{f_i}\right| = \left[\sum_j \left(n_{ij} \frac{dX_j}{X_j}\right)^2\right]^{1/2} \qquad \text{(VIII-10)}$$

There is also the problem of errors introduced by varying the exponents. This is best handled using the techniques of regression analysis.

In the absence of any noteworthy singularities in the equations themselves (such as vanishing denominators or exponents containing independent variables), we can consider the following salient features of any sensitivity analysis.

a) There are discrete discontinuities in the logarithmic derivatives at the points of inflection t_1 and t_2 as defined in Table (VIII,1). A detailed investigation of these singularities is unwarranted, since these are precisely the regions where the model is no longer valid.

b) An unbiased indicator of the relative effect of each of the independent variables can best be obtained by assuming that all the $\delta X_j/X_j$ in (VIII-10) are equal. Then the relative effect of each variable, say the y^{th} variable, on the i^{th} dependent factor would be

$$S_{ij} = \frac{n_{ij}}{\left(\sum_j n_{ij}^2\right)^{1/2}} \qquad \text{(VIII-11)}$$

c) It may turn out that one independent variable is more likely to be unmeasurable or undefined than others. Then, if we assume all other independent variables to be determined with reasonable precision,

$$\frac{df_i}{f_i} \approx n_{ij} \frac{dX_j}{X_j} \qquad \text{(VIII-12)}$$

As an example, consider the formulas in Table 8.1 of Chapter 8 in AMSHAH. There are five dependent variables (we discuss the radial case only):

R_{IG}	the radius in the inertia-gravity regime	- f_1
R_{GV}	the radius in the gravity-viscous regime	- f_2
R_{VT}	the radius in the viscous-surface tension regime	- f_3
t_1	the time for changeover from the gravity-inertia to the gravity-viscous regime	- f_4
t_2	the time for changeover from the gravity-viscous to the viscous-surface tension regime	- f_5

In addition, we might have two other dependent variables:

R_1		- f_6
R_2		- f_7

where R_1 and R_2 are the respective crossover radii for the separate regimes.

For our independent variables, we choose:

V	the spill volume	- x_1
t	the time	- x_2
$J = \rho_\ell G$	an effective gravitational constant (normalized to the density of liquid)	- x_3
ρ_ℓ	the density of liquid	- x_4
μ_ℓ	the viscosity of liquid	- x_5
σ	the surface tension	- x_6
C_{IG}	the constant 1.14 appearing in the equation for r in the inertia-gravity case	- x_7
C_{GV}	the constant 0.8412 appearing in the equation for r in the gravity-viscous case	- x_8
C_{VT}	the constant 1.05 appearing in the equation for r in the viscous-surface tension case	- x_9

The choice of V and t as independent variables is self-explanatory. Note also that

$$J = \frac{\rho_\ell (\rho_w - \rho_\ell) g}{\rho_w} \qquad \text{(VIII-13)}$$

so that

$$\frac{\delta J}{J} = \frac{\delta \rho_\ell}{\rho_\ell} \frac{\rho_w - 2\rho_\ell}{\rho_w - \rho_\ell} \qquad \text{(VIII-14)}$$

and small errors in the estimate of liquid density may be magnified several times in the resulting formulas if $\rho_w \simeq \rho_\ell$.

At the same time, the values of viscosity and surface tension used in these formulas are not necessarily the static published values (presumably determined with reasonably good precision) but dynamical quantities which may not even be constant in time. We thus include them among the independent variables. The last three independent variables are the same semiempirical constants used in the model.

In order to proceed with our analysis, we must rewrite the formulas that appear in Table 8.1 in Chapter 8 of AMSHAH in terms of these variables. This is shown in Table (VIII,2). One can then construct a matrix of the sensitivity parameters n_{ij} as in Table (VIII,3). One can draw several general conclusions from these results.

Thus, by inspecting the first row of Table (VIII,3), one finds that the percentage error in pool radius is equally likely to result from errors in V, J, ρ_ℓ respectively, but twice as likely from an equal error in t; that, if all errors are random, there is a 5% likelihood for it to arise from V, J, ρ_ℓ, but a 70% likelihood for it to arise from C_{IG}, etc.

One should not draw too many far-reaching conclusions from these results, since we do not know that the errors are random. For example, the constants C_{IG}, C_{GV}, C_{VT} depend most certainly on size and geometry (though their ratios may be volume- and shape-independent). The greatest practical difficulty is that of not knowing the initial condition of the spill. Thus, the radius in the gravity-inertia stage will start from a small value (presumably close to zero) and grow to a large value given by

$$R_1 = \left(\frac{C_{GV}{}^4}{C_{IG}}\right)^{1/3} \left(\frac{J\rho_\ell V^5}{\mu_\ell{}^2}\right)^{1/12} \qquad \text{(VIII-15a)}$$

TABLE (VIII,2)

DIMENSIONAL EQUATIONS FOR RADIAL SPREAD WITH LOW VISCOSITY

Gravity-Inertia Regime	Gravity-Viscous Regime	Viscous-Surface Tension Regime
$0 < t < \left(\frac{C_{GV}}{C_{IG}}\right)^{8/3} \left(\frac{V\rho_\ell^2}{J\mu_\ell}\right)^{1/3}$	$\left(\frac{C_{GV}}{C_{IG}}\right)^{8/3} \left(\frac{V\rho_\ell^2}{J\mu_\ell}\right)^{1/3} \leq t \leq \left(\frac{C_{GV}}{C_{VT}}\right)^{8} \left(\frac{JV\mu_\ell}{\sigma^2}\right)$	$t > \left(\frac{C_{GV}}{C_{VT}}\right)^{6} \left(\frac{JV\mu_\ell}{\sigma^2}\right)$
$r = C_{IG} \left(\frac{JV}{\rho_\ell}\right)^{1/4} t^{1/2}$	$r = C_{GV} \left(\frac{JV^3}{\mu_\ell}\right)^{1/8} t^{1/8}$	$r = C_{VT} \left(\frac{\sigma V}{\mu_\ell}\right)^{1/4} t^{1/4}$
$0 < r < \left(\frac{C_{GV}^4}{C_{IG}}\right)^{1/3} \left(\frac{JV^5\rho_\ell}{\mu_\ell^2}\right)^{1/12}$	$\left(\frac{C_{GV}^4}{C_{IG}}\right)^{1/3} \left(\frac{JV^5\rho_\ell}{\mu_\ell^2}\right)^{1/12} \leq r \leq \frac{C_{GV}^2}{C_{VT}} \left(\frac{JV^2}{\sigma}\right)^{1/4}$	$r > \frac{C_{GV}^2}{C_{VT}} \left(\frac{JV^2}{\sigma}\right)^{1/4}$

TABLE (VIII,3)

MATRIX OF SENSITIVITY PARAMETERS (n_{ij}) FOR RADIAL SPREAD OF A POOL

Dependent Variable	Independent Variable									$\left(\sum_j n_{ij}^2\right)^{1/2}$
	V	t	J	ρ_ℓ	μ_ℓ	σ	C_{IG}	C_{GV}	C_{VT}	
R_{IG}	1/4	1/2	1/4	-1/4	0	0	1	0	0	1.20
R_{GV}	3/8	1/8	1/8	0	-1/8	0	0	1	0	1.0897
R_{VT}	1/4	1/4	0	0	-1/4	1/4	0	0	1	1.1180
t_1	1/3	0	-1/3	2/3	-1/3	0	8/3	8/3	0	3.8730
t_2	1	0	1	0	1	-2	0	8	-8	11.6190
R_1	5/12	0	1/12	1/12	-1/6	0	-1/3	4/3	0	1.4506
R_2	1/2	0	1/4	0	0	1/4	0	2	1	2.3184

Note: To determine the percentage error in a given output or dependent variable, i, caused by a given error in an input or independent variable, j, multiply the matrix entry, n_{ij}, by the error in the independent variable, j. For example, if the error in R_{VT}, the radius of spread in the viscous-surface tension regime is sought due to error in C_{VT}, the spread constant pertaining therein, one looks to the entry in the third row (i=3) and ninth column (j=9). In this case, n_{39}=1, and thus a 5% error in C_{VT} will cause a 5% error in R_{VT}. The percentage of the total error caused by variance in C_{VT} is $(1/1.12)^2$ or 79%.

where a point of inflection occurs. Now, if we assume that the initial radius R_0 is of the order $V^{1/3}$

$$\frac{R_1}{R_0} \sim \left(\frac{C_{GV}{}^4}{C_{IG}}\right)^{1/3} \left(\frac{J\rho_\ell V}{\mu_\ell{}^2}\right)^{1/12} \qquad \text{(VIII-15b)}$$

For propylacetate, of density 88 kg/m^3, μ_ℓ = .59 centipoise, σ = 24.3 dynes/cm, we find

$$\frac{R_1}{R_0} \sim .56\ V^{1/12} \qquad \text{(VIII-15c)}$$

where V is in m^3. Thus, for this ratio to be of order 10, one must have a spill of volume 10^{15} m^3. Hence, again the result of (VIII-15b) will not be an asymptotic limit even for the largest spills. Ignoring the initial geometry of the spill is thus unfortunate, considering the inherent character of the model which is based on asymptotic solutions.

In the light of these circumstances, it is proposed that a completely different approach to the problem of scaling and experimental design be attempted. Since, as discussed earlier, the parameters μ and σ may not necessarily be inputs to the model, we can simplify the analysis of the sensitivity studies using some results of dimensional analysis.(5) Thus, consider the parameters R_1, R_2, t_1, t_2. These are given in Table (VIII,2). Note, however, that they are not independent since again they are connected by a relation involving t_1 and t_2. Since the spread law in the gravity-viscous regime is $R \sim t^{1/8}$, we must have

$$\frac{R_2}{R_1} = \left(\frac{t_2}{t_1}\right)^{1/8} \qquad \text{(VIII-16)}$$

Thus, there will be six separate dependent variables, R_{IG}, R_{GV}, R_{VT}, along with R_1, t_1, R_2/R_1 where

$$\frac{R_2}{R_1} = \left(\frac{C_{GV}{}^2 C_{IG}}{C_{VT}{}^3}\right)^{1/3} \left(\frac{J^2 V \mu_\ell{}^2}{\rho_\ell \sigma^3}\right)^{1/12} \qquad \text{(VIII-17)}$$

Note that this ratio has a weak dependence on V. For example,(6) using propylacetate of S.G. 0.88, one obtains

$$\frac{R_2}{R_1} = 0.14\ V^{1/12} \qquad \text{(VIII-18)}$$

where V is in m^3. One thus notes that R_2/R_1 will range in values from 0.14 for very small spills (of order 1 m^3) to 0.45 for very large spills where $V \sim 10^5$. Evidently this parameter is not very sensitive to spill volume. These parameters can be identified by observing the

turning points in the logarithmic derivative of the pool growth rate. (According to the AMSHA model, there should be two such points.) Then from Table (VIII,2) we could propose the following dimensionless equations. For the gravity-inertia regime

$$\lambda = \tau^{1/2} \qquad \text{(VIII-19a)}$$

for $0 < \tau < 1$; for the gravity-viscous regime

$$\lambda = \tau^{1/8} \qquad \text{(VIII-19b)}$$

for $1 < \tau < (R_2/R_1)^8$; and for the viscous-surface tension regime

$$\lambda = (R_1/R_2)(t/t_1)^{1/4} \qquad \text{(VIII-19c)}$$

Here

$$\lambda = R/R_1 \qquad \text{(VIII-19d)}$$

Since we expect the model to be valid in the asymptotic limit, in spite of its shortcomings this seems to be the best procedure for verifying the model and checking out the scaling laws. An improvement, of course, would consist of taking initial conditions of the spill into account and incorporating them as parameters, but this is difficult if not impossible.

D. HACS ERROR ANALYSIS (Chapter 8)

In this section, we explicitly list each HACS Fortran statement at variance with its parent mathematical expression as stated in Chapter 8, "Spreading of a Low-Viscosity Liquid on a High-Viscosity Liquid," in AMSHAH.

MODT obtains data from the subroutines FRCL and IRCL and computes the spread of an immiscible liquid on the water surface at any time after the spill for a liquid with a boiling point greater than the ambient temperature. There is a provision to calculate the size of the spill for the channel spread as well as for the radial spread. It calls subroutines BEGPR, FRCL, IRCL, EPRNT, RLJSP, ENDPR. All these subroutines have been checked for errors.

MODT:

For obtaining surface tension of a liquid in seawater, MODT uses the relation:

surface tension = |72.8 - surface tension of liquid|

where 72.8 dynes/cm is taken as the surface tension of water against air. This value corresponds to the surface tension of water in air at 20°C. However, this value does vary with temperature. At 10°C, it is 74.22 and at 50°C it is 67.91.

There are no errors in this subroutine.

RLJSP:

If $\mu_L > .2\ \mu_W$, this subroutine uses the equations of Chapter 3 of AMSHAH for calculating the size of the spread of the spilled liquid at any time; and, if $\mu_L < .2\ \mu_W$, the equations given in Chapter 8 are used. However, in many cases, agreement between the equations used in this subroutine and those given in Chapters 3 or 8 is lacking.

LN0037 45 IF(T-(.972*A**.75/SQRT(B))**2.66666)50,50,55
RLJSP checks if $\tau \leq 0.927\ \Gamma_W^2/\Sigma_W^{4/3}$ for gravity-viscous regime while the corresponding equation in AMSHAH (p.27) is $\tau \leq 0.989\ \Gamma_W^2/\Sigma_W^{4/3}$.

LN0040 55 S=1.43*SQRT(B/A)*T**.75
RLJSP uses $\chi = 1.43\ \Sigma_L^{1/2}/\Gamma_L^{1/2} * \tau^{3/4}$ for viscous-surface tension regime while AMSHAH (p.111) gives $\chi = 1.2\ \Sigma_L^{1/3}\tau^{1/3}$.

LN0051, 0052 C...START CALCULATIONS FOR THE CASE WHEN THE LIQUID VISCOSITY IS LESS THAN THE VISCOSITY OF WATER

should be: C...START CALCULATIONS FOR THE CASE WHEN THE LIQUID VISCOSITY IS LESS THAN ONE-FIFTH THE VISCOSITY OF WATER

LN0057 90 IF(T-(.81*A**.4)**(15./7.))40,40,100
RLJSP checks if $\tau < 0.6366\ \Gamma_L^{6/7}$ for gravity-inertia regime while the corresponding equation of AMSHAH (p.111) is $\tau < 0.644\ \Gamma_L^{3/14}$.

LN0058 100 IF(T-(.90*A**.4/B**.333333)**7.5)105,105,110
RLJSP checks if $\tau < 0.4537\ \Gamma_L^{3.0}/\Sigma_L^{5/2}$ for gravity-viscous regime while the corresponding equation of AMSHAH (p.111) is $\tau \leq 0.645\ \Gamma_L^{3/4}/\Sigma_L^{5/2}$.

LN0059 105 S=1.13*A**.4*T**.2
RLJSP uses $\chi = 1.13\ \Gamma_L^{2/5}\tau^{1/5}$ for gravity-viscous regime while AMSHAH (p.111) gives $\chi = 1.132\ \Gamma^{1/10}\tau^{1/5}$.

LN0061 110 S=1.26*(B*T)**.333333
RLJSP uses $\chi = 1.26\ \Sigma_L^{1/3}\tau^{1,/3}$ for viscous-surface tension regime while AMSHAH (p.111) gives $\chi = 1.2\ \Sigma_L^{1/3}\tau^{1/3}$.

LN0064 115 IF(T-(.685*A**.25)**2.66666)65,65,125
RLJSP checks if $\tau \leq 0.3646\ \Gamma_L^{2/3}$ for gravity-inertia regime while the corresponding equation of AMSHAH (p.111) is $\tau < 0.4446\ \Gamma_L^{2/3}$.

LN0065 125 IF(T-(.735*(A/B)**.25)**8)130,130,135
RLJSP checks if $\tau \leq 0.08517\ \Gamma_L^2\ \Sigma_L^2$ for gravity-viscous regime while the corresponding equation of AMSHAH (p.111) is $\tau \leq 0.1697\ \Gamma_L^2/\Sigma_L^2$.

LN0066 130 S=.78*A**.25*T**.125
RLJSP uses $\chi = 0.78\ \Gamma_L^{1/4}\tau^{1/8}$ for viscous-gravity regime while AMSHAH (p.111) gives $\chi = 0.8412\ \Gamma_L^{1/4}\tau^{1/8}$.

LN0068 135 S=1.062*(B*T)**.25
RLJSP uses $\chi = 1.062\ \Gamma_L^{1/4}\tau^{1/4}$ for viscous-surface tension regime while AMSHAH (p.111) gives $\chi = 1.05\ \Sigma_L^{1/4}\tau^{1/4}$.

There are no errors in the subroutines BEGPR, FRCL, IRCL, EPRNT, and ENDPR.

E. SUMMARY OF RESULTS

The model described in Chapter 8 of AMSHAH has been reviewed with the following conclusions.

1) There are many minor errors in the text involving numerical data and formulas. These have been cited and the corrections indicated.

2) Except for the erroneous cases noted in (1) above, all formulas and calculations have been checked and found to be correct.

3) Several questionable assumptions in the analysis and modeling have been noted. Among these, the most salient ones are:

a) The parameter σ used in Chapter 8 of AMSHAH may not be valid and may have to be determined empirically as suggested by Fannelop and Waldman.

b) Boundary layer theory as used in Chapter 3 of AMSHAH would have given a better spread law ($t^{1/4}$) in the gravity-viscous regime, and in addition its application would require no artificial dynamical basis for distinguishing high-viscosity liquids from low-viscosity ones.

c) The liquid pool will not spread indefinitely as assumed in Chapter 8. The model gives us no insight into the ultimate extent of the pool. Also, the description of the late stages of pool growth may be highly unrealistic.

d) The boundary conditions assumed are questionable in view of the fact that one assumes asymptotic solutions in the modeling. Also, the Fannelop-Waldman constants used in the AMSHAH model are semiempirical and may not scale up properly, particularly if the boundary conditions are not suitable.

4) A sensitivity study was undertaken, and it was concluded that, in view of the limitations of the model noted in (3) above, it would be best to parameterize the pool growth at the identifiable points of inflection and scale the model accordingly. The subsequent scaling factors would then be highly insensitive to spill volume but sensitive to R_1, R_2, t_1, etc.

F. RECOMMENDATIONS

1) A review of the underlying assumptions involved in viscous spread ought to be undertaken for the purpose of drawing up a rigorous distinction between high-viscosity and low-viscosity flows.

2) A more careful analysis of the spread rate involving surface forces is needed, particularly with regard to determining ultimate limits of pool growth.

3) In the case where parameters entering the model are not well defined, a more careful distinction should be made between data and observed results. Should there be an impasse on this point, one can always reformulate the model and propose an experimental design as has been done in Section C (Sensitivity Analysis), so that the model will scale up properly in spite of its limitations.

G. TABLE OF SYMBOLS USED

A = area of pool

f = dependent variable in sensitivity studies

F_σ = total spreading force due to surface tension

F_ψ = total viscous resistive force against spreading

g = gravitational constant

G = effective gravitational constant $G = g(\rho_w - \rho_\ell)/\rho_w$

J = force density used in sensitivity studies $J = G\rho_\ell$

L = length scale used in AMSHAH models $L = V^{1/3}$

R = radius of pool

T = time scale used in AMSHAH models $T = \sqrt{L/G}$

u = lateral velocity; for radial growth $u = \dot{r}$

v = velocity

V = volume

W = width of channel

x = lateral spread variable; for radial growth $x \equiv r$; in sensitivity studies, x is the independent variable

X = leading edge variable; for radial growth $X = R$

Γ = dimensionless coefficient of viscosity used in AMSHAH models $\Gamma = [L^3 G/V_w^2]^{1/4}$

λ = dimensionless radial extent of pool used in sensitivity studies, $\lambda = R/R_1$

Λ = viscous force

μ = coefficient of viscosity

ρ = mass density

σ = surface tension

Σ = dimensionless surface tension used in AMSHAH models $\Sigma = \sigma \mu_w \sqrt{GL}$

ξ = nondimensional distance in spread direction

χ = nondimensional distance of the spread front from the point of spill

τ = dimensionless time

Subscripts

w = water

ℓ = liquid

H. *LIST OF REFERENCES*

(1) Raj, P. P. K., and A. S. Kalelkar. *Spreading of a low-viscosity liquid on a high-viscosity liquid*, ch. 8, pp. 85-111. *In Assessment Models in Support of the Hazard Assessment Handbook*, Report No. CG-D-65-74, prepared by Arthur D. Little, Inc. for the Department of Transportation, NTIS Document No. AD776617, January 1974.

(2) Fannelop, T. K., and G. D. Waldman. Dynamics of oil slicks, *AIAA Journal 10*(4):506-510, 1972.

(3) This result can be obtained from Laplace's equation. See, for example, Levich, V. G., *Physicochemical Hydrodynamics*, p. 378. Prentice-Hall, Englewood Cliffs, N.J., 1962.

(4) Beers, Y. *Introduction to the Theory of Errors*, pp. 26-35. Addison Wesley Publishing Co., Reading, Mass., 1953.

(5) Duncan, W. J. *Physical Similarity and Dimension Analysis*, ch. V. Edward Arnold & Co., London, 1953.

(6) Weast, R. C. (ed.). *Handbook of Physics and Chemistry*, 53rd ed., p. F41. Chemical Rubber Publishing Co., Cleveland, Ohio, 1972-73.

Chapter 5

"SIMULTANEOUS SPREADING AND EVAPORATION
OF A CRYOGEN ON WATER"
(Chapter 9 of AMSHAH)

INTRODUCTION

The spreading model given in this chapter treats the evaporation of liquid concurrently with the spread of the liquid. Such materials would, of course, principally include the cryogens. In contrast, the spread models of Chapters 3 and 8 of AMSHAH explicitly assume mass conservation for the duration of the spread.

It is perhaps obvious, but it should be recalled that the heat available for vaporization must come from the water and thus the possibility of ice formation presents itself.

A. *REVIEW OF TEXT (Chapter 9)* (1)

(IX,1) *Section 9.1, Aim (p.113)*

(IX,1,a) The aim of the derivation given in this chapter is to obtain the spread rate, time for complete evaporation, and maximum extent of spread of cryogenic spill on water. (√)

(IX,2) *Section 9.2, Introduction (p.113)*

(IX,2,a) Model description is given. (√)

(IX,3) *Section 9.3, Assumptions (pp.113-114)*

(IX,3,a) The liquid spilled is lighter than water and immiscible. (√)

(IX,3,b) The heat for evaporation comes primarily from water. (√)

(IX,3,c) The spread area is a continuous mass of liquid at every instant. (√)

(IX,3,d)* That spill occurs instantaneously is an assumption that is not physically valid yet mathematically tenable.

(IX,3,e) Properties of both liquid and water do not change during the spread. (√)

(IX,4) *Section 9.4, Data Required (p.114)*

(IX,4,a) Physical properties of the cryogenic liquid, such as density, boiling temperature, viscosity, etc. (√)

(IX,4,b)* Whether ice forms or not is a question that can only be resolved by experiment at the present state of the theoretical art.

(IX,4,c) Water and/or ice physical properties. (√)

(IX,4,d) Value of the boiling transfer coefficient between liquid and water (or ice), or equivalently the heat flow from water to liquid. (√)

(IX,4,e) Properties of liquid are constant during spread. (√)

(IX,5) *Section 9.5, Model Details (pp.114-128)*

Section 9.5.1, Radial Spreading

(IX,5.1,a) Equations (9.1), (9.2), (9.3a), (9.4a), and (9.5a) are correct under the *global* rather than local assumptions given. To do this under local continuity conditions is, as stated in the text, difficult but feasible. (√)

(IX,5.1,b)* Equations (9.3b), (9.4b), and (9.5b) are correct if

$$\Delta = \dot{q}/q_{ch} \quad \text{where} \quad q_{ch} = \rho\lambda\sqrt{LG}$$

(IX,5.1,c)** What was to have been evidently equation (9.4c) should read:

$$\frac{d}{d\tau}\left[\chi^3 \frac{dx^2}{d\tau^2}\right] = \frac{\Delta}{C}\chi^2$$

(IX,5.1,d) Equation (9.6) is algebraically correct. (√)

(IX,5.1,e)* Equation (9.7), while algebraically correct, is based on assumptions that may be somewhat tenuous.

(IX,5.1,f)** Following equation (9.9), the reference should be to Eq. (9.3b) rather than (8.3b).

(IX,5.1,g)** The right-hand side of equation (9.10) should be:

$$C\,\frac{\frac{1}{2}\left(B-\frac{\Delta}{C}\tau^2\right)^2-\left(\frac{2\Delta}{C}\right)\left(B\tau^2+\frac{\Delta}{3C}\tau^4\right)}{2\left(B\tau+\frac{\Delta\tau^3}{3C}\right)}$$

(IX,5.1,h) Equations (9.14b) and (9.15b) are correct as given. (√)

(IX,5.1,i)** Equation (9.17) should read

$$\sqrt{\tau_C}=\frac{\Gamma\left[1-2.04\,\tau_C^2\Delta-0.3473\,\tau_C^4\Delta^2\right]}{\pi\left[1.3\,\tau_C+0.442\,\tau_C^3\Delta\right]}$$

(IX,5.1,j)* Note that, again, the neglect of inertial forces comes into play via equation (9.18). The authors do not use boundary layer theory.

(IX,5.1,k) Equation (9.19) is missing. (X)

(IX,5.1,l)** Equation (9.20) should have plus sign in place of minus sign on right-hand side.

(IX,5.1,m)** Equation (9.22) should have a parenthesis after the θ_{cr} term.

(IX,5.1,n)* Equation (9.26a) is based on assumption regarding t which has to be user input.

(IX,5.1,o)** Equation (9.31) should have the exponent 1/6 on the bracketed term of the right-hand side, and 5/12 on V_i .

(IX,5.1,p)** Equation (9.36) should have a plus sign within the bracketed term, rather than a minus sign.

(IX,5.1,q)** Equation (9.39) is missing an integral sign.

(IX,5.1,r)** The denominator on right-hand side of equation (9.46) should be $[1.39\ \tau_c^{2/3} + 0.0966\ \tau_c^{7/3}\ \Delta]$.

Section 9.5.2, One Dimensional Spreading

(IX,5.2,a) All equations in the one-dimensional spread section are correct based on assumptions given. (✓)

(IX,6) *Section 9.6, Computational Algorithm (pp.128-129)*

(IX,6,a) A flow chart is shown in Figure 9.3 for the calculation of Chapter 9 of AMSHAH. (✓)

(IX,7) *Section 9.7, Specific Example (pp.130-131)*

(IX,7,a)** Volume spilled should be 2.353×10^4 m^3.

(IX,7,b)** Characteristic velocity, U_{ch}, should be 12.68 .

(IX,7,c)** Characteristic heat should be 27.527×10^5 kW/m .

(IX,7,d)** Δ should be 3.437×10^{-5}.

(IX,7,e)** τ_c should be 107.1 .

(IX,7,f)** k_c should be 0.142 .

(IX,7,g)** χ_c should be 12.57 .

(IX,7,h)** τ_e should be 115.02 .

(IX,7,i)** χ_{max} should be 13.14 .

(IX,7,j)** For gravity-viscous regime, τ_e should be 115.35 .

(IX,7,k)** For gravity-viscous regime, X_{max} should be 12.69 .

(IX,8) *Section 9.8, Discussions (pp.131-133)*

(IX,8,a) Note is made of difficulty of obtaining instantaneous release which is not recognized by model. (√)

(IX,8,b) Note is made that true heat transfer rate between water and cryogen is a function of temperature difference between them. (√)

(IX,8,c)* The observation is recorded that a continuous sheet of ice is unlikely to form during a cryogenic spill but rather ice in the form of patches. It is generally agreed in cryogenic circles that the only way one can produce a solid ice sheet is to cause the spill to occur in such a manner that the entire surface of water is covered, at least in a local area. Such a condition is unforeseeable in a marine accident, unless it were to occur in drydock.

(IX,8,d)* The effect of heat transfer on the spread radius is claimed to be small. This may not be the case in actual practice, especially when nucleate boiling takes place.

(IX,9) *Section 9.9, Conclusions (p.133)*

(IX,9,a) Equations have been developed to predict the evaporation rate, extent of spread, and time for evaporation of a cryogen on water, for both radial and linear configurations. (√)

(IX,9,b) Model limitations have been discussed and examples given. (√)

(IX,9,c) Validity of all equations not proven due to lack of experimental data; although they are based on sound physical phenomena and theoretical solutions. (√)

(IX,10) *Section 9.10, References (p.134)*

(IX,10,a) References used in report are listed. (√)

(IX,11) *Section 9.11, List of Symbols (pp.134-136)*

(IX,11,a) A list of symbols along with definitions is presented. (√)

F(IX,1) *Figures 9.1a and 9.1b (p.115)*

F(IX,1,a) Figure 9.1a, Spreading and Evaporating Liquid - Thickness of the Film at Various Times, is depicted as showing the actual flow configuration. (√)

F(IX,1,b) Figure 9.1b, The Mean Thicknesses of the Liquid Film Used in the Model at Various Times, is depicted as representing flow as seen from standpoint of model. (√)

F(IX,2) *Figure 9.2 (p.128)*

F(IX,2,a) Figure 9.2, Elliptical Profile for Ice Thickness, depicts geometry of ice formation, should it occur during spill. (√)

F(IX,3) *Figure 9.3 (p.129)*

F(IX,3,a) Flow Chart of Computer Program is shown in Figure 9.3 . (√)

F(IX,4) *Figure 9.4 (p.132)*

F(IX,4,a)* Figure 9.4, Volume & Radius of LNG Spreading on Water, is the result of the calculation of Section 9.7. Since this is in error, the locus of points for both the volume and radius as a function of time is also in error.

T(IX,1) *Table 9.1 (p.137), Radial Spread of a Cryogenic Liquid on Water*

T(IX,1,a) Spread Regimes →	Gravity-Inertia	Gravity-Viscous
One-Dimensional		
Without Ice	(√)	(√)
With Ice	(√)	(√)
Radial		
Without Ice	(X)	(√)
With Ice	(X)	(X)

T(IX,1,b)** In Table 9.1, gravity-inertia regime, radial spread k should read for no ice condition,

$$k = 1 - 2.04\ \tau^2\Delta - 0.347\ \tau^4\Delta^2$$

and for ice condition,

$$k = 1 - 0.867\ \alpha\ \tau^{3/2} - 0.4716\ \alpha^2\ \tau^3$$

T(IX,1,c)** In Table 9.1, in the equations for τ_c for $\mu_\ell/\mu_w \gg 1$ as well as for $\mu_\ell/\mu_w \ll 1$, the term $(+.347\ \tau_c^4\ \Delta^2)$ in the numerator on the right-hand side of the equations should read $(-.347\ \tau_c^4\ \Delta^2)$.

T(IX,2) *Table 9.2 (p.137), One-Dimensional Spread of a Cryogenic Liquid on Water Surface*

T(IX,2,a)** In Table 9.2, $\tau_c^{1/2}$ should read for the case $\dfrac{\mu_\ell}{\mu_w} \ll 1$,

$$\Gamma_\ell\ \frac{(1 - 0.834\ \tau_c^{5/3}\Delta - 0.029\ \tau_c^{10/3}\Delta^2)}{(1.39\ \tau_c^{2/3} + 0.0966\ \tau_c^{7/3}\Delta)}$$

B. *CRITIQUE OF MODEL (Chapter 9)*

The model of Chapter 9 is based on the conservation laws for momentum and mass in the approximate phenomenological limit. Thus, the force conservation law, equation (9.3a), employs the assumption that the inertial term is proportional to the second time derivative of the pool radius. The mass conservation law, equation (9.4a), employs the assumption that the heat flux is approximately constant. These assumptions, though not essential, are reasonable and fair ones provided they are employed properly.

Starting with equations (9.3a) and (9.4a), the model proceeds to develop an expression for the pool radius (9.7) in the initial phase of spread. This yields the result of characteristic flow and self-similarity theory modified by the last term in equation (9.7), the $\Delta\tau^3$ term, which describes the effect of thermal heat transfer on the growth rate. Since the theory is phenomenological, it was necessary to compare the results obtained by integration, equation (9.6), with the model of Chapter 3 of AMSHAH (i.e., Fannelop-Waldmann[2] theory which utilizes boundary layer formulation) in order to obtain explicit expressions for the constants of integration.

There may be some question as to the validity of the result, since it is based on the premise that the second term on the right of equation (9.6), the $A\tau^2$ term, does not depend on thermal processes. This re-

mains to be proven. In any case, regardless of whether equation (9.7) is correct or not, it is to be used for small τ, hence only the first term of the right of equation (9.7) is important.

The gravity-viscous regime is formulated in terms of boundary layer theory, equations (9.16a) and (9.16b), along with a volume scaling law, equation (9.19) which is missing from the text. Again, since the approach is phenomenological, it was necessary to compare this with a constant-volume model taken from a previous development. The result used was that of Chapter 8 in AMSHAH, which predicts a $t^{1/8}$ time-dependence of radial spread. This is in contrast to the $t^{1/4}$ dependence of the Fannelop and Waldmann theory. Since scaling is extremely important in this limit, this matter requires additional investigation. This question is most relevant to the result for boiloff time, equation (9.21).

The treatment of the pool spread with ice formation is also approximate and phenomenological, although a fairly good theory exists within the framework of the classical theory of heat conduction.[2] This could also be extended to include conduction and film boiling, but probably only in an approximate manner. It is difficult to say that the approximate treatment of Chapter 9 has any shortcomings without extensive numerical analysis and detailed comparison with experimental data.

C. SENSITIVITY ANALYSIS (Chapter 9)

A standard approach[3] that is suitable for these relationships is that of assuming that one has a dependent variable f which is defined in terms of a field of independent variables

$$f_i = \phi_i (X_j) \tag{IX-1}$$

More explicitly, it is better to set

$$\ln f_i = \ln \phi_i (\ln X_j)$$

with

$$\frac{1}{f_i} df_i = \frac{\partial \ln \phi_i}{\partial \ln X_j} \frac{dX_j}{X_j} \tag{IX-2}$$

Then

$$\frac{\partial \ln \phi_i}{\partial \ln X_j}$$

represents a matrix connecting the field of dependent fraction increments, $d f_i / f_i$, with the independent ones, $d X_i / X_i$.

What makes our results most amenable to simple calculation is the fact that the dependent variables, f_i, are expressed as products of the independent ones

$$f_i = \phi_i = \prod_j X_j^{n_{ij}} \tag{IX-3}$$

so that

$$\frac{\partial \ln \phi_i}{\partial \ln X_j} = n_{ij} \tag{IX-4}$$

Then one could obtain a composite estimate of the overall sensitivity by setting

$$\left|\frac{df_i}{f_i}\right| = \left[\sum_j \left(n_{ij}\,\frac{dX_j}{X_j}\right)^2\right]^{1/2} \tag{IX-5}$$

There is also the problem of errors introduced by varying the exponents. This is best handled using the techniques of regression analysis.

In the absence of any noteworthy singularities in the equations themselves (such as vanishing denominators or exponents containing independent variables), we can consider the following salient features of any sensitivity analysis.

a) There are discrete discontinuities in the logarithmic derivatives at the point of inflection, τ_c, as defined in Table 9.1. A detailed investigation of the singularities at τ_c is unwarranted, since this is precisely the region where the model is no longer valid.

b) An unbiased indicator of the relative effect of each of the independent variables can best be obtained by assuming that all the $\delta X_j/X_j$ in equation (IX-5) are equal. Then the relative effect of each variable, say the yth variable, on the ith dependent factor would be

$$S_{ij} = \frac{n_{ij}}{\left(\Sigma\, n_{ij}^{\,2}\right)^{1/2}} \tag{IX-6}$$

c) It may turn out that one independent variable is more apt to be unmeasurable or undefined than others. Then, if we assume all other independent variables to be determined with reasonable precision,

$$\frac{df_i}{f_i} \approx n_{ij}\,\frac{dX_j}{X_j} \tag{IX-7}$$

We consider the formulas in Table 9.1 of Chapter 9 in AMSHAH. There are five dimensionless dependent variables (we discuss the radial case only):

χ	the radius	- f_1
k	the volume	- f_2
τ_e	time for evaporation	- f_3
χ_{max}	maximum radius	- f_4
η	layer thickness	- f_5

For our dimensionless independent variables, we choose:

k	the volume	- x_1
τ	the time	- x_2
Δ	ratio of heat fluxes	- x_3
Γ_ℓ	the viscosity of liquid	- x_4
Γ_w	the viscosity of water	- x_5
α	ice heat flux	- x_6
k_c	critical volume	- x_7
τ_c	critical time	- x_8
χ_c	critical radius	- x_9
χ	radius	- x_{10}

The analysis or matrix of n_{ij} is presented in three tables. The first, Table (IX,1), covers the gravity-inertia regime; the second, Table (IX,2), covers the gravity-inertia, ice formation regime; and the third, Table (IX,3), covers the gravity-viscous regime. The functional formulas, upon which the analysis is based. are those of Table 9.1 on page 137 of AMSHAH. Analysis of formulas based on the $\tau^{1/8}$ spread law has been neglected for two reasons: the first being that the law itself is patently incorrect for a cryogen; and the second being that the resulting analysis would be so similar to the given analysis (for $\tau^{1/4}$ spread law) of the gravity-viscous regime that no change in the orders of magnitude experienced would result.

Again, one should not draw too many far-reaching conclusions from these results. For example, had we constructed sensitivity coefficients for the case $(\mu_\ell/\mu_w) \ll 1$, we would almost certainly underestimate the error because of the fact that the $t^{1/8}$ spread law is in itself incorrect, a factor no sensitivity analysis can account for.

In any case, all coefficients showing a non-zero in Tables (IX,1), (IX,2), and (IX,3) are of the order unity for the parameters associated with LNG and other light hydrocarbons.

TABLE (IX,1)

MATRIX OF SENSITIVITY PARAMETERS (n_{ij}) FOR RADIAL SPREAD OF CRYOGEN IN GRAVITY-INERTIA REGIME

Dependent Variable	Independent Variable			
	k	τ	Δ	χ
χ	0	$\frac{1}{2}\left(\frac{1.3\,\tau + 1.326\,\tau^3\Delta}{1.3\,\tau + 0.442\,\tau^3\Delta}\right)$	$\frac{1}{2}\left(\frac{0.442\,\tau^3\Delta}{1.3\,\tau + 0.442\,\tau^3\Delta}\right)$	1
k	1	$-\left(\frac{4.08\,\tau^2\Delta + 1.388\,\tau^4\Delta^2}{1 - 2.04\,\tau^2\Delta - 0.347\,\tau^4\Delta^2}\right)$	$\left(\frac{-2.04\,\tau^2\Delta - 0.694\,\tau^4\Delta^2}{1 - 2.04\,\tau^2\Delta - 0.347\,\tau^4\Delta^2}\right)$	0
η	1	0	0	-2
τ_e	0	0	- 1/2	0
χ_{max}	0	0	- 1/4	0

TABLE (IX,2)

MATRIX OF SENSITIVITY PARAMETERS (n_{ij}) FOR RADIAL SPREAD OF CRYOGEN IN GRAVITY-INERTIA REGIME - ICE FORMATION

Dependent Variable	Independent Variable			
	k	τ	α	χ
χ	0	$\frac{1}{2}\left(\frac{3.537\,\alpha\tau^{5/2} + 1.3\tau}{1.415\,\alpha\tau^{5/2} + 1.3\,\tau}\right)$	$\frac{1}{2}\left(\frac{1.415\,\alpha\tau^{5/2}}{1.415\,\alpha\tau^{5/2} + 1.3\,\tau}\right)$	1
k	1	$-\left(\frac{1.30\,\alpha\tau^{3/2} + 1.41\,\alpha^2\tau^3}{1 - 0.867\,\alpha\tau^{3/2} - 0.4716\,\alpha^2\tau^3}\right)$	$\left(\frac{-0.867\,\alpha\tau^{3/2} - 0.9432\,\alpha^2\tau^3}{1 - 0.867\,\alpha\tau^{3/2} - 0.4716\,\alpha^2\tau^3}\right)$	0
η	1	0	0	-2
τ_e	0	0	- 2/3	0
χ_{max}	0	0	- 1/3	0

TABLE (IX,3)

MATRIX OF SENSITIVITY PARAMETERS (n_{ij}) FOR RADIAL SPREAD OF CRYOGEN IN GRAVITY-VISCOUS REGIME

Dependent Variable	Independent Variable				
	χ_c	τ_c	τ	k_c	Δ
χ	1	-1/4	1/4	0	0
k	$\frac{-2\pi\chi_c^2\tau_c\Delta}{1.5\,\xi}\left[\left(\frac{\tau}{\tau_c}\right)^{1.5}-1\right]$	$\frac{+4\Delta\pi\chi_c^2}{1.5\,\xi}\left(\frac{0.5\,\tau^{1.5}}{\tau_c^{0.5}}+\tau_c\right)$	$\frac{-\Delta\pi\chi_c^2\tau_c}{\xi}\left(\frac{\tau}{\tau_c}\right)^{1.5}$	$\frac{k_c}{\xi}$	$\frac{\Delta\pi\chi_c^2\tau_c}{1.5\,\xi}\left[1-\left(\frac{\tau}{\tau_c}\right)^{1.5}\right]$
τ_e	$\frac{-2\,k_c}{\Phi\pi\chi_c^2\tau_c\Delta}$	$1-\frac{k_c}{\Phi\pi\chi_c^2\tau_c\Delta}$	0	$\frac{k_c}{\Phi\pi\chi_c^2\tau_c\Delta}$	$\frac{-k_c}{\Phi\pi\chi_c^2\tau_c\Delta}$

$$\xi = k_c - \frac{\Delta\pi\chi_c^2\tau_c}{1.5}\left[\left(\frac{\tau}{\tau_c}\right)^{1.5}-1\right] \qquad \Phi = 1+\frac{1.5\,k_c}{\pi\chi_c^2\tau_c\Delta}$$

No scaling was attempted because the models of Chapter 9 are phenomenological in nature, an approach that can and usually does alter if not completely mask any manifestions of scale effects in the theory.

D. HACS ERROR ANALYSIS (Chapter 9)

MOD D obtains data from the subroutines FRCL and IRCL. In case the density of the liquid obtained is equal to or greater than 1 gm/cc, the subroutine prints a warning "THE LIQUID DENSITY OF THE SPILLED CHEMICAL IS SO CLOSE TO WATER THAT IT MAY NOT FLOAT, FOR MODEL IT WILL BE ASSUMED THAT THE DENSITY IS 0.99 gm/cc," assumes density of liquid 0.99 gm/cc and proceeds ahead. It computes the size of the spill of a cryogen on water at a given time, as well as time for complete evaporation. The spill spread may be radial or channel. In each case, two types of heat transfer are considered:

1) constant heat flux
2) ice formation with time- and position-varying heat flux due to water freezing.

MOD D calls the subroutines BEGPR, FRCL, IRCL, EPRNT, CRYSP, COMPQ, FSV, ENDPR. Subroutine CRYSP calls CRIT, GRSPD. All these subroutines have been checked for errors.

MOD D: No error was found.

CRYSP:

LN0001 TIME in the argument list of the subroutine is a user's input supplied by MOD D. If the value of time is greater than the time at which all the liquid evaporates, one obtains from the program negative values of the liquid remaining at the given time. The subroutines CRYSP, CRIT, and GRSPD were run for the radial spread of LNG spill. The volume of the spill was varied while TIME was fixed at 50 sec. The results are shown in Table (IX,4) on the next page.

LN0047, 0048 CRYSP uses C_{ICE} = 0.502 cal/gm*°C
K_{ICE} = 0.005 cal/gm*cm*°C
ρ_{ICE} = 0.92 gm/cc
$\lambda_{s\to\ell}$ = 80 cal/gm

These values check with those obtainable from standard references.

LN0070 TOWE = TOWC*(1.+1.375*KC/(TOWC*KHIC*DEL))*(8./11.)

should be: TOWE = TOWC*(1.+1.375*KC/(TOWC*KHIC*DEL))**(8./11.)

TABLE (IX,4)

V_i, cc	τ_c	k_c	χ_c	V, volume remaining at 50 sec after spill in cc.	R, radius of spill at 50 sec after in cm.	R_{max}, maximum radius of spill in cm.	t_e, time at which all liquid evaporates in sec.
$2.253*10^{10}$	106.517	0.142	12.531	$2.173*10^{10}$	15,263	29,114	256.8
$2.253*10^{9}$	85.957	0.182	11.227	$1.999*10^{9}$	8,637	13,048	144.7
$2.253*10^{8}$	68.914	0.231	10.021	$1.433*10^{8}$	4,952	5,830	81.6
$2.253*10^{7}$	54.802	0.289	8.901	$-3.55*10^{6}$	2,595	2,595	41.6
$2.253*10^{6}$	43.155	0.356	7.863	$-4.04*10^{6}$	1,150	1,150	26.1
$2.253*10^{5}$	33.592	0.430	6.902	$-1.11*10^{6}$	507	507	14.9
$2.253*10^{4}$	25.803	0.510	6.015	$-2.42*10^{5}$	222	222	8.5
$2.253*10^{3}$	19.533	0.590	5.203	$-4.90*10^{4}$	97	97	4.9
$2.253*10^{2}$	14.561	0.668	4.467	$-9.48*10^{3}$	42	42	2.9

LN0104 `TOWE = TOWC*(1.+1.5*KC/(PI*TOWC*DEL*KHI**2))**(2./3.)`

should be: `TOWE = TOWC*(1.+1.5*KC/(PI*TOWC*DEL*KHIC**2))**(2./3.)`

LN0123 `TOWE = TOWC*(1.+0.75*KC/(PI*ALFA*KHIC**2*SQRT(TOWC)))**(4./3.)`

CRYSP uses $\tau_e = \tau_c \left[1 + (3\ k_c)/(4\ \pi \alpha \chi_c^{\,2}\ \tau_c^{\,1/2})\right]^{4/3}$ for radial spread, ice formation, gravity-viscous regime. This agrees with the equation given in Table 9.1 of AMSHAH while it differs from equation (9.36) of AMSHAH. Equation (9.36) is obviously incorrect since it contains a minus sign where there should be a plus sign.

LN0133 `SIZMX = FLOAT(3-IDIM)*L*KHIM`
0134 `TEVAP = TOWE*CHTM`

The values of TOWE and KHIM are obtained from the equations of the gravity-viscous regime. If $\tau_e \leq \tau_c$, i.e., the entire evaporation takes place in the gravity-inertia regime, the values of SIZMX and TEVAP will be incorrect.

GRSPD:

LN0048 `K = 1.-2.04*DEL*TOW**2-0.347*(DEL**2)*(TOW**4)`

GRSPD uses $k = 1 - 2.04\ \Delta\tau^2 - 0.347\ \Delta^2\tau^4$ while AMSHAH (p.137) gives $k = 1 - 2.04\ \Delta\tau^2 + 0.347\ \Delta^2\tau^4$ for constant heat flux in gravity-inertia regime (radial spread).

LN0055 K = 1.-0.867*DEL*TOW**1.5-0.4716*(DEL**2)*(TOW**3)

GRSPD uses $k = 1 - 0.867\,\alpha\,\tau^{3/2} - 0.4716\,\alpha^2\,\tau^3$ while AMSHAH (p.137) gives $k = 1 - 0.867\,\alpha\,\tau^{3/2} + 0.4716\,\alpha^2\,\tau^3$ for ice formation in the gravity-inertia regime (radial spread).

CRIT: This subroutine does not use the equations for critical time for change of regimes given in Tables 9.1 and 9.2 in AMSHAH. Its logic is based on the fact that at the critical time the mean film thickness in the liquid is of the order of magnitude as the mean viscous boundary layer thickness. The boundary layer thickness in this context refers to that in the liquid or water depending, respectively, on whether the liquid viscosity is much smaller than or very much greater than that of water.

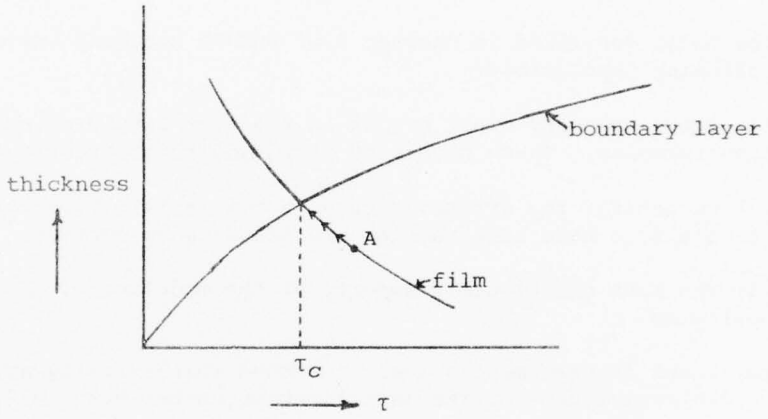

The program presumes that $[\tau_e - \tau_e/100] > \tau_c$ where τ_e is obtained from the equations of gravity-inertia regime. Then it reduces τ_e progressively by increments of $\tau_e/100$ until τ_e becomes $\tau_e \leqslant \tau_c$.

If $[\tau_e - \tau_e/100] \leqslant \tau_c$ to start with, then when the control passes to the statement (LN0028),

```
4     TOWC = TOW+DTOW*E/(E+ABS(E1))
```

E1 will be undefined. The computer may give an error message or use an arbitrary value of E1. E1 is equal to $(\sqrt{\tau_e} - \sqrt{\tau_c})/\Gamma$ where Γ is a dimensionless viscosity.

COMPQ: This subroutine computes the value of heat flux for the 'Constant Heat Flux' situations. It uses the relationship (LN0015) Q = (2.5/181.)*ABS(TINF-TCRY) where TINF = water

temperature, °C and TCRY = boiling temperature of liquid, °C . This equation is not stated anywhere in the text of Chapter 9 of AMSHAH.

For the case of Specific Example, Section 9.7 (p.130) of AMSHAH, let us calculate the value of Q using this equation. μ_w is a strong function of temperature and its value 10^{-3} poise corresponds to a temperature of 20°C. Taking TINF = 20°C, we have

$$Q = (2.5)/(181)\ (298 - 112) = 2.569\ \text{cal/cm}^2\text{*sec} = 107.5\ \text{kW/m}^2 .$$

The value of Q used in AMSHAH example is 94.6 kW/m^2 .

No errors were found in the subroutines BEGPR, FRCL, IRCL, EPRNT, FSV, and ENDPR.

E. SUMMARY OF RESULTS

The model described in Chapter 9 of AMSHAH has been reviewed with the following conclusions.

(1) There are many minor errors in the text involving numerical data and formulas. These have been cited and the corrections indicated.

(2) Except for the erroneous cases noted in (1) above, all formulas and calculations have been checked and found to be correct.

(3) The most questionable aspects of the modeling of Chapter 9 are the following.

(a) Model is phenomenological, a method which finally appeals to empiricism for its justification rather than to first principles.

(b) Spread law giving a radial dependence of time as the one-eighth power of time is erroneous and contrary to properly applied boundary layer theory.

(c) Ice formation, which is claimed to be a factor, will not occur due to a cryogenic spill unless there is no free surface of water present. The analogy of the spill in a drydock is not far-fetched in this regard, as ample experimental evidence has indicated.[4]

F. *RECOMMENDATIONS*

(1) Time-dependence of heat transfer should be investigated.

(2) Hydrodynamic field modeling should be attempted utilizing boundary layer theory, rather than the phenomenological approach already commented on. The kind of difficulty that can be encountered in the latter approach is displayed in Appendix D.

G. *TABLE OF SYMBOLS USED*

C fractional inertia constant = 0.75386

B integration constant = 1.2996

k dimensionless volume

k_c dimensionless critical volume

V volume of liquid

V_i initial volume of liquid

Δ ratio of heat flux to characteristic heat flux

α dimensionless ice heat flux

τ dimensionless time

$\mu_{\ell,w}$ viscosity, liquid or water

τ_c critical time

η dimensionless mean liquid thickness

τ_e evaporation time

$\Gamma_{\ell,w}$ dimensionless viscosity, liquid or water

χ dimensionless spill spread

χ_{max} maximum spread

H. LIST OF REFERENCES

(1) Raj, P. P. K., and A. S. Kalelkar. Simultaneous spreading and evaporation of a cryogen on water, ch. 9, pp. 113-138. In *Assessment Models in Support of the Hazard Assessment Handbook (CG-446-3)*, Report No. CG-D-65-74 (AMSHAH), prepared by Arthur D. Little, Inc. For the Department of Transportation, U.S. Coast Guard, NTIS AD 776617, January 1974.

(2) Fannelop, T. K., and G. D. Waldman. Dynamics of oil slicks. *AIAA Journal 10*(4):506-510, 1972.

(3) Beers, Y. *Introduction to the Theory of Errors*, pp. 26-35. Addison Wesley Publishing Co., Reading, Mass., 1953.

(4) Boyle, G. J., and A. Kneebone. *Laboratory Investigations into the Characteristics of LNG Spills on Water, Evaporation, Spreading and Vapor Dispersion*. Shell Research Ltd., Thornton Research Center, December 1972.

AD-A044 198 ENVIRO CONTROL INC ROCKVILLE MD F/G 13/2
A CRITICAL TECHNICAL REVIEW OF SIX ADDITIONAL HAZARD ASSESSMENT--ETC(U)
MAR 77 A H RAUSCH, R M. /KUMAR, C J LYNCH DOT-CG-33377-A
UNCLASSIFIED USCG-D-54-77 NL

2 OF 3
AD
A044198

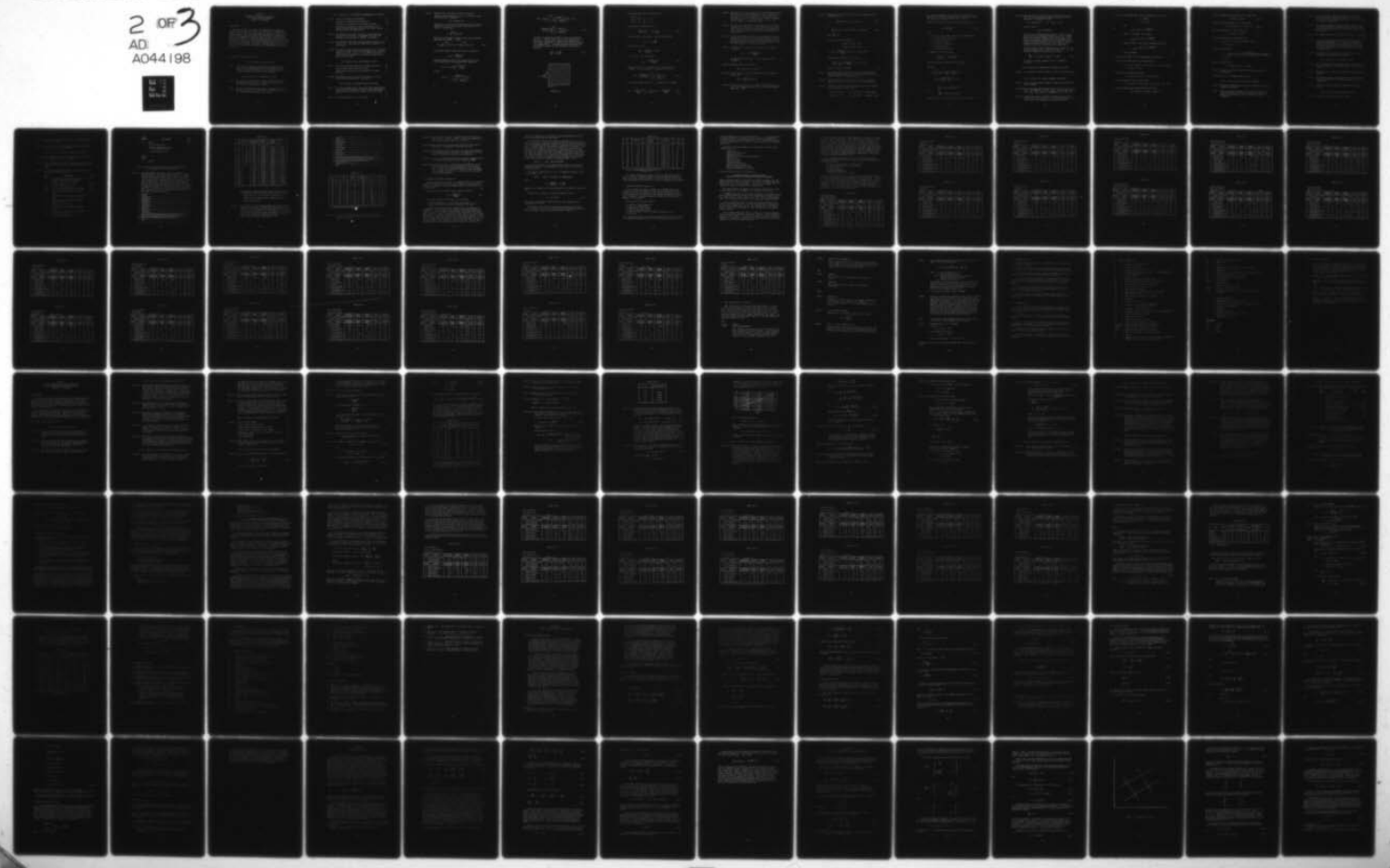

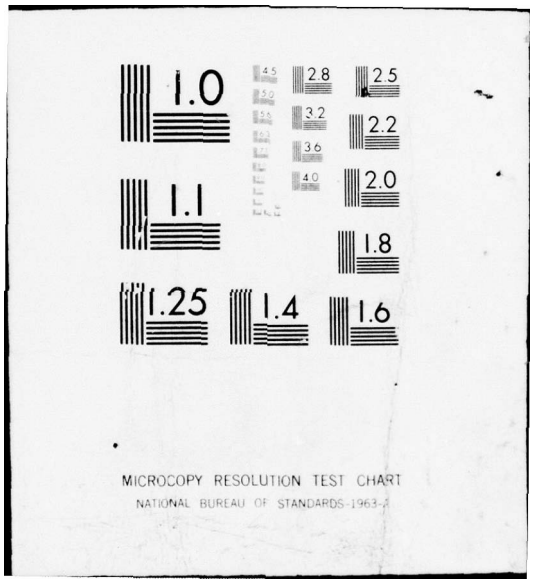
1.0
1.1
1.25
1.4
1.6
1.8
2.0
2.2
2.5
2.8
3.2
3.6
4.0
4.5
5.0
5.6
MICROCOPY RESOLUTION TEST CHART
NATIONAL BUREAU OF STANDARDS-1963-A

Chapter 6

"SIMULTANEOUS SPREADING AND COOLING OF
A HIGH VAPOR PRESSURE CHEMICAL"
(Chapter 10 of AMSHAH)

INTRODUCTION

The model described in Chapter 10 of AMSHAH [2] is designed to determine the specific evaporation rate as well as the extent of the spread after the spill of a fixed and given volume of a high-vapor-pressure liquid. The liquid undergoing spreading and evaporation is assumed to be immiscible with water and less dense. All properties input to this model are assumed constant during the spreading and the evaporation. Further, it is assumed that the mass-transfer coefficient remains constant and that the initial temperature of the liquid is the same as that of the water. This model is predicated on the premise that the spreading and the evaporation are independent, noninteracting phenomena.

A. *REVIEW OF TEXT (Chapter 10)*[1]

(X,1) *Section 10.1, Aim (p.139)*

(X,1,a) The aim of the model is that of obtaining the extent of spread and the vaporization rate at any instant of time after the instantaneous spill of a high-vapor-pressure, lighter-than-water immiscible liquid on water. (√)

(X,2) *Section 10.2, Introduction (p.139)*

(X,2,a)* The chemicals such as diethyl ether and ethyl acetate have limited solubility in water. However, the model treats the chemical as completely immiscible.

(X,2,b) The heat of evaporation comes from the sensible heat of the liquid as well as that of the water. The model presented here takes both these "heats" into account. (√)

(X,3) *Section 10.3, Principles and Assumptions (p.139-141)*

(X,3,a) Liquid is spilled instantaneously. (✓)

Spreading is independent of evaporation. (✓)

Properties of liquid and water assumed constant. (✓)

Evaporation is caused by a vapor concentration difference between the vapor just above the liquid surface and the vapor in the atmosphere. (✓)

(X,3,b) The assumption that entire liquid is at some mean temperature is not correct. The authors state that this assumption has been made to simplify the problem. (✓)

(X,3,c)* Mass-transfer coefficient has been assumed constant. This is incorrect. This point is elaborated in Section B of this chapter.

(X,3,d)* The authors assume that initial temperature of the spilled liquid is the same as that of water temperature. This may not always be true. Also, it is possible to solve the problem when the temperature of water and liquid are different to begin with.

(X,4) *Section 10.4, Data Required (p.141)*

(X,4,a) Physical and thermal properties of water and liquid. (✓)

Vapor pressure equation for the liquid. (✓)

Mass-transfer coefficient for evaporation of liquid into air. (✓)

(X,4,b)** Typographical error in last line of Section 10.4: the word "correction" should be "convection."

(X,5) *Section 10.5, Model Details (p.141-145)*

(X,5,a) The authors assume that at any instant the liquid temperature is uniform throughout, while the water temperature is varying along the radius (or length) as shown in Figure 10.1. (✓)

(X,5,b) The energy equation (10.1) is correct. (✓)

(X,5,c) Equation (10.5) has been arrived at as follows:

The heat flux from water, $q(r,t)$, is a function of both radius and time. Therefore,

$$dQ = (2\pi r dr)q(r,t)$$

where dQ is the rate of heat transferred from an annular differential area on the surface of the water at any instant. Consequently,

$$Q = \int_0^{R(t)} 2\pi r q(r,t) dr$$

where R is the radius of spread at any instant and mean heat flux, $\overline{q} = Q/(\pi R^2)$. Thus,

$$\overline{q} = \frac{1}{\pi R^2} \int_0^{R(t)} 2\pi r\, q(r,t)\, dr = \frac{2}{R^2} \int_0^{R(t)} r\, q(r,t)\, dr \qquad \text{(X-1)}$$

If the heat transfer takes place only by conduction,

$$q(r,t) = \frac{K_w(T_w - T)}{Y(r,t)}$$

Assuming elliptical profile for boundary layer profile for the variation of the boundary layer dimension,

$$Y(r,t) = Y_0(t) * \sqrt{1 - \left(\frac{r}{R(t)}\right)^2}$$

we have,

$$q(r,t) = \frac{K_w(T_w - T)}{Y_0(t) * \left[1 - \left(\frac{r}{R(t)}\right)^2\right]^{1/2}}$$

or

$$\bar{q}(t) = \frac{2}{R^2(t)} \int_0^{R(t)} \frac{K(T_w - T)}{Y_0(t)\left[1 - \left(\frac{r}{R(t)}\right)^2\right]^{1/2}} * r\,dr$$

$$= \frac{2\,K_w(T_w - T)}{R^2(t)\,Y_0(t)} \int_0^{R(t)} \frac{r\,dr}{\left[1 - \left(\frac{r}{R(t)}\right)^2\right]^{1/2}} \qquad \text{(X-2)}$$

To obtain an expression for $\bar{q}(t)$, we need an expression for $Y_0(t)$. Consider semi-infinite fluid (water) shown in Figure (X,1) maintained as some initial temperature T_w. The surface temperature is suddenly lowered and maintained at a temperature T_0. Assuming constant properties, the differential equation for the temperature distribution $T(x,t)$ is

$$\frac{\partial^2 T}{\partial x^2} = \frac{1}{\alpha_w} \frac{\partial T}{\partial t} \qquad \text{(X-3)}$$

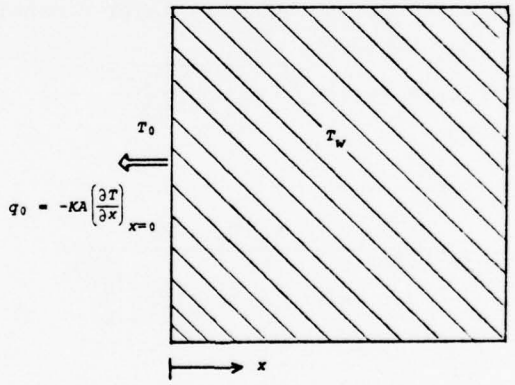

FIGURE (X,1)

The boundary and initial conditions are:

$$T(x,0) = T_w$$
$$T(0,t) = T_0 \quad \text{for} \quad t > 0$$
$$T(\infty,t) = T_w \quad \text{for} \quad t > 0$$

The solution of equation (X-3) is:

$$\frac{T(x,t) - T_0}{T_w - T_0} = erf \frac{x}{2\sqrt{\alpha_w t}} \tag{X-4}$$

The heat flow at any position x may be obtained from

$$q_x = - K_w \frac{\partial T}{\partial x}$$

From equation (X-4),

$$\frac{\partial T}{\partial x} = \frac{T_w - T_0}{\sqrt{\pi \alpha_w t}} e^{-x^2/4\alpha_w t}$$

At the surface, the heat flow is

$$q\Big|_{x=0} = \frac{K_w(T_w - T_0)}{\sqrt{\pi \alpha_w t}} \tag{X-5}$$

From equation (X-5), it appears that we can take $Y_0(t) = \sqrt{\pi \alpha_w t}$. Substituting this in equation (X-2), we get

$$\overline{q}(t) = \frac{2\ K_w(T_w - T)}{R^2(t)\ \sqrt{\pi \alpha_w t}} \int_0^{R(t)} \frac{r\, dr}{\left[1 - \left(\frac{r}{R(t)}\right)^2\right]^{1/2}} \tag{X-6}$$

For radial spread, using $r/R = \xi$, equation (X-6) becomes

$$\overline{q}(t) = \frac{K_w(T_w - T)}{\sqrt{\pi \alpha_w t}} \int_0^1 \frac{2\,\xi}{[1 - \xi^2]^{1/2}}\, d\xi = 2\, \frac{K_w(T_w - T)}{\sqrt{\pi \alpha_w t}} \tag{10.7}$$

(✓)

(X,5,d)* Equation (X-5) is the solution to the differential equation (X-3) when the surface temperature is kept constant. In the present case, the temperature of the liquid, which is the same as the surface temperature of water, is changing and equation (X-5) is not the solution. Hence, using $Y_0(t) = \sqrt{\pi \alpha_w t}$ is a fundamental error.

(X,5,e)* As the water temperature at the interface is less than in the main body, convection currents will be set up. They will increase the rate of heat transfer. The analysis in (X,5,c) was based on pure conduction as the only mode of heat transfer.

(X,5,f)* In the real situation, eddies may be present in the water, and the chief mechanism of heat exchange will be one involving macroscopic lumps of water moving about. In that case, $\overline{q}(t)$ obtained from equation (10.5) in AMSHAH can be an underestimate by an order of magnitude.

(X,5,g) Proceeding as in section (X,5,c) above, it is possible to derive

$$\overline{q}(t) = \frac{\pi}{2} \cdot \frac{K_w (T_w - T)}{\sqrt{\pi \alpha_w t}}$$

for one-dimensional spread. This is equation (10.6) in AMSHAH. (✓)

(X,5,h)** Equation (10.7a) should read:

$$\dot{E}'' = h_p \, P_{sat}(T) = a \, h_p \, e^{-b/T}$$

(X,5,i)** In the footnote on p.142 of AMSHAH, the first equation should read:

$$\overline{q}(t) = \left(\frac{2}{R^2}\right) \int_0^R r \, q(r,t) \, dr$$

(X,5,j)** In the footnote on p.142 of AMSHAH, the denominator of the first term on the right-hand side of the second equation should be: $\sqrt{\pi \alpha_w t}$

(X,5,k) Equation (10.8a) follows from the energy equation (10.1). By equation (10.1):

$$\frac{d}{dt}\left[M\, I_{liq}(T)\right] = Q - \dot{E}\, I_{vap}(T) \qquad (10.1)$$

or

$$M\,\frac{d}{dt}\, I_{liq}(T) + I_{liq}(T) \cdot \frac{dM}{dt} = Q - \dot{E}\, I_{vap}(T) \qquad (X\text{-}7)$$

Now, $\frac{dM}{dt} = -\dot{E}$

If T_R is the base temperature,

$$I_{liq}(T) = C_{liq}(T - T_R)$$

$$I_{vap}(T) = C_{liq}(T - T_R) + \lambda$$

$$Q = \bar{q}A = \frac{c\,A\,K_W(T_W - T)}{\sqrt{\pi\alpha_W t}} \quad \text{and} \quad \dot{E} = a\,A\,h_p\, e^{-b/T}$$

Substituting the above in (X-7) yields

$$M\,\frac{dT}{dt} = \frac{A}{C_{liq}}\left[c\,\frac{K_W(T_W - T)}{\sqrt{\pi\alpha_W t}} - \lambda\, h_p\, a\, e^{-b/T}\right]$$

equation (10.8a) in AMSHAH. (√)

(X,5,l) The authors solve equations (10.8a) and (10.9a) with the initial conditions equation (10.10a) using forward integration method of the Runge-Kutta type. (√)

(X,5,m)* The mass-transfer coefficient, h_p, is assumed constant during the solution of these equations. It is incorrect.

(X,5,n) Treybal[2] lists the following equations for mass transfer for flow parallel to flat plates:

For $Re_x < 80{,}000$ $\quad J_H = 0.664\, Re_x^{-0.5}$ (laminar flow)

For $Re_x > 5 \times 10^5$ $\quad J_H = 0.036\, Re_x^{-0.2}$ (turbulent flow)

The authors of AMSHAH do not consider the transition flow. They use the equation of laminar flow for $Re_L \leq 5 \times 10^5$ and the equation of turbulent flow for $Re_L > 5 \times 10^5$.

Treybal (2) states that for flow over flat plates, $J_H = J_D$.

$$J_D = \frac{k_x}{cU} \left(\frac{\mu}{\rho D}\right)^{2/3} \qquad \text{(X-8)}$$

where

k_x is local mass transfer coefficient, moles/cm^2 sec

c is concentration, moles/cc

U is velocity, cm/sec

μ is viscosity, gm/cm sec

ρ is density, gm/cc

D is diffusivity, cm^2/sec

For laminar flow, we then have

$$\frac{k_x}{cU} \left(\frac{\mu}{\rho D}\right)^{2/3} = 0.664 \left(\frac{x\rho U}{\mu}\right)^{-0.5}$$

Mean mass transfer coefficient, $\bar{k} = \frac{1}{2} \int_0^L k_x \, dx$

Therefore,

$$\bar{k} = \frac{1}{L} \int_0^L 0.664 \, cU \left(\frac{\mu}{\rho D}\right)^{-2/3} \left(\frac{x\rho U}{\mu}\right)^{-0.5} dx$$

$$= 1.328 \, cU \left(\frac{\rho D}{\mu}\right)^{2/3} \left(\frac{U\rho}{\mu}\right)^{-0.5} L^{-0.5}$$

or

$$\frac{\bar{k}L}{cD} = 1.328 \, (Sc)^{1/3} (Re_L)^{1/2}$$

or

$$\frac{\bar{h}_D L}{D} = 1.328 \, (Sc)^{1/3} (Re_L)^{1/2}$$

where $\bar{h}_D = \bar{k}/c$. This is equation (10.11a) of AMSHAH. (√)

(X,5,o)** Different sources report different constants in the turbulent flow equation for heat transfer during flow over a flate plate. Baumeister[3] lists:

$$J_H = 0.0148\ Re_x^{-0.2} \qquad \text{for} \quad Re_x > 4 \times 10^5$$

Polter[4] gives:

$$J_H = 0.029\ Re_x^{-0.2} \tag{X-9}$$

We will use the equation given by Polter, since it gives, on integration, an equation resembling (10.11b) of AMSHAH. Whenever a turbulent boundary layer develops over a flat plate, there exists a certain part of the boundary layer near the leading edge where the flow is laminar. Therefore, integration must be carried out in two steps, over the laminar part and over the turbulent part separately.

Assuming laminar boundary layer exists up to $Re_L = 5 \times 10^5$ and the boundary layer is turbulent for $Re_L > 5 \times 10^5$, integration of equation (X-9) with $J_H = J_D$ yields,

$$\frac{\bar{h}_D L}{D} = 0.036\ (Sc)^{1/3}\ [(Re_L)^{0.8} - 23{,}100] \tag{X-10}$$

In view of the above, equation (10.12) in AMSHAH is incorrect.

(X,6) *Section 10.6, Algorithm for Computation (p.145)*

(X,6,a) A flow chart is shown in Figure 10.3 for the calculations. (✓)

(X,7) *Section 10.7, Specific Example (pp.145-148)*

(X,7,a) Data. All data correct except for latent heat of vaporization of liquid.

(X,7,b)** Since the properties being used are at 20°C, we use λ_{liq} at 20°C. From Weast[5], p. E-26, λ_{liq} = 94.44 cal/gm = 395.14 $\times 10^3$ J/kg. That reported in AMSHAH is 355.4 $\times 10^3$ J/kg .

(X,7,c)* Although the values for D and σ correspond to 20°C, the value of the $\mu_{liq} = 0.2842 \times 10^{-3}$ N s/m^2 corresponds to 0°C. We are unable to understand the reason behind this.

(X,7,d) For diethyl ether, we have from Weast (5, p.D-155)

$$A = 6946.2$$

$$B = 7.7756659$$

and

$$\log_{10} P_{sat}(T) = \frac{-0.2185\ A}{T} + B$$

where P is in mmHg. This yields,

$$P_{sat}(T) = e^{\left(22.7969 - \frac{3494.736}{T}\right)}$$

where P is N/m^2. This agrees reasonably well with

$$P_{sat} = e^{\left(22.7522 - \frac{3496.736}{T}\right)}$$

given in AMSHAH. (✓)

(X,7,e)** The symbol for the Schmidt number should be Sc.

(X,7,f)** The third line on p.148 should read:

$$\overline{h}_D = [0.037 \times 1.685^{1/3} \times (3.61 \times 10^6)^{0.8}] \times 8.9 \times 10^{-6}/10.83$$

$$= 6.375 \times 10^{-3} \text{ m/s}$$

(X,7,g)** Gas constant should read:

$$R = 8.314 \times 10^3/74.12 = 112.169 \text{ J/kg °K}$$

(X,7,h)** Using Eq. (10.12) should read:

$$h_p = 6.375 \times 10^{-3}/112.169 \times 293 = 1.9397 \times 10^{-7} \text{ s/m}$$

(X,7,i)** Characteristic temperature should read:

$$T_{ch} = 395.14 \times 10^3/2200 = 179.61 \text{ °K}$$

(X,7,j)** Saturated vapor pressure at T_i should read:

$$P_{sat}(T_i) = 52547.5 \quad N/m^2$$

(X,7,k)** Initial evaporation rate should read:

$$\dot{E}''_i = h_p \, P_{sat}(T_i) = 1.0193 \times 10^{-2} \quad kg/m^2 \, s$$

(X,7,l)** Characteristic area should read:

$$A_i = [V_i]^{2/3} = 117.30 \quad m^2$$

(X,7,m)** Characteristic time should read:

$$t_{ch} = 1.27 \times 10^3 \times 715/(1.0193 \times 10^{-2} \times 117.3)$$

$$= 7.595 \times 10^5 \quad s$$

(X,7,n)** Δ should read:

$$\Delta = 2 \times \frac{0.6 \times 179.61}{1.0193 \times 10^{-2} \times 395.14 \times 10^3 \sqrt{\pi \times 1.43 \times 10^{-7} \times 7.595 \times 10^5}}$$

$$= 0.0916$$

(X,7,o)** β should read:

$$\beta = 3494.736/179.61 = 19.4574$$

(X,7,p)** ρ_ℓ and C_ℓ on p.145 of AMSHAH should read ρ_{liq} and C_{liq}, respectively.

(X,7,q)** T_B on p.147 of AMSHAH should read T_b.

(X,8) *Section 10.8, Discussions (pp.148-149)*

(X,8,a) The model considers the spread and the evaporation as two independent phenomena. (√)

(X,8,b) The heat necessary to supply latent heat of vaporization comes from sensible heat of the liquid (which therefore cools) and also from the water on which the liquid is spreading. (√)

(X,8,c) The model neglects temperature gradient in the liquid. That is, the entire liquid is considered at the same temperature as the water-liquid interface. This is cited as a weakness of the model. (√)

(X,8,d) Analytical solutions of equations (10.7b) through (10.9b) are impossible because of coupling between equations and their highly nonlinear character (primarily from the vapor pressure term). (√)

(X,8,e) The example worked out illustrates the utility of the model. (√)

(X,8,f) If the liquid temperature falls below the water-freezing temperature (see Table 10.1), ice may form beneath the spreading liquid surface. Ice formation is assumed as a continuous sheet formed over the whole area at the same time and conductivity of ice K_{ice} instead of K_w is used in equation (10.5). (√)

(X,8,g)* The present version of HACS has no provision to include complexities introduced by ice formation.

(X,9) *Section 10.9, Conclusions (p.149)*

(X,9,a) Model has been developed to predict rate of evaporation and extent of spread of a high-vapor-pressure liquid spilled on water. (√)

(X,9,b) Models derived for spread of nonvolatile liquids have been utilized. (√)

(X,9,c) Model based primarily on heat transfer from water and the change of sensible heat of liquid to supply the heat of evaporation. (√)

(X,9,d) Solution to governing equations obtained by numerical methods. (√)

(X,10) *Section 10.10, References (p.150)*

(X,10,a) References used in Section 10 are listed. (√)

(X,10,b)** Typographical error in reference (3). Author should be Weast, R. C. (ed.).

(X,10,c)* It would be helpful if the authors had mentioned page numbers for the cited references.

(X,11) *Section 10.11, List of Symbols (pp.150-152)*

(X,11,a)** For m, dimensionless mass of liquid, there should be no units listed, i.e., kg is incorrect.

(X,11,b)** Since the symbol $\dot{q}''(t)$, heat flux at time t, has not been used in the text, it should be deleted from the list of symbols.

(X,11,c)* The following symbols have been used in the text but are not listed in Section 10.11.

Symbol	Description	Unit
$\overline{h}_D$	mass transfer coefficient defined in equations (10.11a) and (10.11b)	m/s
K_w	thermal conductivity of water	W/m °K
K_{ice}	thermal conductivity of ice	W/m °K
$q(r,t)$	local heat flux from water at any time	J/m^2 s
$\overline{q}(t)$	mean heat flux from water at any time	J/m^2 s
r	radius	m
R	maximum radius at any time for a radial spill	m
T_{ch}	characteristic temperature defined in equation (10.11)	
T_F	freezing point of liquid	°C
t_{ch}	characteristic time defined in equation (10.11)	
$Y_0(t)$	thickness of boundary layer at the point of spill at any time	m
$Y(r,t)$	thickness of boundary layer	m

Greek Letters	Description	Unit
ρ	density	kg/m^3
ξ	r/R for radial spill	
	$\frac{\text{distance from point of spill}}{0.5 \times \text{size of spill}}$ for one-dimensional spill	

Sub-scripts	
i	initial

T(X,1) *Table 10.1 (p.153), Evaporation Rate and Temperature of a Spreading Pool of Diethyl Ether*

T(X,1,a) The program shown below uses the data of Section 10.7, Specific Example. This program was used with the subroutines RLJSP, FCT, OUTP, HMTC, PKRHI, PKRRK. We set TIME =3000.0. With IOUT=1, we were able to get intermediate results which can be compared with the corresponding values given in Table 10.1. The values of the temperature at times up to 1380 were obtained from the subroutine PKRHI as they are not printed by the subroutine OUTP. The value of temperature, where not available, has been left blank in Table (X,1). Units of the results obtained from HACS have been converted so that the comparison between Table (X,1) and Table 10.1 may become easy.

```
      IOUT=1
      IDIM=2
      VOLI=1.27E9
      DENL=.715
      VISL=.002842
      SURT=10.7
      XLAT=94.44
      CL=.478
      A=7.7756659
      B=1517.7447
      C=273.15
      TW=20.0
      DIFCO=.089
      XMOL=74.12
      TIME=3000.0
      CALL PKRHI(IDIM,CHNLW,VOLI,DENL,VISL,SURT,XLAT,CL,A,B,C,TW,
     *TIME,DIFCO,XMOL,VOL,SIZE,TEMP,SPEVA,TMEND,AREA,IOUT)
      WRITE(6,100) TIME,VOL,SIZE,TEMP,SPEVA,TMEND,AREA
  100 FORMAT(//,4(F16.4,2X),F16.8,2X,2(F16.4,2X))
      STOP
      END
```

TABLE (X,1)

Time (sec)	Temperature (°C)	Fraction of Initial Mass Remaining	Actual Mass Remaining (kg)	Specific Evaporation kg/s m^2	Pool Area m^2
0	20	1.00000	0.90805E06	0	0
120	16.77	0.98235	0.89202E06	0.88993E-02	0.29179E05
240	9.51	0.93437	0.84846E06	0.77794E-02	0.58358E05
360	1.94	0.86509	0.78555E06	0.67087E-02	0.87538E05
480	-3.86	0.78177	0.70989E06	0.59561E-02	0.10917E06
600	-7.58	0.69448	0.63062E06	0.55040E-02	0.12206E06
720	-10.11	0.60409	0.54854E06	0.52089E-02	0.13371E06
840	-12.03	0.51042	0.46349E06	0.49928E-02	0.14442E06
960	-13.60	0.41359	0.37556E06	0.48201E-02	0.15439E06
1080	-14.95	0.31382	0.28496E06	0.46747E-02	0.16376E06
1200	-16.15	0.21135	0.19191E06	0.45488E-02	0.17261E06
1320	-17.22	0.10641	0.96621E05	0.44460E-02	0.18104E06
1380	-17.71	0.053084	0.48203E05	0.44359E-02	0.18511E06
1410		0.026295	0.23877E05	0.46615E-02	0.18711E06
1417.5		0.019396	0.17613E05	0.43775E-02	0.18761E06
1425		0.012636	0.11474E05	0.43519E-02	0.18810E06
1432.5		0.00588	0.53390E04	0.43808E-02	0.18860E06
1433.4		0.00418	0.37991E04	0.43440E-02	0.18872E06
1436.2		0.00249	0.22626E04	0.43409E-02	0.18884E06
1438.1		0.00081	0.73222E03	0.47834E-02	0.18897E06
1438.4		0.00059	0.53368E03	0.43709E-02	0.18898E06
1438.6		0.00038	0.34121E03	0.43437E-02	0.18900E06
1438.8		0.00016	0.14944E03	0.44708E-02	0.18901E06
1438.9		0.00006	0.52982E02	0.11688E00	0.18902E06

At time=1438.9, IHLF had become 11 and control passed to the calling program with the following result printed out:

TIME=3000.0 sec, VOL=209000 cc, SIZE=24528.89 cm,

TEMP=-16.89°C, SPEVA=0.000447, TMEND=1438.9453 sec,

AREA=$1.89019*10^9 cm^2$

T(X,1,b) The results of Table (X,1) indicate that the output may be misleading for values of TIME greater than about 1438 sec. Therefore, we set TIME=60.0 and increased it by 60 sec each time until it became 3000.0 sec with IOUT=0. This program is listed below and the results for TIME≥1440 sec at intervals of 120 seconds are listed in Table (X,2). This output is exactly the same as obtained by MODV.

```
      IOUT=0
      IDIM=2
      VOLI=1.27E9
      DENL=.715
      VISL=.002342
      SURT=10.7
      XLAT=34.44
      CL=.473
      A=7.7756659
      B=1517.7447
      C=273.15
      TW=20.0
      DIFCO=.133
      XMOL=74.12
      TIME=60.0
   10 CALL PKRHI(IDIM,CHNLW,VOLI,DENL,VISL,SURT,XLAT,CL,A,B,C,TW,
     *TIME,DIFCO,XMOL,VOL,SIZE,TEMP,SPEVA,TMEND,AREA,IOUT)
      WRITE(6,100) TIME,VOL,SIZE,TEMP,SPEVA,TMEND,AREA
  100 FORMAT(///,4(F16.4,2X),F16.8,2X,2(F16.4,2X))
      TIME=TIME+60.0
      IF(TIME.LE.3000.0) GO TO 10
      STOP
      END.
```

TABLE (X,2)

Time, sec	Volume, cc	Size, cm	Temperature, °C	Specific Evaporation, gm/s cm^2	TMEND, sec	Pool Area, cm^2
1400	90601	24528	-17.86	.0004371	1438.65	1.89×10^9
1560	92889	24529	-16.92	.0004468	1438.98	1.89×10^9
1680	93200	24528	-18.06	.0004351	1438.96	1.89×10^9
1800	170800	24528	-12.05	.0004990	1438.96	1.89×10^9
1920	106412	24528	-17.12	.0004447	1438.05	1.89×10^9
2040	182396	24528	-17.16	.0004430	1438.76	1.89×10^9
2160	89834	24529	158.63	.0049767	1439.02	1.89×10^9
2280	96406	24527	349.66	.0146377	1438.45	1.89×10^9
2400	75569	24529	-17.98	.0004359	1439.06	1.89×10^9
2520	185189	24528	-17.43	.0004415	1438.96	1.89×10^9
2640	292831	24529	31.01	.001137	1438.90	1.89×10^9
2760	210408	24528	-17.83	.000437	1438.88	1.89×10^9
2880	91266	24529	2.82	.000683	1438.99	1.89×10^9
3000	209000	24529	-16.89	.000447	1438.94	1.89×10^9

The results of this table are discussed in Section D of this chapter. TMEND is the time at which the computations end in the subroutine PKRRX.

T(X,1,c)** It is evident from Table (X,1) that time for complete evaporation is close to 1439 sec and is not 1206.8 sec as listed in Table 10.1.

T(X,1,d)** The variation of specific evaporation with time given in Table 10.1 is incorrect. There is hardly any agreement for this quantity between Tables 10.1 and (X,1).

T(X,1,e)** The results for pool area agree during the first 360 sec. Thereafter, the agreement is progressively lost.

T(X,1,f)** The agreement between the values for actual mass remaining is progressively lost with time. The same is true of fraction of initial mass remaining, and temperature.

T(X,1,g)* At t=0, the subroutine OUTP prints specific evaporation rate =0.0 rather than initial specific evaporation rate.

T(X,1,h)** At time t=0.0 sec, it gives pool area=0.00000E00. By the initial conditions, at t=0, M=M_i and pool area cannot be zero. However, the subroutine RLJSP will give size=0 at t=0. In fact, the equations of Chapters 3 and 8 of AMSHAH are applicable only at t>0. In view of this, RLJSP needs to be slightly modified.

B. CRITIQUE OF THE MODEL (Chapter 10)

The model described in Chapter 10 of AMSHAH consists of a numerical solution of equations (10.8b), the energy equation, and (10.9b), the continuity equation. The major assumptions made in the derivation of this model are:

1) Mean heat flux from water at any instant is given by:

$$\overline{q} = c\,\frac{K_w(T_w - T)}{\sqrt{\pi\alpha_w t}} \qquad (10.5)$$

2) The mass transfer coefficient, h_p, is constant.

3) Liquid temperature is a function of time alone, i.e., it does not vary with the space coordinates at any time.

As discussed in Section (X,5), equation (10.5) is based on two assumptions: 1) the liquid-water interface temperature remains constant and 2) the only mode of heat exchange is the molecular conduction. Obviously, both these assumptions are unrealistic. The liquid temperature is certainly changing with time. Due to temperature gradients in water, convection currents will invariably be present. In addition, navigational waters will have an appreciable eddy activity, and the major mode of heat exchange is likely to be the result of eddy-mixing rather than molecular conduction as implied in equation (10.5).

Therefore, equation (10.5) will give a gross underestimation of the heat flux from the water to the liquid.

The assumption that the mass-transfer coefficient, h_p, is a constant is incorrect. Equations (10.8b) and (10.9b) can be obtained from the corresponding dimensional equations (10.8a) and (10.9a) without the need of assuming that the mass-transfer coefficient is constant. However, to obtain equation (10.7b) it is necessary to assume that the mass-transfer coefficient is constant. From equations (10.11a) and (10.11b), it is clear that $\bar{h}_D$ is a function of the size of the spread; and since the value of the size is available at different times from the subroutine RLJSP, it is possible to incorporate it in the computation of h_p. Again, h_p is obtained from $\bar{h}_D$ (calculated by equations (10.11a) and (10.11b)) in LN0015 if subroutine HMTC. It is

```
LN0015   3   HMP = HBAR/(RVAP*TEMP)
```

i.e., $h_p = h_D/RT$ where T is a constant equal to 293°K. The correct temperature to use is the temperature of the liquid $T(t)$, which is a function of time.

The specific evaporation rate, $\dot{E}''$, is computed in LN0082 of subroutine PKRHI; i.e.,

```
LN0082    SPEVA = -ZMI*AUX(2,2)/(TIMEC*AREA)
```

that is,

$$\dot{E}'' = \frac{-M\, dm/d\tau}{t_{ch} \times A} = -\frac{1}{A} \times \frac{dM}{dt}$$

SPEVA is also computed by an analogous equation in LN0038 of subroutine OUTP.

Another way to compute the specific evaporation rate is:

$$\dot{E}'' = h_p\, a\, e^{-b/T} \qquad \text{(X-11)}$$

where h_p has been assumed constant and the liquid temperature T is independent of (x,y,z).

The values of the specific evaporation rate obtained from HACS, i.e., from Table (X,1), as well as the values calculated from equation (X-11) for various times are tabulated below in Table (X,3).

TABLE (X,3)

Time, s	Temperature, °C	$\dot{E}''$ from Table (X,1), kg/s m^2	$\dot{E}''$ from Equation (X-11)	% Error[a]
120	-16.77	0.88993×10^{-2}	0.89173×10^{-2}	0.21
240	9.51	0.77794×10^{-2}	0.65422×10^{-2}	19
360	1.94	0.67087×10^{-2}	0.46546×10^{-2}	44
480	-3.86	0.59561×10^{-2}	0.35432×10^{-2}	68
600	-7.58	0.55040×10^{-2}	0.29511×10^{-2}	86
720	-10.11	0.52089×10^{-2}	0.26001×10^{-2}	100
840	-12.03	0.49928×10^{-2}	0.23579×10^{-2}	112
960	-13.60	0.48201×10^{-2}	0.21745×10^{-2}	122
1080	-14.95	0.46747×10^{-2}	0.20266×10^{-2}	131
1200	-16.15	0.45488×10^{-2}	0.19024×10^{-2}	139
1320	-17.22	0.44460×10^{-2}	0.17972×10^{-2}	147
1380	-17.71	0.44359×10^{-2}	0.17507×10^{-2}	153

[a] $\% \text{ Error} = \dfrac{[\dot{E}'' \text{ (from Col. 3)} - \dot{E}'' \text{ (from Col. 4)}]}{\dot{E}'' \text{ (from Col. 4)}} \times 100$

The results of Table (X,3) point to the fact that there exists a lack of internal consistency among the values of specific evaporation rates obtained by different methods. This indicates that results obtained from HACS are not sound, even if all the assumptions were obeyed.

C. *SENSITIVITY ANALYSIS (Chapter 10)*

Since the model described in Chapter 10 of AMSHAH consists of a numerical solution of equations (10.8b), the energy equation, and (10.9b), the continuity equation, an analytical sensitivity analysis as performed in the case of some of the chapters of AMSHAH is not possible. Therefore, a computer technique is used for the sensitivity analysis of this chapter.

MODV calculates six items, namely:

1) volume of liquid remaining,
2) size of the liquid pool,
3) temperature of the liquid,
4) specific evaporation rate
5) specified time or time for complete evaporation, and
6) pool area.

These calculated quantities (dependent variables) are functions of the two independent variables, viz., 1) initial volume of the spill and

2) water temperature, and of eight parameters, i.e., 1) liquid density, 2) liquid viscosity, 3) surface tension, 4) heat of vaporization, 5) liquid specific heat, 6) coefficient A of the vapor pressure equation, 7) coefficient B of the vapor pressure equation, and 8) diffusion coefficient.

The units for various quantities as they appear in Tables (X,4) through (X,29) are:

volume in cc
size of the pool in cm
temperature in °C
specific evaporation rate in gm/cm^2 sec
time in sec
density in gm/cc
pool area in cm^2
viscosity in gm/cm sec
surface tension in dyne/cm
heat of vaporization in cal/gm
diffusion coefficient in cm^2/sec

The sensitivity coefficient is defined as:

$$\frac{\text{fractional change in dependent varible}}{\text{fractional change in independent variable or parameter}}$$

where fractional change in independent variable or parameter has been taken to be +5% of its normal value. The normal values have been taken from Section 10.7, Specific Example, of Chapter 10 of AMSHAH. The results are reported in Tables (X,4) through (X,29).

The authors report the sensitivity analysis of Chapter 10 on pages 235-236 (Section 14. 9) of AMSHAH. Our review of this follows.

1) AMSHAH states that the main input parameters of the model are the mass of the spill and the vapor pressure temperature relationships for the liquid spilled. However, mass of the spill is not an input parameter. It is, in fact, the volume of the spill that is input to MODV.

2) It is stated that time for complete evaporation varies as the cube root of the mass spilled. Now, the mass spilled is proportional to the initial volume of the spill. The reported value (1/3) agrees with the sensitivity coefficient (0.2856) obtained by us for initial volume of spill.

3) The authors report the effect of changes in the liquid temperature on the time for complete evaporation. However, liquid temperature is not an input to MODV. It is always assumed to be equal to the water temperature. Therefore, changes in water temperature are equivalent to changes in the initial liquid temperature.

4) The increase in initial liquid temperature results in a smaller time for complete evaporation. This agrees with our sensitivity coefficient for water temperature, since it is negative. However, the figures reported for the changes in time for complete evaporation for various changes in the liquid temperature do not appear to agree with the sensitivity coefficient obtained by us. It can be seen from Table (X,4) that, for increase in water (liquid) temperature from 20°C (293°K) to 21°C (294°K), the fractional decrease in time for complete evaporation is (1 - 0.97948) or approximately 2%. That is, for about 1/3% increase in temperature (based on absolute temperature), the decrease in time for complete evaporation is 2%.

5) It can be seen from Table (X,4) that the importance of the variables/parameters that affect the time for complete evaporation can be ordered as follows:

a) vapor pressure equation, coefficient B
b) vapor pressure equation, coefficient A
c) liquid density
d) water temperature
e) diffusion coefficient
f) heat of vaporization of liquid

We expect that the values of the vapor pressure equation coefficients A and B, as available from the literature, are very accurate. The same is true of liquid density and latent heat of of vaporization. The diffusion coefficient obtained from the subroutine COMPD is likely to be inaccurate, since the equation used is meant for crude calculations. Therefore, the errors introduced in time for complete evaporation, as a consequence of the inaccurate data, are likely to be due to the errors in the value of the diffusion coefficient.

TABLE (X,4)

RESULTS FOR DIETHYL ETHER

TIME FOR COMPLETE EVAPORATION

Normal Value Is 1438.8 sec

INDEX	VARIABLE	SENSITIVITY COEFFICIENT	VARIABLE NORMAL	VARIABLE CHANGED	OUTPUT	FRACTION
1	Initial Volume of Spill	0.28561	1.27×10^9	1.3335×10^9	1459.4	1.01428
2	Water Temperature	-0.41049	20.0	21.0	1409.3	0.97948
INDEX	PARAMETER	SENSITIVITY COEFFICIENT	PARAMETER NORMAL	PARAMETER CHANGED	OUTPUT	FRACTION
1	Liquid Density	1.43780	0.715	0.75075	1542.3	1.07189
2	Liquid Viscosity	0.0000	0.002842	0.0029841	1438.8	1.0000
3	Surface Tension	0.0000	10.7	11.235	1438.8	1.0000
4	Heat of Vaporization of Liquid	0.29538	94.44	99.162	1460.1	1.01477
5	Liquid Specific Heat	-0.03584	0.478	0.5019	1436.2	0.99821
6	Vapor Pressure Equation Coefficient A	-6.35826	7.7756659	8.164492	981.4	0.68209
7	Vapor Pressure Equation Coefficient B	6.94141	1517.7447	1593.631935	1938.2	1.34707
8	Diffusion Coefficient	-0.32796	0.089	0.09345	1415.2	0.98360

TABLE (X,5)

RESULTS FOR DIETHYL ETHER

POOL RADIUS

Normal Value Is 6814.7 At Time = 60 sec

INDEX	VARIABLE	SENSITIVITY COEFFICIENT	VARIABLE NORMAL	VARIABLE CHANGED	OUTPUT	FRACTION
1	Initial Volume of Spill	0.24544	1.27×10^9	1.3335×10^9	6898.3	1.01227
2	Water Temperature	0.0000	20.0	21.0	6814.7	1.0000
INDEX	PARAMETER	SENSITIVITY COEFFICIENT	PARAMETER NORMAL	PARAMETER CHANGED	OUTPUT	FRACTION
1	Liquid Density	-0.65906	0.715	0.75075	6590.1	0.96705
2	Liquid Viscosity	0.0000	0.002842	0.0029841	6814.7	1.0000
3	Surface Tension	0.0000	10.7	11.235	6814.7	1.0000
4	Heat of Vaporization of Liquid	0.0000	94.44	99.162	6814.7	1.0000
5	Liquid Specific Heat	0.0000	0.478	0.5019	6814.7	1.0000
6	Vapor Pressure Equation Coefficient A	0.0000	7.7756659	8.164492	6814.7	1.0000
7	Vapor Pressure Equation Coefficient B	0.0000	1517.7447	1593.631935	6814.7	1.0000
8	Diffusion Coefficient	0.0000	0.089	0.09345	6814.7	1.0000

TABLE (X,6)

RESULTS FOR DIETHYL ETHER

POOL RADIUS

Normal Value Is 16692.5 At Time = 360 sec

INDEX	VARIABLE	SENSITIVITY COEFFICIENT	VARIABLE NORMAL	VARIABLE CHANGED	OUTPUT	FRACTION
1	Initial Volume of Spill	0.24544	1.27×10^9	1.3335×10^9	16897.4	1.01227
2	Water Temperature	0.0000	20.0	21.0	16692.5	1.0000
INDEX	PARAMETER	SENSITIVITY COEFFICIENT	PARAMETER NORMAL	PARAMETER CHANGED	OUTPUT	FRACTION
1	Liquid Density	-0.65906	0.715	0.75075	16142.5	0.967051
2	Liquid Viscosity	0.0000	0.002842	0.0029841	16692.5	1.0000
3	Surface Tension	0.0000	10.7	11.235	16692.5	1.0000
4	Heat of Vaporization of Liquid	0.0000	94.44	99.162	16692.5	1.0000
5	Liquid Specific Heat	0.0000	0.478	0.5019	16692.5	1.0000
6	Vapor Pressure Equation Coefficient A	0.0000	7.7756659	8.164492	16692.5	1.0000
7	Vapor Pressure Equation Coefficient B	0.0000	1517.7447	1593.631935	16692.5	1.0000
8	Diffusion Coefficient	0.0000	0.089	0.09345	16692.5	1.0000

TABLE (X,7)

RESULTS FOR DIETHYL ETHER

POOL RADIUS

Normal Value Is 20186.1 At Time = 660 sec

INDEX	VARIABLE	SENSITIVITY COEFFICIENT	VARIABLE NORMAL	VARIABLE CHANGED	OUTPUT	FRACTION
1	Initial Volume of Spill	0.32793	1.27×10^9	1.3335×10^9	20517.1	1.01640
2	Water Temperature	0.0000	20.0	21.0	20186.1	1.0000
INDEX	PARAMETER	SENSITIVITY COEFFICIENT	PARAMETER NORMAL	PARAMETER CHANGED	OUTPUT	FRACTION
1	Liquid Density	-0.44182	0.715	0.75075	19740.2	0.97791
2	Liquid Viscosity	0.0000	0.002842	0.0029841	20186.1	1.0000
3	Surface Tension	0.0000	10.7	11.235	20186.1	1.0000
4	Heat of Vaporization of Liquid	0.0000	94.44	99.162	20186.1	1.0000
5	Liquid Specific Heat	0.0000	0.478	0.5019	20186.1	1.0000
6	Vapor Pressure Equation Coefficient A	0.0000	7.7756659	8.164492	20186.1	1.0000
7	Vapor Pressure Equation Coefficient B	0.0000	1517.7447	1593.631935	20186.1	1.0000
8	Diffusion Coefficient	0.0000	0.089	0.09345	20186.1	1.0000

TABLE (X,8)

RESULTS FOR DIETHYL ETHER

POOL RADIUS

Normal Value Is 22168.4 At Time = 960 sec

INDEX	VARIABLE	SENSITIVITY COEFFICIENT	VARIABLE NORMAL	VARIABLE CHANGED	OUTPUT	FRACTION
1	Initial Volume of Spill	0.32793	1.27×10^9	1.3335×10^9	22531.9	1.01640
2	Water Temperature	0.0000	20.0	21.0	22168.4	1.0000
INDEX	PARAMETER	SENSITIVITY COEFFICIENT	PARAMETER NORMAL	PARAMETER CHANGED	OUTPUT	FRACTION
1	Liquid Density	-0.44182	0.715	0.75075	21678.	0.97791
2	Liquid Viscosity	0.0000	0.002842	0.0029841	22168.4	1.0000
3	Surface Tension	0.0000	10.7	11.235	22168.4	1.0000
4	Heat of Vaporization of Liquid	0.0000	94.44	99.162	22168.4	1.0000
5	Liquid Specific Heat	0.0000	0.478	0.5019	22168.4	1.0000
6	Vapor Pressure Equation Coefficient A	0.0000	7.7756659	8.164492	22168.4	1.0000
7	Vapor Pressure Equation Coefficient B	0.0000	1517.7447	1593.631935	22168.4	1.0000
8	Diffusion Coefficient	0.0000	0.089	0.09345	22168.4	1.0000

TABLE (X,9)

RESULTS FOR DIETHYL ETHER

POOL RADIUS

Normal Value Is 23727.9 At Time = 1260 sec

INDEX	VARIABLE	SENSITIVITY COEFFICIENT	VARIABLE NORMAL	VARIABLE CHANGED	OUTPUT	FRACTION
1	Initial Volume of Spill	0.32793	1.27×10^9	1.3335×10^9	24117.0	1.01640
2	Water Temperature	0.0000	20.0	21.0	23727.0	1.0000
INDEX	PARAMETER	SENSITIVITY COEFFICIENT	PARAMETER NORMAL	PARAMETER CHANGED	OUTPUT	FRACTION
1	Liquid Density	-0.44182	0.715	0.75075	23203.7	0.97791
2	Liquid Viscosity	0.0000	0.002842	0.0029841	23727.9	1.0000
3	Surface Tension	0.0000	10.7	11.235	23727.9	1.0000
4	Heat of Vaporization of Liquid	0.0000	94.44	99.162	23727.9	1.0000
5	Liquid Specific Heat	0.0000	0.478	0.5019	23727.9	1.0000
6	Vapor Pressure Equation Coefficient A	-1.20828	7.7756659	8.164492	22294.4	0.93959
7	Vapor Pressure Equation Coefficient B	0.0000	1517.7447	1593.631935	23727.9	1.0000
8	Diffusion Coefficient	0.0000	0.089	0.09345	23727.9	1.0000

TABLE (X,10)

RESULTS FOR DIETHYL ETHER

VOLUME OF LIQUID REMAINING

Normal Value Is 1.264×10^9 At Time = 60 sec

INDEX	VARIABLE	SENSITIVITY COEFFICIENT	VARIABLE NORMAL	VARIABLE CHANGED	OUTPUT	FRACTION
1	Initial Volume of Spill	1.00257	1.27×10^9	1.3335×10^9	1.328×10^9	1.05013
2	Water Temperature	-0.00372	20.0	21.0	1.264×10^9	0.99981
INDEX	PARAMETER	SENSITIVITY COEFFICIENT	PARAMETER NORMAL	PARAMETER CHANGED	OUTPUT	FRACTION
1	Liquid Density	0.00984	0.715	0.75075	1.2649×10^9	1.00049
2	Liquid Viscosity	0.0000	0.002842	0.0029841	1.264×10^9	1.0000
3	Surface Tension	0.0000	10.7	11.235	1.264×10^9	1.0000
4	Heat of Vaporization of Liquid	0.0000	94.44	99.162	1.264×10^9	1.0000
5	Liquid Specific Heat	0.0000	0.478	0.5019	1.264×10^9	1.0000
6	Vapor Pressure Equation Coefficient A	-0.12872	7.7756659	8.164492	1.2561×10^9	0.99356
7	Vapor Pressure Equation Coefficient B	0.04052	1517.7447	1593.631935	1.2668×10^9	1.00203
8	Diffusion Coefficient	-0.00297	0.089	0.09345	1.264×10^9	0.99985

TABLE (X,11)

RESULTS FOR DIETHYL ETHER

VOLUME OF LIQUID REMAINING

Normal Value Is 1.09866×10^9 At Time = 360 sec

INDEX	VARIABLE	SENSITIVITY COEFFICIENT	VARIABLE NORMAL	VARIABLE CHANGED	OUTPUT	FRACTION
1	Initial Volume of Spill	1.07785	1.27×10^9	1.3335×10^9	1.15787×10^9	1.05389
2	Water Temperature	-0.10938	20.0	21.0	1.0926×10^9	0.99453
INDEX	**PARAMETER**	**SENSITIVITY COEFFICIENT**	**PARAMETER NORMAL**	**PARAMETER CHANGED**	**OUTPUT**	**FRACTION**
1	Liquid Density	0.30131	0.715	0.75075	1.115×10^9	1.01507
2	Liquid Viscosity	0.0000	0.002842	0.0029841	1.0986×10^9	1.0000
3	Surface Tension	0.0000	10.7	11.235	1.0986×10^9	1.0000
4	Heat of Vaporization of Liquid	0.02618	94.44	99.162	1.10×10^9	1.00131
5	Liquid Specific Heat	-0.01803	0.478	0.5019	1.0977×10^9	0.99910
6	Vapor Pressure Equation Coefficient A	-2.97922	7.7756659	8.164492	0.935×10^9	0.85104
7	Vapor Pressure Equation Coefficient B	1.26283	1517.7447	1593.631935	1.168×10^9	1.06314
8	Diffusion Coefficient	-0.08456	0.089	0.09345	1.094×10^9	0.99577

TABLE (X,12)

RESULTS FOR DIETHYL ETHER

VOLUME OF LIQUID REMAINING

Normal Value Is 0.825×10^9 At Time = 660 sec

INDEX	VARIABLE	SENSITIVITY COEFFICIENT	VARIABLE NORMAL	VARIABLE CHANGED	OUTPUT	FRACTION
1	Initial Volume of Spill	1.22079	1.27×10^9	1.3335×10^9	0.8755×10^9	1.06104
2	Water Temperature	-0.32958	20.0	21.0	0.8115×10^9	0.98352
INDEX	**PARAMETER**	**SENSITIVITY COEFFICIENT**	**PARAMETER NORMAL**	**PARAMETER CHANGED**	**OUTPUT**	**FRACTION**
1	Liquid Density	0.92983	0.715	0.75075	0.863×10^9	1.04649
2	Liquid Viscosity	0.0000	0.002842	0.0029841	0.825×10^9	1.0000
3	Surface Tension	0.0000	10.7	11.235	0.825×10^9	1.0000
4	Heat of Vaporization of Liquid	0.15163	94.44	99.162	0.831×10^9	1.00758
5	Liquid Specific Heat	-0.06122	0.478	0.5019	0.8226×10^9	0.99694
6	Vapor Pressure Equation Coefficient A	-7.91603	7.7756659	8.164492	0.4985×10^9	0.60420
7	Vapor Pressure Equation Coefficient B	3.95604	1517.7447	1593.631935	0.988×10^9	1.1978
8	Diffusion Coefficient	-0.24706	0.089	0.09345	0.8149×10^9	0.98765

TABLE (X,13)

RESULTS FOR DIETHYL ETHER

VOLUME OF LIQUID REMAINING

Normal Value Is 5.253×10^8 At Time = 960 sec

INDEX	VARIABLE	SENSITIVITY COEFFICIENT	VARIABLE NORMAL	VARIABLE CHANGED	OUTPUT	FRACTION
1	Initial Volume of Spill	1.55101	1.27×10^9	1.3335×10^9	5.66×10^8	1.07755
2	Water Temperature	-0.81227	20.0	21.0	5.039×10^8	0.95939
INDEX	PARAMETER	SENSITIVITY COEFFICIENT	PARAMETER NORMAL	PARAMETER CHANGED	OUTPUT	FRACTION
1	Liquid Density	2.42179	0.715	0.75075	5.8886×10^8	1.12109
2	Liquid Viscosity	0.0000	0.002842	0.0029841	5.253×10^8	1.0000
3	Surface Tension	0.0000	10.7	11.235	5.253×10^8	1.0000
4	Heat of Vaporization of Liquid	0.46940	94.44	99.162	5.376×10^8	1.02347
5	Liquid Specific Heat	-0.11442	0.478	0.5019	5.222×10^8	0.99428
6	Vapor Pressure Equation Coefficient A	-18.6646	7.7756659	8.164492	0.3507×10^8	0.06677
7	Vapor Pressure Equation Coefficient B	9.86645	1517.7447	1593.631935	7.8438×10^8	1.49332
8	Diffusion Coefficient	-0.59889	0.089	0.09345	5.0953×10^8	0.97006

TABLE (X,14)

RESULTS FOR DIETHYL ETHER

VOLUME OF LIQUID REMAINING

Normal Value Is 2.021×10^8 At Time = 1260 sec

INDEX	VARIABLE	SENSITIVITY COEFFICIENT	VARIABLE NORMAL	VARIABLE CHANGED	OUTPUT	FRACTION
1	Initial Volume of Spill	3.01575	1.27×10^9	1.3335×10^9	2.326×10^8	1.15079
2	Water Temperature	-2.90523	20.0	21.0	1.728×10^8	0.85474
INDEX	PARAMETER	SENSITIVITY COEFFICIENT	PARAMETER NORMAL	PARAMETER CHANGED	OUTPUT	FRACTION
1	Liquid Density	9.06196	0.715	0.75075	2.937×10^8	1.45310
2	Liquid Viscosity	0.0000	0.002842	0.0029841	2.021×10^8	1.0000
3	Surface Tension	0.0000	10.7	11.235	2.021×10^8	1.0000
4	Heat of Vaporization of Liquid	1.90842	94.44	99.162	2.214×10^8	1.09542
5	Liquid Specific Heat	-0.31053	0.478	0.5019	1.99×10^8	0.98447
6	Vapor Pressure Equation Coefficient A	-19.99717	7.7756659	8.164492	0.2859×10^8	0.00014
7	Vapor Pressure Equation Coefficient B	35.50873	1517.7447	1593.631935	5.61×10^8	2.77544
8	Diffusion Coefficient	-2.11824	0.089	0.09345	1.7277×10^8	0.89409

TABLE (X,15)

RESULTS FOR DIETHYL ETHER

LIQUID TEMPERATURE

Normal Value Is 19.13 At Time = 60 sec

INDEX	VARIABLE	SENSITIVITY COEFFICIENT	VARIABLE NORMAL	VARIABLE CHANGED	OUTPUT	FRACTION
1	Initial Volume of Spill	0.02392	1.27×10^9	1.3335×10^9	19.16	1.00120
2	Water Temperature	1.0079	20.0	21.0	20.10	1.05040
INDEX	PARAMETER	SENSITIVITY COEFFICIENT	PARAMETER NORMAL	PARAMETER CHANGED	OUTPUT	FRACTION
1	Liquid Density	0.09589	0.715	0.75075	9.23	1.00479
2	Liquid Viscosity	0.0000	0.002842	0.0029841	19.13	1.0000
3	Surface Tension	0.0000	10.7	11.235	19.13	1.0000
4	Heat of Vaporization of Liquid	-0.04491	94.44	99.162	19.09	0.99775
5	Liquid Specific Heat	0.04157	0.478	0.5019	19.17	1.00208
6	Vapor Pressure Equation Coefficient A	-1.29325	7.7756659	8.164492	17.90	0.93534
7	Vapor Pressure Equation Coefficient B	0.40548	1517.7447	1593.631935	19.52	1.02027
8	Diffusion Coefficient	-0.02977	0.089	0.09345	19.11	0.99851

TABLE (X,16)

RESULTS FOR DIETHYL ETHER

LIQUID TEMPERATURE

Normal Value Is 1.94 At Time = 360 sec

INDEX	VARIABLE	SENSITIVITY COEFFICIENT	VARIABLE NORMAL	VARIABLE CHANGED	OUTPUT	FRACTION
1	Initial Volume of Spill	2.71269	1.27×10^9	1.3335×10^9	2.20	1.13563
2	Water Temperature	3.65481	20.0	21.0	2.29	1.18274
INDEX	PARAMETER	SENSITIVITY COEFFICIENT	PARAMETER NORMAL	PARAMETER CHANGED	OUTPUT	FRACTION
1	Liquid Density	10.61704	0.715	0.75075	2.97	1.53085
2	Liquid Viscosity	0.0000	0.002842	0.0029841	1.94	1.0000
3	Surface Tension	0.0000	10.7	11.235	1.94	1.0000
4	Heat of Vaporization of Liquid	-7.36223	94.44	99.162	1.22	0.63189
5	Liquid Specific Heat	4.09319	0.478	0.5019	2.33	1.20466
6	Vapor Pressure Equation Coefficient A	-180.93958	7.7756659	8.164492	-15.59	-8.04698
7	Vapor Pressure Equation Coefficient B	76.24396	1517.7447	1593.631935	9.32	4.81220
8	Diffusion Coefficient	-5.12253	0.089	0.09345	1.44	0.74387

TABLE (X,17)

RESULTS FOR DIETHYL ETHER

LIQUID TEMPERATURE

Normal Value Is -8.95 At Time = 660 sec

INDEX	VARIABLE	SENSITIVITY COEFFICIENT	VARIABLE NORMAL	VARIABLE CHANGED	OUTPUT	FRACTION
1	Initial Volume of Spill	-0.29609	1.27×10^9	1.3335×10^9	-8.82	0.98520
2	Water Temperature	-0.32076	20.0	21.0	-8.81	0.98396
INDEX	PARAMETER	SENSITIVITY COEFFICIENT	PARAMETER NORMAL	PARAMETER CHANGED	OUTPUT	FRACTION
1	Liquid Density	-0.91275	0.715	0.75075	-8.54	0.95436
2	Liquid Viscosity	0.0000	0.002842	0.0029841	-8.95	1.0000
3	Surface Tension	0.0000	10.7	11.235	-8.95	1.0000
4	Heat of Vaporization of Liquid	2.00366	94.44	99.162	-9.85	1.10018
5	Liquid Specific Heat	-0.30808	0.478	0.5019	-8.81	0.98460
6	Vapor Pressure Equation Coefficient A	42.69191	7.7756659	8.164492	-28.06	3.13460
7	Vapor Pressure Equation Coefficient B	-23.15634	1517.7447	1593.631935	1.41	-0.15782
8	Diffusion Coefficient	1.40287	0.089	0.09345	-9.58	1.07014

TABLE (X,18)

RESULTS FOR DIETHYL ETHER

LIQUID TEMPERATURE

Normal Value Is -13.60 At Time = 960 sec

INDEX	VARIABLE	SENSITIVITY COEFFICIENT	VARIABLE NORMAL	VARIABLE CHANGED	OUTPUT	FRACTION
1	Initial Volume of Spill	-0.13457	1.27×10^9	1.3335×10^9	-13.51	0.99327
2	Water Temperature	-0.13531	20.0	21.0	-13.51	0.99323
INDEX	PARAMETER	SENSITIVITY COEFFICIENT	PARAMETER NORMAL	PARAMETER CHANGED	OUTPUT	FRACTION
1	Liquid Density	-0.23346	0.715	0.75075	-13.44	0.98833
2	Liquid Viscosity	0.0000	0.002842	0.0029841	-13.60	1.0000
3	Surface Tension	0.0000	10.7	11.235	-13.60	1.0000
4	Heat of Vaporization of Liquid	1.37637	94.44	99.162	-14.53	1.06882
5	Liquid Specific Heat	-0.04996	0.478	0.5019	-13.56	0.99750
6	Vapor Pressure Equation Coefficient A	28.15503	7.7756659	8.164492	-32.74	2.40775
7	Vapor Pressure Equation Coefficient B	-16.38696	1517.7447	1593.631935	-2.46	0.18065
8	Diffusion Coefficient	0.95585	0.089	0.09345	-14.25	1.04779

TABLE (X,19)

RESULTS FOR DIETHYL ETHER

LIQUID TEMPERATURE

Normal Value Is -16.70 At Time = 1260 sec

INDEX	VARIABLE	SENSITIVITY COEFFICIENT	VARIABLE NORMAL	VARIABLE CHANGED	OUTPUT	FRACTION
1	Initial Volume of Spill	-0.10047	1.27×10^9	1.3335×10^9	-16.61	0.99498
2	Water Temperature	-0.06485	20.0	21.0	-16.64	0.99676
INDEX	PARAMETER	SENSITIVITY COEFFICIENT	PARAMETER NORMAL	PARAMETER CHANGED	OUTPUT	FRACTION
1	Liquid Density	-0.12122	0.715	0.75075	-16.60	0.99394
2	Liquid Viscosity	0.0000	0.002842	0.0029841	-16.70	1.0000
3	Surface Tension	0.0000	10.7	11.235	-16.70	1.0000
4	Heat of Vaporization of Liquid	1.15178	94.44	99.162	-17.66	1.05759
5	Liquid Specific Heat	-0.00798	0.478	0.5019	-16.69	0.99960
6	Vapor Pressure Equation Coefficient A	-25.82163	7.7756659	8.164492	4.86	-0.29108
7	Vapor Pressure Equation Coefficient B	-13.96302	1517.7447	1593.631935	-5.04	0.30185
8	Diffusion Coefficient	0.79959	0.089	0.09345	-17.36	1.03998

TABLE (X,20)

RESULTS FOR DIETHYL ETHER

SPECIFIC EVAPORATION RATE

Normal Value Is 0.00092844 At Time = 60 sec

INDEX	VARIABLE	SENSITIVITY COEFFICIENT	VARIABLE NORMAL	VARIABLE CHANGED	OUTPUT	FRACTION
1	Initial Volume of Spill	-0.05683	1.27×10^9	1.3335×10^9	0.92581×10^{-3}	0.99716
2	Water Temperature	0.81626	20.0	21.0	0.96634×10^{-3}	1.04081
INDEX	PARAMETER	SENSITIVITY COEFFICIENT	PARAMETER NORMAL	PARAMETER CHANGED	OUTPUT	FRACTION
1	Liquid Density	0.03265	0.715	0.75075	0.92996×10^{-3}	1.00163
2	Liquid Viscosity	0.0000	0.002842	0.0029841	0.92844×10^{-3}	1.0000
3	Surface Tension	0.0000	10.7	11.235	0.92844×10^{-3}	1.0000
4	Heat of Vaporization of Liquid	-0.01528	94.44	99.162	0.92774×10^{-3}	0.99924
5	Liquid Specific Heat	0.01415	0.478	0.5019	0.9291×10^{-3}	1.00071
6	Vapor Pressure Equation Coefficient A	27.88691	7.7756659	8.164492	2.223×10^{-3}	2.39435
7	Vapor Pressure Equation Coefficient B	-8.90902	1517.7447	1593.631935	0.51487×10^{-3}	0.55455
8	Diffusion Coefficient	0.65080	0.089	0.09345	0.95866×10^{-3}	1.03254

TABLE (X,21)

RESULTS FOR DIETHYL ETHER

SPECIFIC EVAPORATION RATE

Normal Value Is 0.00067086 At Time = 360 sec

INDEX	VARIABLE	SENSITIVITY COEFFICIENT	VARIABLE NORMAL	VARIABLE CHANGED	OUTPUT	FRACTION
1	Initial Volume of Spill	0.04043	1.27×10^{9}	1.3335×10^{9}	0.672×10^{-3}	1.00202
2	Water Temperature	0.60928	20.0	21.0	0.6913×10^{-3}	1.03046
INDEX	PARAMETER	SENSITIVITY COEFFICIENT	PARAMETER NORMAL	PARAMETER CHANGED	OUTPUT	FRACTION
1	Liquid Density	0.41578	0.715	0.75075	0.6848×10^{-3}	1.02079
2	Liquid Viscosity	0.0000	0.002842	0.0029841	0.67086×10^{-3}	1.0000
3	Surface Tension	0.0000	10.7	11.235	0.67086×10^{-3}	1.0000
4	Heat of Vaporization of Liquid	-0.28512	94.44	99.162	0.6613×10^{-3}	0.98574
5	Liquid Specific Heat	0.15965	0.478	0.5019	0.676×10^{-3}	1.00798
6	Vapor Pressure Equation Coefficient A	13.61563	7.7756659	8.164492	1.1276×10^{-3}	1.68078
7	Vapor Pressure Equation Coefficient B	-7.3923	1517.7447	1593.631935	0.4229×10^{-3}	0.63038
8	Diffusion Coefficient	0.45603	0.089	0.09345	0.6862×10^{-3}	1.0228

TABLE (X,22)

RESULTS FOR DIETHYL ETHER

SPECIFIC EVAPORATION RATE

Normal Value Is 0.00053428 At Time = 660

INDEX	VARIABLE	SENSITIVITY COEFFICIENT	VARIABLE NORMAL	VARIABLE CHANGED	OUTPUT	FRACTION
1	Initial Volume of Spill	-0.00738	1.27×10^{9}	1.3335×10^{9}	0.5341×10^{-3}	0.99963
2	Water Temperature	0.52748	20.0	21.0	0.548×10^{-3}	1.02637
INDEX	PARAMETER	SENSITIVITY COEFFICIENT	PARAMETER NORMAL	PARAMETER CHANGED	OUTPUT	FRACTION
1	Liquid Density	0.17836	0.715	0.75075	0.539×10^{-3}	1.00892
2	Liquid Viscosity	0.0000	0.002842	0.0029841	0.534×10^{-3}	1.0000
3	Surface Tension	0.0000	10.7	11.235	0.534×10^{-3}	1.0000
4	Heat of Vaporization of Liquid	-0.38793	94.44	99.162	0.524×10^{-3}	0.9806
5	Liquid Specific Heat	0.0609	0.478	0.5019	0.536×10^{-3}	1.0030
6	Vapor Pressure Equation Coefficient A	11.26734	7.7756659	8.164492	0.835×10^{-3}	1.56337
7	Vapor Pressure Equation Coefficient B	-6.547	1517.7447	1593.631935	0.3594×10^{-3}	0.67265
8	Diffusion Coefficient	0.38014	0.089	0.09345	0.544×10^{-3}	1.01901

TABLE (X,23)

RESULTS FOR DIETHYL ETHER

SPECIFIC EVAPORATION RATE

Normal Value Is 0.000482 At Time = 960 sec

INDEX	VARIABLE	SENSITIVITY COEFFICIENT	VARIABLE NORMAL	VARIABLE CHANGED	OUTPUT	FRACTION
1	Initial Volume of Spill	-0.02377	1.27×10^9	1.3335×10^9	0.481×10^{-3}	0.99881
2	Water Temperature	0.50596	20.0	21.0	0.494×10^{-3}	1.0253
INDEX	PARAMETER	SENSITIVITY COEFFICIENT	PARAMETER NORMAL	PARAMETER CHANGED	OUTPUT	FRACTION
1	Liquid Density	0.07169	0.715	0.75075	0.4837×10^{-3}	1.00358
2	Liquid Viscosity	0.0000	0.002842	0.0029841	0.482×10^{-3}	1.0000
3	Surface Tension	0.0000	10.7	11.235	0.482×10^{-3}	1.0000
4	Heat of Vaporization of Liquid	-0.41925	94.44	99.162	0.472×10^{-3}	0.97904
5	Liquid Specific Heat	0.01533	0.478	0.5019	0.4824×10^{-3}	1.00077
6	Vapor Pressure Equation Coefficient A	10.7145	7.7756659	8.164492	0.7402×10^{-3}	1.5357
7	Vapor Pressure Equation Coefficient B	-6.27615	1517.7447	1593.631935	0.331×10^{-3}	0.6862
8	Diffusion Coefficient	0.35984	0.089	0.09345	0.491×10^{-3}	1.01799

TABLE (X,24)

RESULTS FOR DIETHYL ETHER

SPECIFIC EVAPORATION RATE

Normal Value Is 0.00044908 At Time = 1260 sec

INDEX	VARIABLE	SENSITIVITY COEFFICIENT	VARIABLE NORMAL	VARIABLE CHANGED	OUTPUT	FRACTION
1	Initial Volume of Spill	-0.02628	1.27×10^9	1.3335×10^9	0.4485×10^{-3}	0.99869
2	Water Temperature	0.48907	20.0	21.0	0.4601×10^{-3}	1.02445
INDEX	PARAMETER	SENSITIVITY COEFFICIENT	PARAMETER NORMAL	PARAMETER CHANGED	OUTPUT	FRACTION
1	Liquid Density	0.04680	0.715	0.75075	0.450×10^{-3}	1.00234
2	Liquid Viscosity	0.0000	0.002842	0.0029841	0.4491×10^{-3}	1.0000
3	Surface Tension	0.0000	10.7	11.235	0.4491×10^{-3}	1.0000
4	Heat of Vaporization of Liquid	-0.44107	94.44	99.162	0.4392×10^{-3}	0.97795
5	Liquid Specific Heat	0.00308	0.478	0.5019	0.4492×10^{-3}	1.00015
6	Vapor Pressure Equation Coefficient A	57.50538	7.7756659	8.164492	1.74×10^{-3}	3.87527
7	Vapor Pressure Equation Coefficient B	-6.08342	1517.7447	1593.631935	0.3125×10^{-3}	0.69583
8	Diffusion Coefficient	0.34422	0.089	0.09345	0.4568×10^{-3}	1.01721

TABLE (X,25)

RESULTS FOR DIETHYL ETHER

POOL AREA

Normal Value Is 1.4589607×10^8 At Time = 60 sec

INDEX	VARIABLE	SENSITIVITY COEFFICIENT	VARIABLE NORMAL	VARIABLE CHANGED	OUTPUT	FRACTION
1	Initial Volume of Spill	0.49390	1.27×10^9	1.3335×10^9	1.495×10^8	1.02470
2	Water Temperature	0.0000	20.0	21.0	1.459×10^8	1.0000
INDEX	PARAMETER	SENSITIVITY COEFFICIENT	PARAMETER NORMAL	PARAMETER CHANGED	OUTPUT	FRACTION
1	Liquid Density	-1.29640	0.715	0.75075	[illegible] $\times 10^8$	0.93518
2	Liquid Viscosity	0.0000	0.002842	0.0029841	1.459×10^8	1.0000
3	Surface Tension	0.0000	10.7	11.235	1.459×10^8	1.0000
4	Heat of Vaporization of Liquid	0.0000	94.44	99.162	1.459×10^8	1.0000
5	Liquid Specific Heat	0.0000	0.478	0.5019	1.459×10^8	1.0000
6	Vapor Pressure Equation Coefficient A	0.0000	7.7756659	8.164492	1.459×10^8	1.0000
7	Vapor Pressure Equation Coefficient B	0.0000	1517.7447	1593.631935	1.459×10^8	1.0000
8	Diffusion Coefficient	0.0000	0.089	0.09345	1.459×10^8	1.0000

TABLE (X,26)

RESULTS FOR DIETHYL ETHER

POOL AREA

Normal Value Is 8.75376×10^8 At Time = 360

INDEX	VARIABLE	SENSITIVITY COEFFICIENT	VARIABLE NORMAL	VARIABLE CHANGED	OUTPUT	FRACTION
1	Initial Volume of Spill	0.49390	1.27×10^9	1.3335×10^9	8.9699×10^8	1.02470
2	Water Temperature	0.0000	20.0	21.0	8.7538×10^8	1.0000
INDEX	PARAMETER	SENSITIVITY COEFFICIENT	PARAMETER NORMAL	PARAMETER CHANGED	OUTPUT	FRACTION
1	Liquid Density	-1.29640	0.715	0.75075	8.1863×10^8	0.93518
2	Liquid Viscosity	0.0000	0.002842	0.0029841	8.7538×10^8	1.0000
3	Surface Tension	0.0000	10.7	11.235	8.7538×10^8	1.0000
4	Heat of Vaporization of Liquid	0.0000	94.44	99.162	8.7538×10^8	1.0000
5	Liquid Specific Heat	0.0000	0.478	0.5019	8.7538×10^8	1.0000
6	Vapor Pressure Equation Coefficient A	0.0000	7.7756659	8.164492	8.7538×10^8	1.0000
7	Vapor Pressure Equation Coefficient B	0.0000	1517.7447	1593.631935	8.7538×10^8	1.0000
8	Diffusion Coefficient	0.0000	0.089	0.09345	8.7538×10^8	1.0000

TABLE (X,27)

RESULTS FOR DIETHYL ETHER

POOL AREA

Normal Value Is 1.280134×10^9 At Time = 660 sec

INDEX	VARIABLE	SENSITIVITY COEFFICIENT	VARIABLE NORMAL	VARIABLE CHANGED	OUTPUT	FRACTION
1	Initial Volume of Spill	0.66123	1.27×10^9	1.3335×10^9	1.3224×10^9	1.03306
2	Water Temperature	0.0000	20.0	21.0	1.2801×10^9	1.0000
INDEX	PARAMETER	SENSITIVITY COEFFICIENT	PARAMETER NORMAL	PARAMETER CHANGED	OUTPUT	FRACTION
1	Liquid Density	-0.87388	0.715	0.75075	1.2242×10^9	0.95631
2	Liquid Viscosity	0.0000	0.002842	0.0029841	1.2801×10^9	1.0000
3	Surface Tension	0.0000	10.7	11.235	1.2801×10^9	1.0000
4	Heat of Vaporization of Liquid	0.0000	94.44	99.162	1.2801×10^9	1.0000
5	Liquid Specific Heat	0.0000	0.478	0.5019	1.2801×10^9	1.0000
6	Vapor Pressure Equation Coefficient A	0.0000	7.7756659	8.164492	1.2801×10^9	1.0000
7	Vapor Pressure Equation Coefficient B	0.0000	1517.7447	1593.631935	1.2801×10^9	1.0000
8	Diffusion Coefficient	0.0000	0.089	0.09345	1.2801×10^9	1.0000

TABLE (X,28)

RESULTS FOR DIETHYL ETHER

POOL AREA

Normal Value Is 1.5439×10^9 At Time = 960 sec

INDEX	VARIABLE	SENSITIVITY COEFFICIENT	VARIABLE NORMAL	VARIABLE CHANGED	OUTPUT	FRACTION
1	Initial Volume of Spill	0.66123	1.27×10^9	1.3335×10^9	1.5949×10^9	1.03306
2	Water Temperature	0.0000	20.0	21.0	1.5439×10^9	1.0000
INDEX	PARAMETER	SENSITIVITY COEFFICIENT	PARAMETER NORMAL	PARAMETER CHANGED	OUTPUT	FRACTION
1	Liquid Density	-0.87388	0.715	0.75075	1.4764×10^9	0.95631
2	Liquid Viscosity	0.0000	0.002842	0.0029841	1.5439×10^9	1.0000
3	Surface Tension	0.0000	10.7	11.235	1.5439×10^9	1.0000
4	Heat of Vaporization of Liquid	0.0000	94.44	99.162	1.5439×10^9	1.0000
5	Liquid Specific Heat	0.0000	0.478	0.5019	1.5439×10^9	1.0000
6	Vapor Pressure Equation Coefficient A	0.0000	7.7756659	8.164492	1.5439×10^9	1.0000
7	Vapor Pressure Equation Coefficient B	0.0000	1517.7447	1593.631935	1.5439×10^9	1.0000
8	Diffusion Coefficient	0.0000	0.089	0.09345	1.5439×10^9	1.0000

TABLE (X,29)

RESULTS FOR DIETHYL ETHER

POOL AREA

Normal Value Is 1.76876×10^9 At Time = 1260 sec

INDEX	VARIABLE	SENSITIVITY COEFFICIENT	VARIABLE NORMAL	VARIABLE CHANGED	OUTPUT	FRACTION
1	Initial Volume of Spill	0.66123	1.27×10^9	1.3335×10^9	1.8272×10^9	1.03306
2	Water Temperature	0.0000	20.0	21.0	1.7688×10^9	1.0000
INDEX	PARAMETER	SENSITIVITY COEFFICIENT	PARAMETER NORMAL	PARAMETER CHANGED	OUTPUT	FRACTION
1	Liquid Density	-0.87388	0.715	0.75075	1.6915×10^9	0.95631
2	Liquid Viscosity	0.0000	0.002842	0.0029841	1.7688×10^9	1.0000
3	Surface Tension	0.0000	10.7	11.235	1.7688×10^9	1.0000
4	Heat of Vaporization of Liquid	0.0000	94.44	99.162	1.7688×10^9	1.0000
5	Liquid Specific Heat	0.0000	0.478	0.5019	1.7688×10^9	1.0000
6	Vapor Pressure Equation Coefficient A	-2.34356	7.7756659	8.164492	1.5615×10^9	0.88282
7	Vapor Pressure Equation Coefficient B	0.0000	1517.7447	1593.631935	1.7688×10^9	1.0000
8	Diffusion Coefficient	0.0000	0.089	0.09345	1.7688×10^9	1.0000

D. HACS ERROR ANALYSIS (Chapter 10)

MODV obtains data from the State File and computes 1) volume, 2) size, 3) temperature, 4) specific evaporation rate, 5) time at which computation terminates, and 6) pool area for any given time. There is a provision to obtain the above items in the case of spill for the channel spread as well as for the radial spill. It calls subroutines BEGPR, FRCL, IRCL, EPRNT, COMPD, PKRHI, FSV, ENDPR. The subroutine PKRHI calls HMTC, PKRRK, OUTP, FCT. All the subroutines have been checked for errors.

MODV:

```
LN0046      TMAX=TW
  0047      IF(TA.GT.TMAX)TMAX=TA
```

MODV considers the possibility that air temperature and water temperature could be different. They are user's input values. However, the subroutine HMTC, instead of using the input air temperature to calculate the air properties, uses a constant temperature of 293°K.

LN0049 PRES=10.**(A-(B/(TMAX+C)))

MODV sets the greater of air temperature, water temperature as TMAX to evaluate the initial vapor pressure of the spill. However, the correct temperature to use is the temperature of the spilled liquid itself.

HMTC:

LN0006 TEMP=293.

HMTC assumes the air temperature to be constant at 293°K.

LN0009 VELCO=450.

HMTC assumes the wind velocity to be constant at 450 cm/sec.

PKRHI:

LN0047 CONDW=.0013

PKRHI uses a constant value for the thermal conductivity of water, K_W = .0013 cal/cm sec °C. However, K_W = .001348 cal/cm sec °C at 0°C and .001429 cal/cm sec °C at 20°C.

LN0052 AI = FACT*VOLI**0.666667

PKRHI uses $A_i = 10\, V_i^{2/3}$ while AMSHAH (p.143) defines

$$A_i = \left(\frac{M_i}{\rho_{liq}}\right)^{2/3}$$

LN0054 PVAPI = (10.**(A-(B/(TW+C))))/760 .

PKRHI uses water temperature to calculate the initial vapor pressure of the spill. MODV uses the greater of air temperature, water temperature to calculate the same quantity.

COMPD: This subroutine calculates the diffusion coefficient of vapor in air using the equation

$$D = 0.0043 \frac{T^{3/2}}{P(V_1^{1/3} + V_2^{1/3})^2} \sqrt{\frac{1}{M_1} + \frac{1}{M_2}}$$

where D = gas diffusivity, cm^2/s
T = absolute temperature, °K
V_1, V_2 = molal volumes of components 1 and 2 at normal boiling point, cc/g mole
P = absolute pressure, atm

This equation checks with equation (14-59) of Emmert and Pigford[6] and is meant for crude calculations. Table 14-46 of reference (6) lists approximate error for gas diffusivity prediction using this equation: average deviation 20%; maximum deviation 47%.

This equation is nowhere stated in AMSHAH.

PKRRK: Table (X,2) depicts the completely erratic results obtained from HACS if the given value of time is more than about 1439 seconds in this case. In view of this, the subroutine PKRRK must be modified so that misleading results are not obtained. Although the time in each case was more than TMEND, transfer to statement number 50 never took place and ISKIP was always zero. IHLF had already become 11. The authors can run the program listed in T(X,1,b) which appears on page A-16 of this appendix and satisfy themselves that the present version of subroutine PKRRK must be modified to avoid getting misleading results.

FCT: The subroutine evaluates the right-hand side of equations (10.8b) and (10.9b) of AMSHAH for use in PKRRK.

LN0011 ETA=EXP(-BETA*(1./Y(1)-1./THETW))

FCT uses:

$$\eta = e^{-\beta(1/\theta - 1/\theta_w)}$$

while AMSHAH (p.144) gives:

$$\eta = e^{-\beta(1/\theta - 1/\theta_i)}$$

That is, FCT assumes $\theta_i = \theta_w$ or $T_i = T_w$

We found no errors in the subroutines BEGPR, FRCL, IRCL, EPRNT, FSV, ENDPR.

E. SUMMARY OF RESULTS

The model described in Chapter 10 of AMSHAH has been reviewed with the following conclusions.

1) There are several minor errors in the text involving numerical data and formulas. These have been cited and the corrections indicated.

2) Except for erroneous results noted in (1) above, all formulas and calculations have been checked and found to be correct.

3) Several questionable assumptions in the analysis and modeling have been noted. Among these, the most salient one is: the use of equation (10.5) for calculating the mean heat flux from water to the liquid.

4) It has been found that HACS gives erroneous results for the values of time greater than time for complete evaporation. This is evident from the study of Table (X,2).

5) There is a lack of internal consistency among the values of the specific evaporation rate obtained by different methods [refer to Table (X,3)].

F. RECOMMENDATIONS

1) The use of equation (10.5) for calculating the heat flux from water to the liquid is likely to give grossly underestimated values of the mean heat flux from the water to the liquid. This equation ought to be replaced.

2) As noted in (4) and (5) above in Section E, the appropriate subroutines in HACS ought to be modified in order to get intelligible results.

3) Since it is possible to incorporate easily the variation of the mass-transfer coefficient in the course of spreading and simultaneous evaporation, it is recommended that it be done.

4) Equation (10.2) should be replaced by equation (X-10) and this change included in the subroutine HMTC.

5) This model needs to be expanded to include the situation of the occurrence of ice formation in the course of simultaneous spreading and evaporation.

G. TABLE OF SYMBOLS USED

a	=	constant in equation (10.7a)
A	=	pool area at any time
b	=	constant in equation (10.7a)
c	=	constant defined in equation (10.5) [in equation (X-8), c is concentration]
C	=	specific heat
D	=	diffusion coefficient of vapor in air
$\dot{E}$	=	total evaporation rate from pool at any time
$\dot{E}''$	=	specific evaporation rate at any time
$\dot{E}''_i$	=	initial specific evaporation rate
h	=	heat transfer coefficient
$\overline{h}_D$	=	mass transfer coefficient defined in equations (10.11a) and (10.11b)
h_p	=	mass transfer coefficient, $h_p = \overline{h}_D/RT$
I	=	enthalpy
J_D	=	defined in equation (X-8)
J_H	=	defined by $\dfrac{h}{P_{air}C_{air}U_{wind}}\left(\dfrac{C_{air}\,U_{air}}{K_{air}}\right)^{2/3}$
$\overline{k}$	=	mean mass transfer coefficient
k_x	=	local mass transfer coefficient defined in equation (X-8)
K_w	=	thermal conductivity of water
L	=	characteristic length
m	=	dimensionless mass of liquid
M	=	mass of liquid remaining at any time
$P_{sat}(T)$	=	saturated vapor pressure at temperature T
$q(r,t)$	=	local heat flux from water at any time
$\overline{q}(t)$	=	mean heat flux from water at any time
Q	=	rate of total heat into liquid from water
r	=	radius
R	=	maximum radius at any time for radial spill (in defining equation for $h_p = \overline{h}_D/RT$, R is gas constant)

Re_L = Reynolds number, $U_{wind}\ L/\nu_{air}$

Re_x = same as Re_L

t = time

t_{ch} = characteristic time defined in equation (10.11)

T = temperature

T_{ch} = characteristic temperature defined in equation (10.11)

T_0 = constant surface temperature of water

T_R = base temperature in energy balance

U_{wind} = wind velocity

U = same as U_{wind}

V = volume of liquid at any point

$Y(r,t)$ = thickness of boundary layer

$Y_0(t)$ = thickness of boundary layer at the point of spill at any time

α = thermal diffusivity

β = constant defined in equation (10.11)

Δ = characteristic heat flux defined in equation (10.11)

σ = dimensionless temperature

μ = viscosity

ν = kinematic viscosity

λ = latent heat of vaporization of liquid

τ = dimensionless time

Subscripts

liq = liquid

w = water

air = air

i = initial

H. *LIST OF REFERENCES*

(1) Raj, P. P. K., and A. S. Kalelkar. Simultaneous spreading and cooling of a high vapor pressure chemical, ch. 10, pp. 139-153. In *Assessment Models in Support of the Hazard Assessment Handbook, (CG-446-3)*, Report No. CG-D-65-74 (AMSHAH), prepared by Arthur D. Little, Inc. for the Department of Transportation, U.S. Coast Guard, NTIS AD 776617, January 1974.

(2) Treybal, R. E. *Mass-Transfer Operations*, 2nd ed., p. 63. McGraw-Hill Book Co., New York, 1968.

(3) Baumeister, T. (ed.). *Marks' Standard Handbook for Mechanical Engineers*, 7th ed., pp. 4-100. McGraw-Hill Book Co., New York, 1967.

(4) Polter, James H. (ed.). *Handbook of Engineering Sciences*, vol. II, p. 100. D. Van Nostrand Co., Inc., Princeton, N.J., 1967.

(5) Weast, R. C. (ed.). *Handbook of Physics and Chemistry*, 53rd ed. Chemical Rubber Publishing Co., Cleveland, Ohio, 1972-1973.

(6) Emmert, R. E., and R. L. Pigford. Gas absorption and solvent extraction, section 14. In R. H. Perry, C. H. Chilton, and S. D. Kirkpatrick (eds.), *Chemical Engineers' Handbook*, 4th ed. McGraw-Hill Book Co., New York, 1963.

Chapter 7

"BOILING RATE MODEL FOR HEAVY LIQUIDS WITH
BOILING TEMPERATURES LESS THAN AMBIENT"
(Chapter 12 of AMSHAH)

INTRODUCTION

The boiling rate model for heavy liquids with low boiling temperatures is used to obtain the rate of evaporation and total time for evaporation for a spilled liquid that sinks rapidly. Since the boiling point of the liquid is presumed to be less than that of water but far above that of a cryogen, the evaporation rate is akin to, say, ammonia or perhaps butane.

The importance of determining the boiling rate is highlighted by the fact that chemicals fitting this chapter's category of physical-chemical properties are often toxic, and thus it is important to determine vapor dispersion behavior. The boiling rate is a prime input parameter to the vapor dispersion model designed to assess toxic hazard.

A. REVIEW OF TEXT (Chapter 12) [1]

(XII,1) *Section 12.1, Aim (p.171)*

(XII,1,a) The aim of the model is that of obtaining the rate of evaporation when a liquid is spilled on water and sinks. The boiling point of the liquid is less than that of water. (√)

(XII,1,b)* It does not really calculate the total time for which a liquid will evaporate. It has been roughly approximated that, in any case, time for complete evaporation is characteristic time divided by 0.95.

(XII,1,c)* The subroutine EVDRP also computes the volume of liquid left at any time, and this value is passed to MODI.

(XII,2) *Section 12.2, Introduction (pp.171-175)*

(XII,2,a)* There are many liquids immiscible with water having densities greater than water and normal boiling points less than ambient. When such liquids are spilled on water, they sink and evaporate at the same time. If the vapor is toxic, it is necessary to compute vapor liberation rate so that it can be fed to the vapor dispersion model to assess the hazard. However, the present version of HACS has no provision to calculate concentration, $C(x,y,z,t)$, when vapor is released continuously.

(XII,2,b)* The sinking blob of heavy liquid breaks up at Weber numbers from 8 to 10. Levich[2] does not give the value of critical Weber number to be 8 to 10. He gives the value to be 2.3 (2, p. 456).

(XII,2,c)* The cluster of drops so formed sinks at increasing velocities, accelerated by gravity. This appears to disagree with the model used. It can be seen from Table (XII,17) that at first the drop velocity increases slightly, but that after a while the drop velocity progressively decreases.

(XII,2,d)* It is assumed in the derivation of the model that drops formed are of uniform size given by equation (12.10). However, the experimental evidence is that this equation is incorrect, to the extent that drops formed are of varying size.

(XII,2,e)* The authors determine the drop size by satisfying both the stability criterion and the terminal velocity criterion simultaneously. In reality, the blob will break up as soon as its Weber number exceeds 8 into relatively large drops. These large drops further break up into small drops when (and if) their Weber number exceeds 8.

(XII,3) *Section 12.3, Principles and Assumptions (p.175)*

(XII,3,a)* The basic principle of the derivation is that the blob of heavy liquid breaks up into small drops and after that evaporation due to heat transfer from the surrounding medium takes place. That is, the time to reach

the terminal velocity is negligible compared to the life of the drop. This is one of the very important assumptions which has been accepted without proof. In those cases where the time to reach the terminal settling velocity is not negligible compared to the life of the drop, neglecting the evaporation during this period will be unjustified.

(XII,3,b)* All drops formed are of the same size. The authors agree that in reality drops formed are of varying size.

(XII,3,c)* The drop cluster formed has a high porosity; that is, laws of free settling apply. The critical Weber number is 8. Forced convection heat and mass transfer results apply. Levich[2, p.456] gives the value of critical Weber number to be 2.3. The assumption of high porosity is also questionable. In fact, the drops formed will be close together and interaction between the drops will play an important role in determining the nature of motion of the system.

(XII,4) *Section 12.4, Data Required (pp.175-176)*

(XII,4,a) Density of the liquid. (√)

Surface tension of the liquid. (√)

Normal boiling temperature of the liquid. (√)

Latent heat of vaporization of the liquid. (√)

Properties of water, such as its density, viscosity, and Prandtl number. (√)

Water temperature. (√)

(XII,4,b)** The surface tension of the liquid to be used is against water. However, the value actually being used in the program is against air.

(XII,5) *Section 12.5, Model Details (pp.176-181)*

(XII,5,a)* For a nondeformable spherical drop, the terminal velocity is

$$V = \left[\frac{8}{3}\frac{g}{C_D}\left(\frac{\rho}{\rho_m} - 1\right)R\right]^{1/2} \qquad (12.3)$$

with $C_D = 0.4$ and $400 < Re_D < 5000$.

Boucher and Alves[3] lists $C_D = 0.44$ for $1000 < Re_d < 200{,}000$ for spherical particles and $C_D = 18.5/Re_d^{0.6}$ for $0.3 < Re_d < 1000$. Levich (2, p.430) lists this constant to be of the order of 0.5 for a large spherical drop.

(XII,5,b)** On p. 176, Re_D should read Re_d.

(XII,5,c) Levich (2, p.431) gives the following equation for fall of a bean-like drop in air

$$U \approx \left[\frac{4\rho' g\sigma}{K_f \rho^2}\right]^{1/4}$$

In the terminology of AMSHAH, it is

$$U \approx \left[\frac{4\rho' g\sigma}{C_D \rho_m^2}\right]^{1/4}$$

If the fall of the drop were in a dense medium, then this equation will be

$$U \approx \left[\frac{4(\rho - \rho_m) g\sigma}{C_D\ \rho_m^2}\right]^{1/4} = \left[\frac{4g}{C_D}\left(\frac{\rho}{\rho_m} - 1\right)\frac{\sigma}{\rho_m}\right]^{1/4}$$

where the value of C_D is close to unity according to Levich (2, p.431). This checks with equation (12.4) except for the value of C_D. (√)

(XII,5,d)** Definition of U on p.177 should read:

U = terminal velocity of a drop of radius R given by Eq. (12.4).

(XII,5,e) $$We = We^*[1 - 0.1\ We^* + 7.2 \times 10^{-3}(We^*)^2 - 1.93 \times 10^{-4}(We^*)^3]$$

for $We^* < 11.5$ (12.8a)

and

$$We = We^*[0.6635 - 0.01374\ We^*]$$

for $11.5 < We^* < 24$ (12.8b)

These equations appear to have been arrived at as follows:

$$U = V\left[(1 - \delta)\ \frac{1 + A(1 - \delta)^{3/2}}{A}\right]^{1/2} \qquad (12.5a)$$

where $$\delta = 0.056\ We \tag{12.6a}$$

$$We = \rho_m U^2 R/\sigma \tag{12.6b}$$

$$A = 1.778$$

$$We^* = \rho_m V^2 R/\sigma$$

By substitution of these in equation (12.5a), one gets

$$We = We^* \left[(1 - 0.056\ We)\ \frac{1 + 1.778\ (1 - 0.056\ We)^{3/2}}{2.778} \right] \quad \text{(XII-1)}$$

For various values of *We*, one can obtain from this equation corresponding values of *We**. The plot of *We/We** versus *We** is given in Figure 12.3. It can be seen from this plot that *We/We** becomes a linear function of *We** at *We** > 11.5 and hence the equation (12.8b) for 11.5 < *We** < 24. For *We** < 11.5, a fourth-degree equation in *We** has been fitted to data obtained as above. Some results of the fit are given below in Table (XII,1).

TABLE (XII,1)

We	*We** from Eq.(XII,1)	*We*,cal from Eq.(12.8a) or (12.8b) for *We** obtained from col. 2	$E = \left\lvert \frac{We,cal - We}{We} \right\rvert \cdot 100$
1.00	1.12	1.00	0.00
1.50	1.78	1.50	0.00
2.00	2.51	1.99	0.54
2.50	3.34	2.47	1.26
3.00	4.26	2.94	2.00
3.50	5.30	3.41	2.55
4.00	6.46	3.89	2.67
4.50	7.77	4.41	2.05
5.00	9.25	4.98	0.44
5.50	10.91	5.62	2.24
6.00	12.79	6.24	4.00
6.50	14.93	6.84	5.28
7.00	17.35	7.38	5.38
7.50	20.12	7.79	3.83
8.00	23.28	8.00	0.00

The fit is good up to *We* = 8.00. Above this value, the results obtained deviate enormously. At *We* = 10.00, the percent error is 61.60. However, the range of interest of the Weber number is only up to 8.0. (√)

(XII,5,f)** On p. 178, the last part of the first line of text after equation (12.11) should read: "...., a factor of 1.778."

(XII,5,g)** The factor of 2.07 on the right-hand side of equation (12.11) should be 2.069.

(XII,5,h)** The factor of 1.87 on the right-hand side of equation (12.10) should be 1.869.

(XII,5,i)** $U_C^2\rho_m R_i/\sigma = 8 = 0.3434\ [V_C^2\rho_m R_i/\sigma]$ should be:

$U_C^2\rho_m R_i/\sigma = 8 = 0.3436\ [V_C^2\rho_m R_i/\sigma]$

(XII,5.1) *Section 12.5.1, Heat Transfer (pp.178-179)*

(XII,5.1,a)** The authors of AMSHAH state, on p.178, "The reduced drop size results in a larger drag and hence the drop velocity changes." This appears to be incorrect.

For a bean-like drop, Levich (2, p.431) gives

$$\text{Drag force} = C_D \frac{V\rho^2 U^4}{4\sigma} \qquad \text{(XII-2)}$$

where V is the volume of drop and U is the terminal velocity.

Writing equation (XII-2) as

$$\text{Drag force} = \frac{C_D[K_1 r^3]\rho^2 u^4 V_i^4 R_i^3}{4\sigma}$$

where $K_1 r^3$ is the volume of the drop, K_1 being a constant

$$= K r^3 u^4$$

where K is a constant for a specific case

Let us use figures from Table (XII,17) to compute the drag force variation with radius. The results are tabulated in Table (XII,2). We find that drag force progressively decreases with a decrease in radius.

TABLE (XII,2)

r	Drag force/K
1.0	1
0.9	0.8186
0.8	0.5848
0.7	0.3659
0.6	0.1983

(XII,5.1,b) *Spalding*(4,p.56) *gives* the following relations for heat transfer coefficient when the interface element lies on the external surface of a solid spherical pellet embedded in a heap of such pellets. In the terminology of AMSHAH, they are:

$$St = 1.625\ Re_d^{-0.507} Pr^{-2/3} \qquad 15 \leqslant Re_d \leqslant 120 \qquad \text{(XII-3)}$$

$$St = 0.687\ Re_d^{-0.327} Pr^{-2/3} \qquad 120 \leqslant Re_d \leqslant 2000 \qquad \text{(XII-4)}$$

AMSHAH uses equation (12.12c) which closely approximates (XII-4). The applicability of this equation according to Spalding (4) is $120 \leqslant Re_d \leqslant 2000$, while AMSHAH gives $20 < Re_d < 5 \times 10^4$. Again, equation (XII-4) is meant for use when heat transfer takes place in the absence of mass transfer. Although the model is concerned with a situation in which there is simultaneous heat and mass transfer, the value of heat transfer coefficient in Stanton number to be used in equation (12.13) should be the one which is in the absence of mass transfer. (√)

(XII,5.1,c)* The authors on p.179 state: "McAdams correlation for heat transfer for flow of a liquid over an isolated single sphere is of the form

$$St = 1.2\ Re_d^{-0.6} Pr^{-2/3} \qquad \text{(12.12b)"}$$

Since $St = Nu/RePr$, we get

$$Nu = 1.2\ Re^{0.4} Pr^{1/3}$$

McAdams (5, p.267) gives the following figure showing data for flow of water and of spindle oil (Prandtl number from 7.3 to 380 and Δt from 11 to 71°F) past single spheres, having diameters from 0.279 to 0.496 in.

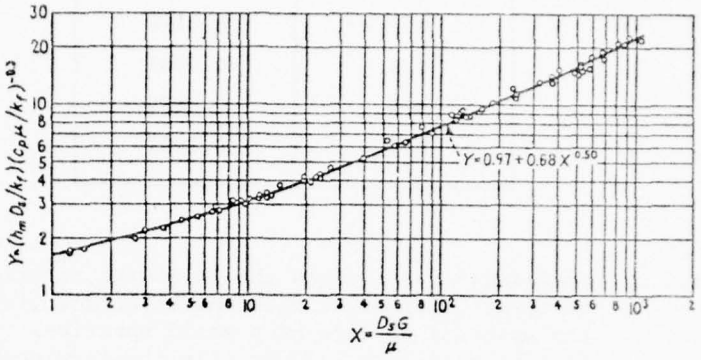

The corresponding equation is:

$$NuPr^{-0.3} = 0.97 + 0.68\ Re_d^{0.5}$$

This equation is valid for Re_d ranging from 50 to 10,000. McAdams (5, p.267) gives another equation involving five constants:

$$Nu = 0.42\ Pr^{0.2} + 0.57\ Pr^{0.33}\ Re^{0.5}$$

Neither of these equations compares with equation (12.12b) of AMSHAH.

(XII,5.2) *Section 12.5.2, Mass Transfer (pp.179-181)*

(XII,5.2,a)* Since the evaporation of the sinking liquid is accompanied simultaneously by the transfer of heat from water, we have a situation of simultaneous heat and mass transfer. An excellent treatment of this subject is available in Bird et al. (6, pp.656-676). High mass transfer rate alters the transfer coefficients for mass, heat, and momentum. Since we want to compute mass transfer rate from the knowledge of heat transfer, the appropriate expression to use is equation (21.5.35) of Bird et al. (6). This equation for the present case, written in the terminology of AMSHAH, is:

$$1 + \frac{(T_m - T)C_V}{\lambda} = exp\ \frac{\dot{m}''C_V}{h}$$

where C_V is the specific heat of the vapor of boiling liquid,

or

$$\dot{m}'' = \frac{h}{C_V}\ \ell n\left[1 + \frac{(T_m - T)C_V}{\lambda}\right]$$

$$= \frac{h}{C_m G} \times \frac{C_m G}{C_V} \times \ell n\left[1 + \frac{(T_m - T)C_V}{\lambda}\right]$$

or

$$\dot{m}'' = St\ G\ \frac{C_m}{C_V}\ \ell n\left[1 + \frac{(T_m - T)C_V}{\lambda}\right] \qquad \text{(XII-5)}$$

The equation used in AMSHAH is:

$$\dot{m}'' = St\ G\ \ell n\left[1 + \frac{(T_m - T)C_m}{\lambda}\right] \qquad (12.13)$$

which, according to the treatment given in Bird et al. (6), is incorrect.

(XII,5.2,b)* It can be easily seen that the expression

$$\dot{m}'' = -\rho\ \frac{dR}{dt} \qquad (12.15a)$$

is true only for a spherical drop. Although the authors take into account the deformation of the drop in determining terminal velocity, they have neglected the same in the derivation of $\dot{m}''$ in equation (12.15a).

(XII,5.2,c)** Equation (12.16) should read:

$$t_{ch} = \frac{R_i}{0.69\ (\rho_m/\rho)U_i\ Re_i^{-0.3}\ Pr^{-2/3}\ \ell n(1 + B)} = \frac{R_i \rho}{m_i''}$$

(XII,5.2,d)** The second line from the bottom of p.180 should read: "In Eq. (12.17), u is a function of r given by Eqs. (12.8a) and (12.8b). ..."

(XII,5.2,e)** Equation (12.17) should read: $dr/d\tau = -u^{0.7}/r^{0.3}$

(XII,5.2,f)** Equation (12.18a) should read:

$$u = r^{0.5} v_i [(1 - 0.1\ r^2 v_i^2 We_i) + 7.2 \times 10^{-3} (r^2 v_i^2 We_i)^2$$

$$- 1.93 \times 10^{-4} (r^2 v_i^2 We_i)^3]^{1/2}$$

for $r < 0.4936$

(XII,5.2,g)** Equation (12.18b) should read:

$$u = r^{0.5} v_i [0.6635 - 0.01374\ r^2 v_i^2 We_i]^{1/2}$$

for $1.00 > r > 0.4936$

It is shown below why the limits of r are wrong in AMSHAH equations (12.18a) and (12.18b).

We^* < 11.5 for equation (12.18a) since it results from (12.8a) and 24 > We^* > 11.5 for equation (12.18b) since it results from (12.8b).

$$We^* = \frac{\rho_m V^2 R}{\sigma} = \frac{R \rho_m U_i^2}{\sigma} \times \frac{V^2}{V_i^2} \times \frac{V_i^2}{U_i^2} \qquad \text{(XII-6)}$$

By equation (12.3)

$$V = \left[\frac{8}{3} \frac{g}{C_D} \left(\frac{\rho}{\rho_m} - 1\right) R\right]^{1/2}$$

$$\therefore \frac{V^2}{V_i^2} = \frac{R}{R_i} = r$$

By equation (12.19), $\frac{V_i}{U_i} = v_i$

Therefore, by substituting the above in equation (XII.6), one gets $We^* = We_i\ r\ v_i^2$

For (12.18a), $We^* = We_i\ r\ v_i^2 < 11.5$

or $(8)(r)(1/.586)^2 < 11.5$

or $r < 0.4936$

For (12.18b), $We^* = We_i\ r\ v_i^2 < 24.0$

or $r < 1.0$

TABLE (XII.12)

(XII,5.2,h)* With conditions $\tau = 0$: $r = 1$, $u = 1$

$$dr/d\tau = -u^{0.7} r^{-0.3} \qquad (12.17)$$

At the time the blob breaks up, the drops formed will have a velocity close to that of the blob. Let us consider the case of specific example 12.7.

Radius of the blob = 5.465 m (considering the blob to be spherical)

This blob will break up at $We = 8$

or $\frac{U_c^2 \rho_m R}{\sigma} = 8$

$$U_c = \left[\frac{8 \times 2 \times 10^{-2}}{10^3 \times 5.465}\right]^{1/2} = 0.541 \times 10^{-2} \quad \text{m/s}$$

while $U_i = 0.2$ m/s

Since, at the time of break up of the blob, the velocity of the drops formed will be close to the velocity of the blob itself, we have at $\tau = 0$

$$u = \frac{0.541 \times 10^{-2}}{0.2} = 2.7 \times 10^{-2}$$

which is far different from $\tau = 0$, $u = 1$.

In those cases where t' is *not* much less than t_{ch} where t' is the time to reach the terminal settling velocity, the initial condition $\tau = 0$, $u = 1$ will be grossly in error.

(XII,6) *Section 12.6, Computational Algorithm (p.181)*

(XII,6,a) A flow chart is shown in Figure 12.4 for the procedure of the computational algorithm. (√)

(XII,6,b)** The second sentence in section 12.6 should read: "Using these values and Eqs. (12.16), (12.17), and (12.18a) or (12.18b) yields the evaporation rate as a function of time."

(XII,7) *Section 12.7, Specific Example (pp.181-183)*

(XII,7,a)** Under properties of liquid, heat of vaporization should be:

$$\lambda = 1.5 \times 10^5 \quad J/kg$$

(XII,7,b)** In the equation for the size of drop formed, the factor preceding the radical sign should be 1.869.

(XII,7,c)** In the equation for terminal velocity of a non-deformable drop, V_i, the term preceding the bracketed factor should be: 3.53. And the final term should be: 0.343.

(XII,7,d)** Terminal velocity of a deformable drop should be:

$$U_i = 0.586 \times .343 = 0.2 \text{ m/s}$$

(XII,7,e)** The authors of AMSHAH use the surface tension of Freon 114 against air. This value reported in Weast[7] is 12 dynes/cm at 25°C. This is equivalent to 1.2×10^{-2} N/m. However, the value needed is at 3.8°C. Since the surface tension increases with decrease in temperature, it is reasonable to assume that surface tension of Freon 114 at 3.8°C is $\sim 2 \times 10^{-2}$ N/m. But what we need to use in the example is the surface tension of Freon 114 water system and not the surface tension of pure Freon 114 in air. This is a serious error.

(XII,8) *Section 12.8, Discussions (pp.183-184)*

(XII,8,a) In view of the lack of quantitative information available and the necessity to have a reasonably simple model, it has been necessary to assume that the blob breaks up into uniformly sized drops. (√)

(III,8,b) Assumption of single-sphere drag leads to higher settling velocity owing to lack of interaction among the drops. It can be seen from equation (12.12c) that it leads to higher heat transfer coefficient and from (12.13), it is clear that it leads to still higher mass transfer rate. (√)

(XII,8,c) To obtain the heat transfer coefficient, correlation for closely packed spheres has been used as it gives rise to highest heat transfer coefficient. (√)

(XII,8,d)* We have noted that incorrect values of surface tension of system liquid-air are being used for the system liquid-water. Study of Table (XII,16) suggests that there is no relation between the two values. It is strongly recommended that values of the surface tension of systems liquid-water be stored in data files for those chemicals for which values are available (if any). For other chemicals for which no suitable values of the interfacial tension are available, the use of the model is questionable.

(XII,8,e)* HACS was run with the data of Specific Example, 12.7. The time for complete evaporation obtained was 25.2 sec, as against 3 sec reported in AMSHAH. With life of drop of the order of 25 sec, it should be necessary to take into account the rise in boiling point of the liquid with increase in hydrostatic head. However, it will complicate the model.

(XII,9) *Section 12.9, Conclusions (p.184)*

(XII,9,a) Evaporative model worked out based on assumption of drop formation when a blob of heavy, low-boiling-point liquid is spilled on a water surface. A heat-mass similarity model is used to predict vaporization rate. To obtain a conservative vapor hazard estimate, packed sphere bed heat transfer correlations have been used. Rate of spill itself can be used for vapor liberation rate to predict evaporation rate in the case of continuous spill. (√)

(XII,9,b)* It is difficult to say how realistic the model is in predicting the actual situation in the absence of experimental data. In any case, it will give conservative estimates of the evaporation rates when the time to reach the terminal settling velocity is much less than the life of the drop. For liquids at very low temperatures, like tetrafluoroethylene at -76°C, the drops formed may evaporate even before they reach their terminal velocity. In those cases, this model will not apply at all.

(XII,10) *Section 12.10, References (p.185)*

(XII,10,a) References used in Section 12 are listed. (√)

(XII,11) *Section 12.11, List of Symbols (pp.185-187)*

(XII,11,a)** The following symbols have been used in the text and either incorrectly listed or not listed in this section.

Symbol	Description	Value	Units
A	a constant = 1.778		
B	transfer factor defined by Eq.(12.14)		
F	force (drag or weight)		N
G	mass flux of medium	$= \rho U$	kg/m^2 s
$\dot{m}''$	evaporation rate from a unit area of the spherical drop		kg/m^2 s
$\dot{m}$	evaporation rate per drop		kg/s
$\dot{M}$	total evaporation rate (for all drops)		kg/s
N	number of drops formed		
τ	non-dimensional time = t/t_{ch}		

F(XII,3) *Figure 12.3 (p.174), Relationship Between the Terminal Velocities of a Deformable Drop and a Non-Deformable Drop, Falling Within a Medium*

F(XII,3,a)** For $We^* < 11.5$, the equation should be:

$$We = We^*[1 - 0.1\ We^* + 7.20 \times 10^{-3}(We^*)^2 - 1.93 \times 10^{-4}(We^*)^3]$$

to correspond to equation (12.8a) given on p.177 of AMSHAH.

F(XII,3,b)** Equation following "Curves are for" should be:

$$\delta = 0.056\ We$$

F(XII,4) *Figure 12.4(p.182), Flow Chart for the Calculation of Evaporation Rate of a Liquid Sinking in Water*

F(XII,4,a)** The equation for U_i should be:

$$U_i = 2.069\left[\frac{g\sigma}{\rho_m}\left(\frac{\rho}{\rho_m} - 1\right)\right]^{1/4}$$

F(XII,4,b)** The equation for $\dot{m}_i''$ should be:

$$\dot{m}_i'' = \rho_m U_i [0.69\ Re_i^{-0.3}\ Pr^{-2/3}]\ \ln(1 + B)$$

F(XII,4,c)** After the first equation for u, it should read:

for $r < 0.4936$

and after the second equation for u, it should read:

for $1.0 > r > 0.4936$

F(XII,4,d)** The equation for $\dot{m}(t)$ should be:

$$\dot{m}(t) = \dot{m}_i r^{1.7}\ u^{0.7}$$

B. CRITIQUE OF THE MODEL (Chapter 12)

The model presented in Chapter 12 of AMSHAH is based on the following major assumptions.

1) Time to reach the terminal velocity is exceedingly small compared to the life of the drop.
2) The blob of liquid breaks up into drops of uniform size determined by simultaneously satisfying the stability criterion and terminal velocity criterion.
3) For heat transfer calculations, the cluster of drops is considered a packed bed of spheres, while the model neglects any interaction among the drops for calculating the terminal velocity.
4) It is assumed that the life of a drop is small enough so that elevation of boiling point due to hydrostatic head can be neglected.

Assumption (1): When time to reach terminal velocity is not negligible compared to the life of the drop, this model will not be applicable since the initial conditions $\tau = 0$, $u = 1$, and $r = 1$ will not hold.

Assumption (2): In reality, the blob will break up as soon as its Weber number exceeds 8 into relatively large drops. These large drops then break up into smaller drops, if their Weber number exceeds 8. However, to derive a reasonably simple model, it is necessary to assume that the blob breaks up into drops of uniform size which is determined by simultaneously satisfying the stability criterion and the terminal velocity criterion. This is a good assumption if the time to reach the terminal velocity is negligible compared to the life of the drop.

Assumption (3): Since models in AMSHAH attempt to obtain conservative values whenever the calculation of realistic results becomes complicated, this assumption is justified.

Assumption (4): This assumption will be strictly true only if the life of the drop is exceedingly small. However, neglecting the elevation in boiling point will only lead to more conservative results (i.e., larger values of the specific evaporation rate). Since this assumption simplifies the model appreciably, it is justified.

As explained in Section 12.5.2, equation (12.13) used for calculation of the specific evaporation rate does not check with equation (XII-5) derived by us following Bird et al. (6).

In summary, we may assert that the model developed represents a good first attempt at solving this rather difficult problem. The major difficulty with this model is that of obtaining the necessary data for computations. We do not know of a single chemical which a) is heavier than water, b) is immiscible with water, and c) has a boiling point less than water (so that this model may apply), of which the interfacial tension (needed for calculations) is known. This is, in fact, one of the severe limitations of the several models described in AMSHAH.

C. *SENSITIVITY ANALYSIS (Chapter 12)*

Due to the nature of the equations involved in the final solution, it was decided to perform the sensitivity analysis numerically by using the computer rather than employing the analytical techniques used in the sensitivity analyses of chapters 3 and 8 of AMSHAH.

MODI calculates three items:

1) time for complete evaporation,
2) total evaporation rate, and
3) volume of liquid remaining.

These calculated quantities (dependent variables) are functions of three independent variables, viz., 1) initial volume of the spill, 2) water temperature, and 3) liquid temperature; and of six parameters, viz., 1) surface tension, 2) heat of vaporization of liquid, 3) liquid density, 4) water viscosity, 5) water density, and 6) water specific heat.

The units for the various quantities as they appear in the following tables are:

volume in cc
total evaporation rate in gm/cm^2 sec
time in sec

temperature in °C
surface tension in dyne/cm
density in gm/cc
water specific heat in cal/gm °C
sensitivity coefficient dimensionless

The sensitivity coefficient used is:

$$\frac{\text{fractional change in dependent variable}}{\text{fractional change in independent variable or parameter}}$$

where fractional change in independent variable/parameter has been taken to be about 0.05 of its normal value. Normal values have been taken from Section 12.7, Specific Example. The authors report their sensitivity analysis of this chapter on pp.237-238 in AMSHAH. Our review of this as well as additional comments follow.

1) The time for complete evaporation varies almost as the square root of the surface tension. For a 1% change in the value of surface tension, the total time of evaporation varies by 0.475. This is correct.

2) The time for complete evaporation is very sensitive to water density. However, the water density variation with temperature is very small. Therefore, assuming its value to be a constant at 1.00 gm/cc (as the subroutine EVDRP does) is justified. The time for complete evaporation is also very sensitive to liquid density.

3) The authors state in AMSHAH that evaporation rate is an extremely weak function of the surface tension. For a 100% change in surface tension, the change in evaporation rate is approximately 2.5%. As can be seen from the following tables [Tables (XII,3) through (XII,15) which appear at the end of this section], sensitivity coefficient of evaporation rate to the surface tension is a function of time. To begin with it is negative and at a later time it becomes positive. Therefore, it is incorrect to say that a 100% change in surface tension causes a 2.5% change in evaporation rate.

4) MODI does not determine the size of the drop. Therefore, we have not computed its sensitivity coefficient to any of the dependent variables.

5) Instead of evaluating the sensitivity coefficient of the density difference of water and liquid, the effect of each of the two parameters was determined separately as these quantities are inputted to the computer program independently. However, the computer program assumes density of water to be a constant. Since the density of liquid does not always appear as $(\rho - \rho_m)$ in the computations for evaporation rate, it is not possible to compute the sensitivity coefficient to $(\rho - \rho_m)$ from the knowledge about the sensitivity coefficient to ρ. It is incorrect

to say that a 1% change in density difference cause a 0.3% change in evaporation rate, since this quantity is a function of time and it does vary appreciably with time.

6) For a 5% increase in liquid density we have, from Table (XII,3), change in time for complete evaporation as 7.09%. And a 5% increase in liquid density corresponds to 16.24% increase in $(\rho - \rho_m)$ with ρ_m being constant. This means that for a 1% increase in $(\rho - \rho_m)$ due to change in liquid density, the time for complete evaporation will alter by 0.44%. This is different from the value reported in AMSHAH of 0.825%. Again, density differences $(\rho - \rho_m)$ resulting from changes in ρ and ρ_m will affect the time for complete evaporation to different extents, depending upon whether this change is due to change in ρ or ρ_m. For a 1% change in $(\rho - \rho_m)$ due to water density, the change in time for complete evaporation is 0.57%.

7) It is clear from the tables on sensitivity analysis that sensitivity coefficients for the water and the liquid temperatures are functions of time. In view of this, it is incorrect to say that a 1% change in temperature difference causes a 1% change in evaporation rate.

8) Since temperatures always appear as $(T - T_m)$ in the computations, it is possible to compute the sensitivity coefficient to $(T - T_m)$ from the knowledge of sensitivity coefficient to T or T_m.

$$\text{Sensitivity coefficient to } T_m = \frac{\delta f/f}{\delta T_m/T_m} = \frac{\delta f}{f} \times \frac{T_m}{\delta T_m}$$

Now $\delta(T_m - T) = \delta T_m$ since T is a constant.

$$\text{Sensitivity coefficient to } T_m = \frac{\delta f}{f} \times \frac{(T_m - T)}{\delta(T_m - T)} \times \frac{T_m}{(T_m - T)}$$

Hence,

$$\text{Sensitivity coefficient to } (T_m - T) = \frac{(T_m - T)}{T_m} \times \text{sensitivity coefficient to } T_m$$

For time for complete evaporation, sensitivity coefficient to water temperature is -0.9571. Therefore, sensitivity coefficient to $(T_m - T)$

$$= -0.9571 \times \frac{(20 - 3.8)}{20} = -0.775$$

That is, a 1% change in temperature difference will bring about a 0.775% change in the time for complete evaporation. This agrees reasonably well with the figure given in AMSHAH.

9) It is incorrect to say that the temperature has the greatest effect on the final results. Evaporation rate is a function of time, and its sensitivity coefficients vary with time. On study of Tables (XII,4) through (XII,9), liquid density appears to have more effect on the evaporation rate than does the temperature difference. Also, liquid density has a greater effect on the time for complete evaporation than does the temperature difference.

10) No doubt the sensitivity coefficients for surface tension are generally lower than the corresponding values for liquid density; the errors in surface tension will be several times the errors in liquid density. Instead of the interfacial tension, the computer program uses the surface tension of the liquid in air, and this can be enormously different from the interfacial tension as can be seen from Table (XII,16). In fact, nonavailability of the data on interfacial tension appears to be the most severe limitation of this model.

The numerical values for the sensitivity coefficients of 1) time for complete evaporation, 2) total evaporation rate, and 3) volume of liquid remaining follow.

TABLE (XII,3)

RESULTS FOR FREON 114

TIME FOR COMPLETE EVAPORATION

Normal Value Is 25.2015 sec

INDEX	VARIABLE	SENSITIVITY COEFFICIENT	VARIABLE NORMAL	VARIABLE CHANGED	OUTPUT	FRACTION
1	Initial Volume of Spill	1.0000	687.3×10^6	721.665×10^6	25.2015	1.0000
2	Water Temperature	-0.9571	20.0	21.0	23.9955	0.9521
3	Liquid Temperature	0.1952	3.80	3.99	25.4475	1.0098
INDEX	PARAMETER	SENSITIVITY COEFFICIENT	PARAMETER NORMAL	PARAMETER CHANGED	OUTPUT	FRACTION
1	Surface Tension	0.4689	20.0	21.0	25.7924	1.0234
2	Heat of Vaporization	0.8221	32.51	34.1355	26.2374	1.0411
3	Liquid Density	-1.4187	1.455	1.52775	23.4138	0.9291
4	Water Viscosity	-0.2906	0.01	0.0105	24.8353	0.9855
5	Water Density	1.2768	1.00	1.05	26.8104	1.0638
6	Water Specific Heat	-0.7838	1.00	1.05	24.2139	0.9608

TABLE (XII,4)

RESULTS FOR FREON 114

TOTAL EVAPORATION RATE

Normal Value Is 114.82×10^6 At Time = 1 sec

INDEX	VARIABLE	SENSITIVITY COEFFICIENT	VARIABLE NORMAL	VARIABLE CHANGED	OUTPUT	FRACTION
1	Initial Volume of Spill	1.0000	687.3×10^6	721.665×10^6	120.57×10^6	1.0500
2	Water Temperature	0.9112	20.0	21.0	120.06×10^6	1.0456
3	Liquid Temperature	-0.1762	3.80	3.99	113.81×10^6	0.9912
INDEX	PARAMETER	SENSITIVITY COEFFICIENT	PARAMETER NORMAL	PARAMETER CHANGED	OUTPUT	FRACTION
1	Surface Tension	-0.4182	20.0	21.0	112.42×10^6	0.9791
2	Heat of Vaporization	-0.7219	32.51	34.1355	110.68×10^6	0.9639
3	Liquid Density	2.4498	1.455	1.52775	128.89×10^6	1.1225
4	Water Viscosity	0.2682	0.01	0.0105	116.36×10^6	1.0134
5	Water Density	-1.0995	1.00	1.05	108.51×10^6	0.9450
6	Water Specific Heat	0.7401	1.00	1.05	119.07×10^6	1.0370

TABLE (XII,5)

RESULTS FOR FREON 114

TOTAL EVAPORATION RATE

Normal Value Is 77.75×10^6 At Time = 5 sec

INDEX	VARIABLE	SENSITIVITY COEFFICIENT	VARIABLE NORMAL	VARIABLE CHANGED	OUTPUT	FRACTION
1	Initial Volume of Spill	1.0000	687.3×10^6	721.665×10^6	81.64×10^6	1.0500
2	Water Temperature	0.4454	20.0	21.0	79.49×10^6	1.0233
3	Liquid Temperature	-0.0909	3.80	3.99	77.40×10^6	0.9955
INDEX	PARAMETER	SENSITIVITY COEFFICIENT	PARAMETER NORMAL	PARAMETER CHANGED	OUTPUT	FRACTION
1	Surface Tension	-0.2183	20.0	21.0	76.91×10^6	0.9891
2	Heat of Vaporization	-0.3823	32.51	34.1355	76.27×10^6	0.9809
3	Liquid Density	1.6917	1.455	1.52775	84.33×10^6	1.0846
4	Water Viscosity	0.1354	0.01	0.0105	78.28×10^6	1.0068
5	Water Density	-0.5925	1.00	1.05	75.45×10^6	0.9704
6	Water Specific Heat	0.3650	1.00	1.05	79.17×10^6	1.0182

TABLE (XII,6)

RESULTS FOR FREON 114

TOTAL EVAPORATION RATE

Normal Value Is 42.10×10^6 At Time = 10 sec

INDEX	VARIABLE	SENSITIVITY COEFFICIENT	VARIABLE NORMAL	VARIABLE CHANGED	OUTPUT	FRACTION
1	Initial Volume of Spill	1.0000	687.3×10^6	721.665×10^6	44.20×10^6	1.0500
2	Water Temperature	-0.4648	20.0	21.0	44.12×10^6	0.9768
3	Liquid Temperature	0.0794	3.80	3.99	42.26×10^6	1.0040
INDEX	PARAMETER	SENSITIVITY COEFFICIENT	PARAMETER NORMAL	PARAMETER CHANGED	OUTPUT	FRACTION
1	Surface Tension	0.1829	20.0	21.0	42.48×10^6	1.0091
2	Heat of Vaporization	0.3032	32.51	34.1355	42.73×10^6	1.0152
3	Liquid Density	0.2246	1.455	1.52775	42.57×10^6	1.0112
4	Water Viscosity	-0.1275	0.01	0.0105	41.83×10^6	0.9936
5	Water Density	0.4379	1.00	1.05	43.02×10^6	1.0219
6	Water Specific Heat	-0.3708	1.00	1.05	41.31×10^6	0.9815

TABLE (XII,7)

RESULTS FOR FREON 114

TOTAL EVAPORATION RATE

Normal Value Is 17.8×10^6 At Time = 15 sec

INDEX	VARIABLE	SENSITIVITY COEFFICIENT	VARIABLE NORMAL	VARIABLE CHANGED	OUTPUT	FRACTION
1	Initial Volume of Spill	1.0000	687.3×10^6	721.665×10^6	18.69×10^6	1.0500
2	Water Temperature	-2.2017	20.0	21.0	15.84×10^6	0.8899
3	Liquid Temperature	0.4191	3.80	3.99	18.17×10^6	1.0210
INDEX	PARAMETER	SENSITIVITY COEFFICIENT	PARAMETER NORMAL	PARAMETER CHANGED	OUTPUT	FRACTION
1	Surface Tension	0.9900	20.0	21.0	18.68×10^6	1.0495
2	Heat of Vaporization	1.6980	32.51	34.1355	19.31×10^6	1.0849
3	Liquid Density	-2.5187	1.455	1.52775	15.56×10^6	0.8741
4	Water Viscosity	-0.6427	0.01	0.0105	17.23×10^6	0.9679
5	Water Density	2.5631	1.00	1.05	20.08×10^6	1.1282
6	Water Specific Heat	-1.7849	1.00	1.05	16.21×10^6	0.9108

TABLE (XII,8)

RESULTS FOR FREON 114

TOTAL EVAPORATION RATE

Normal Value Is 4.16×10^6 **At Time =** 20 sec

INDEX	VARIABLE	SENSITIVITY COEFFICIENT	VARIABLE NORMAL	VARIABLE CHANGED	OUTPUT	FRACTION
1	Initial Volume of Spill	1.0000	687.3×10^6	721.665×10^6	4.37×10^6	1.0500
2	Water Temperature	-6.7846	20.0	21.0	2.75×10^6	0.6608
3	Liquid Temperature	1.4294	3.80	3.99	4.46×10^6	1.0715
INDEX	PARAMETER	SENSITIVITY COEFFICIENT	PARAMETER NORMAL	PARAMETER CHANGED	OUTPUT	FRACTION
1	Surface Tension	3.4466	20.0	21.0	4.88×10^6	1.1723
2	Heat of Vaporization	6.0608	32.51	34.1355	5.42×10^6	1.3030
3	Liquid Density	-9.3225	1.455	1.52775	2.22×10^6	0.5339
4	Water Viscosity	-2.1067	0.01	0.0105	3.72×10^6	0.8947
5	Water Density	9.4253	1.00	1.05	6.12×10^6	1.4713
6	Water Specific Heat	-5.5947	1.00	1.05	3.00×10^6	0.7203

TABLE (XII,9)

RESULTS FOR FREON 114

TOTAL EVAPORATION RATE

Normal Value Is 3.738×10^3 **At Time =** 25 sec

INDEX	VARIABLE	SENSITIVITY COEFFICIENT	VARIABLE NORMAL	VARIABLE CHANGED	OUTPUT	FRACTION
1	Initial Volume of Spill	1.0000	687.3×10^6	721.665×10^6	3.925×10^3	1.0500
2	Water Temperature	--	20.0	21.0	**	--
3	Liquid Temperature	88.4735	3.80	3.99	2.027×10^4	5.4237
INDEX	PARAMETER	SENSITIVITY COEFFICIENT	PARAMETER NORMAL	PARAMETER CHANGED	OUTPUT	FRACTION
1	Surface Tension	336.73	20.0	21.0	6.668×10^4	17.8367
2	Heat of Vaporization	864.29	32.51	34.1355	1.653×10^5	44.2146
3	Liquid Density	--	1.455	1.52775	**	--
4	Water Viscosity	--	0.01	0.0105	**	--
5	Water Density	1857.47	1.00	1.05	3.51×10^5	93.8734
6	Water Specific Heat	--	1.00	1.05	**	--

**No output since 25 sec is greater than time for complete evaporation.

TABLE (XII,10)

RESULTS FOR FREON 114

VOLUME OF LIQUID REMAINING

Normal Value Is 604.8×10^6 cc At Time = 1 sec

INDEX	VARIABLE	SENSITIVITY COEFFICIENT	VARIABLE NORMAL	VARIABLE CHANGED	OUTPUT	FRACTION
1	Initial Volume of Spill	1.0000	687.3×10^6	721.665×10^6	635.05×10^6	1.0500
2	Water Temperature	-0.1309	20.0	21.0	600.8×10^6	0.9935
3	Liquid Temperature	0.0252	3.80	3.99	605.57×10^6	1.0013
INDEX	PARAMETER	SENSITIVITY COEFFICIENT	PARAMETER NORMAL	PARAMETER CHANGED	OUTPUT	FRACTION
1	Surface Tension	0.0598	20.0	21.0	606.2×10^6	1.0030
2	Heat of Vaporization	0.1032	32.51	34.1355	607.93×10^6	1.0052
3	Liquid Density	-0.1986	1.455	1.52775	598.80×10^6	0.9901
4	Water Viscosity	-0.0385	0.01	0.0105	603.64×10^6	0.9981
5	Water Density	0.1570	1.00	1.05	609.56×10^6	1.0079
6	Water Specific Heat	-0.1063	1.00	1.05	601.60×10^6	0.9947

TABLE (XII,11)

RESULTS FOR FREON 114

VOLUME OF LIQUID REMAINING

Normal Value Is 341.86×10^6 cc At Time = 5 sec

INDEX	VARIABLE	SENSITIVITY COEFFICIENT	VARIABLE NORMAL	VARIABLE CHANGED	OUTPUT	FRACTION
1	Initial Volume of Spill	1.0000	687.3×10^6	721.665×10^6	358.96×10^6	1.0500
2	Water Temperature	-0.7752	20.0	21.0	328.6×10^6	0.9612
3	Liquid Temperature	0.1515	3.80	3.99	344.4×10^6	1.0076
INDEX	PARAMETER	SENSITIVITY COEFFICIENT	PARAMETER NORMAL	PARAMETER CHANGED	OUTPUT	FRACTION
1	Surface Tension	0.3603	20.0	21.0	348.02×10^6	1.0180
2	Heat of Vaporization	0.6237	32.51	34.1355	352.52×10^6	1.0312
3	Liquid Density	-1.1694	1.455	1.52775	321.88×10^6	0.9415
4	Water Viscosity	-0.2296	0.01	0.0105	337.94×10^6	0.9885
5	Water Density	0.9532	1.00	1.05	358.16×10^6	1.0477
6	Water Specific Heat	-0.6307	1.00	1.05	331.08×10^6	0.9685

TABLE (XII,12)

RESULTS FOR FREON 114

VOLUME OF LIQUID REMAINING

Normal Value Is 139.27×10^6 cc At Time = 10 sec

INDEX	VARIABLE	SENSITIVITY COEFFICIENT	VARIABLE NORMAL	VARIABLE CHANGED	OUTPUT	FRACTION
1	Initial Volume of Spill	1.0000	687.3×10^6	721.665×10^6	146.23×10^6	1.0500
2	Water Temperature	-2.0146	20.0	21.0	125.24×10^6	0.8993
3	Liquid Temperature	0.4044	3.80	3.99	142.08×10^6	1.0202
INDEX	PARAMETER	SENSITIVITY COEFFICIENT	PARAMETER NORMAL	PARAMETER CHANGED	OUTPUT	FRACTION
1	Surface Tension	0.9674	20.0	21.0	146.01×10^6	1.0484
2	Heat of Vaporization	1.6868	32.51	34.1355	151.02×10^6	1.0843
3	Liquid Density	-3.0036	1.455	1.52775	118.36×10^6	0.8498
4	Water Viscosity	-0.6062	0.01	0.0105	135.05×10^6	0.9697
5	Water Density	2.6010	1.00	1.05	157.38×10^6	1.1301
6	Water Specific Heat	-1.6461	1.00	1.05	127.81×10^6	0.9177

TABLE (XII,13)

RESULTS FOR FREON 114

VOLUME OF LIQUID REMAINING

Normal Value Is 39.52×10^6 cc At Time = 15 sec

INDEX	VARIABLE	SENSITIVITY COEFFICIENT	VARIABLE NORMAL	VARIABLE CHANGED	OUTPUT	FRACTION
1	Initial Volume of Spill	1.0000	687.3×10^6	721.665×10^6	41.50×10^6	1.0500
2	Water Temperature	-4.3058	20.0	21.0	31.01×10^6	0.7847
3	Liquid Temperature	0.9115	3.80	3.99	41.32×10^6	1.0456
INDEX	PARAMETER	SENSITIVITY COEFFICIENT	PARAMETER NORMAL	PARAMETER CHANGED	OUTPUT	FRACTION
1	Surface Tension	2.2058	20.0	21.0	43.88×10^6	1.1103
2	Heat of Vaporization	3.9013	32.51	34.1355	47.23×10^6	1.1951
3	Liquid Density	-6.2687	1.455	1.52775	27.13×10^6	0.6866
4	Water Viscosity	-1.3375	0.01	0.0105	36.88×10^6	0.9331
5	Water Density	6.1215	1.00	1.05	51.62×10^6	1.3061
6	Water Specific Heat	-3.5484	1.00	1.05	32.51×10^6	0.8226

TABLE (XII,14)

RESULTS FOR FREON 114

VOLUME OF LIQUID REMAINING

Normal Value Is 4.71×10^6 cc At Time = 20 sec

INDEX	VARIABLE	SENSITIVITY COEFFICIENT	VARIABLE NORMAL	VARIABLE CHANGED	OUTPUT	FRACTION
1	Initial Volume of Spill	1.0000	687.3×10^6	721.665×10^6	4.94×10^6	1.0500
2	Water Temperature	-9.8487	20.0	21.0	2.39×10^6	0.5076
3	Liquid Temperature	2.4428	3.80	3.99	5.29×10^6	1.1221
INDEX	PARAMETER	SENSITIVITY COEFFICIENT	PARAMETER NORMAL	PARAMETER CHANGED	OUTPUT	FRACTION
1	Surface Tension	6.1100	20.0	21.0	6.15×10^6	1.3055
2	Heat of Vaporization	11.2509	32.51	34.1355	7.36×10^6	1.5625
3	Liquid Density	-13.3259	1.455	1.52775	1.57×10^6	0.3337
4	Water Viscosity	-3.3664	0.01	0.0105	3.92×10^6	0.8317
5	Water Density	18.5268	1.00	1.05	9.07×10^6	1.9263
6	Water Specific Heat	-8.3299	1.00	1.05	2.75×10^6	0.5835

TABLE (XII,15)

RESULTS FOR FREON 114

VOLUME OF LIQUID REMAINING

Normal Value Is 163.97 cc At Time = 25 sec

INDEX	VARIABLE	SENSITIVITY COEFFICIENT	VARIABLE NORMAL	VARIABLE CHANGED	OUTPUT	FRACTION
1	Initial Volume of Spill	1.0000	687.3×10^6	721.665×10^6	172.1691	1.0500
2	Water Temperature	--	20.0	21.0	**	--
3	Liquid Temperature	220.87	3.80	3.99	1974.8	12.0434
INDEX	PARAMETER	SENSITIVITY COEFFICIENT	PARAMETER NORMAL	PARAMETER CHANGED	OUTPUT	FRACTION
1	Surface Tension	1382.66	20.0	21.0	1.150×10^4	70.1330
2	Heat of Vaporization	5409.71	32.51	34.1355	4.45×10^4	271.4855
3	Liquid Density	--	1.455	1.52775	**	--
4	Water Viscosity	--	0.01	0.0105	**	--
5	Water Density	16845.87	1.00	1.05	1.3827×10^5	843.2937
6	Water Specific Heat	--	1.00	1.05	**	--

**No output since 25 sec is greater than time for complete evaporation.

D. HACS ERROR ANALYSIS (Chapter 12)

In this section, we explicitly list each HACS Fortran statement at variance with its parent mathematical expression as stated in Chapter 12, "Boiling Rate Model for Heavy Liquids with Boiling Temperatures Less Than Ambient," in AMSHAH.

MODI obtains data from the state file and computes, for a given time, 1) the total rate of evaporation, 2) volume of liquid remaining, and 3) time for complete evaporation. It calls subroutine EVDRP which has been checked for errors.

MODI:

In the HACS error analysis of Chapter 10, "Simultaneous Spreading and Cooling of a High Vapor Chemical," we had in MODV the following statements:

```
LN0031   CALL FRCL(1008,SURT,IS,IR)
LN0032   SURT = ABS(72.8-SURT)
```

The same is true of MODT used for "Spreading of a High Viscosity and Low Viscosity Liquid on Water":

```
LN0022   CALL FRCL(1008,SURT,IS,IR)
LN0023   SURT = ABS(72.8-SURT)
```

That is, the data files contain the values of surface tension of liquids against air. To obtain the value against water, the relationship used is:

$$\sigma_{\ell w} = \left| 72.8 - \sigma_{\ell a} \right|$$

where $\sigma_{\ell w}$ is the surface tension of liquid in water while $\sigma_{\ell a}$ is the value against air obtained from the state file.

According to Liley et al.[8] the interfacial tension of immiscible liquids is less than the larger of the surface tensions of the component liquids. Quantitative prediction may be made with Antonoff's rule which states that, for two saturated liquid layers in equilibrium, the interfacial tension is equal to the difference between the individual surface tensions of two *mutually saturated* phases under a common vapor or gas:

$$\sigma_i = \sigma_{1s} - \sigma_{2s} \qquad \text{(XII-7)}$$

where σ_i = interfacial tension between components 1 and 2

σ_{1s}, σ_{2s} = surface tensions of mutually saturated phases of components 1 and 2 against a common vapor or gas.

If pure component surface tensions are used in equation (XII-7), this rule proves quite inaccurate since $\sigma_i < (\sigma_1 - \sigma_2)$ and the error will often exceed 100%. If, however, saturated-phase surface tensions are used, estimates within 15% may be made for both organic-water and organic-organic systems. As an illustration, some results are tabulated below in Table (XII,16). Values have been obtained from Lange[9].

TABLE (XII,16)

Component #1	Component #2	Surface Tension σ_1, dyne/cm	Surface Tension σ_2, dyne/cm	$\lvert\sigma_1 - \sigma_2\rvert$ dyne/cm	Interfacial Tension σ_i dyne/cm	% Error*
benzene	water	28.9	72.8	43.9	35.0	25.4
n-hexane	water	18.4	72.8	54.4	51.1	6.5
ethyl ether	water	17.0	72.8	55.8	10.7	421.5
n-butyronitrile	water	26.7	72.8	46.1	10.38	349.5
iso-amyl alcohol	water	23.8	72.8	49.0	5.0	880
iso-butyl alcohol	water	22.8	72.8	50.0	2.1	2281

* % Error = $\dfrac{\left|\lvert\sigma_1 - \sigma_2\rvert - \sigma_i\right|}{\sigma_i} \times 100$

Therefore, the relationship used by MODV and MODT to obtain interfacial tension needed for computations is completely inadequate.

MODI gets the value of surface tension of liquid in air by:

```
LN0026    CALL FRCL(1008,SURT,IS,IR)
```

For use in subroutine EVDRP, the value of surface tension of the system liquid-water is needed. The value actually being used is for the system liquid-air. Since the two values bear no relation to each other, the results computed will be erroneous.

```
LN0026    RO = 0.094*SQRT(SURT/DELRO)
```

EVDRP uses $R_i = 0.094\sqrt{\sigma/(\rho - \rho_m)}$ while the corresponding equation in AMSHAH, p.178, is $R_i = 1.87\sqrt{\sigma/[g(\rho - \rho_m)]}$. With R_i in cm (as in EVDRP), this becomes $R_i = 0.0597\sqrt{\sigma/(\rho - \rho_m)}$.

LN0027 UO = 30.2*SQRT(RO*DELRO)

EVDRP uses $U_i = 9.259\ [\sigma(\rho - \rho_m)]^{1/4}$ while AMSHAH, p.178, gives

$$U_i = 2.07 \left[\frac{g\sigma}{\rho_m}\left(\frac{\rho}{\rho_m} - 1\right)\right]^{1/4}$$

With U_i in cm/sec as in EVDRP, this equation becomes:

$$U_i = 11.582 \left(\frac{\sigma(\rho - \rho_m)}{\rho_m^2}\right)^{1/4}$$

LN0031 STANT = 0.057*REY**(-0.3)

EVDRP uses $St_i = 0.057\ Re_i^{-0.3}$ while the corresponding equation in AMSHAH, p.179, is $St_i = 0.69\ Re_i^{-0.3}\ Pr^{-2/3}$. For water, $Pr = 7$. This equation then becomes:

$$St_i = 0.1884\ Re_i^{-0.3}$$

LN0041 ETA = (1.-0.95*TOW)**(1./0.95)
LN0042 TOTEV = EVAPO*ETA**2.05
LN0043 V = VI*ETA**3

Total evaporation rate is calculated by the subroutine EVDRP by the relationship:

$$\dot{M}(t) = \dot{M}_i \times (1 - 0.95\tau)^{2.05/0.95} \qquad \text{(XII-8)}$$

It is easy to prove from the equations given in Chapter 12 that,

$$\dot{M}(t) = \dot{M}_i\, r^{1.7}\, u^{0.7} \qquad \text{(XII-9)}$$

where

$$u = 1.7065\ r^{0.5}\ [1 - 2.33\ r^2 + 3.9\ r^4 - 2.44\ r^6]^{1/2}$$

for $r < 0.4936$

$$u = 1.7065\ r^{0.5}\ [0.6635 - 0.32\ r^2]^{1/2}$$

for $1.00 > r > 0.4936$

and

$$\frac{dr}{d\tau} = -u^{0.7}\ r^{-0.3}$$

It follows from the above that

$$\frac{d\tau}{dr} = -0.6879\ r^{-0.05}\ [1 - 2.33\ r^2 + 3.9\ r^4 - 2.44\ r^6]^{-0.35}$$

for $r < 0.4936$ (XII-10)

and

$$\frac{d\tau}{dr} = -0.6879\ r^{-0.05}\ [0.6635 - 0.32\ r^2]^{-0.35} \qquad \text{(XII-11)}$$

for $1.00 > r > 0.4936$

From any value of r, τ can be calculated from the numerical solution of the above differential equations (XII-10) and (XII-11). Then $(1 - 0.95\ \tau)^{2.05/0.95}$ can be computed. For this value of r, the corresponding value of u can be obtained from the appropriate equations, and $r^{1.7}\ u^{0.7}$ can then be calculated. The results are given below in Table (XII,17).

TABLE (XII,17)

$r = \frac{R}{R_i}$	$u = \frac{U}{U_i}$	τ	$(1 - 0.95\ \tau)^{\frac{2.05}{0.95}}$	$u^{0.7}\ r^{1.7}$	Error, %
0.999	1.0006	0.001	0.9980	0.9983	0.035
0.950	1.0181	0.049	0.9017	0.9165	1.612
0.900	1.0294	0.097	0.8112	0.8360	2.971
0.850	1.0344	0.144	0.7276	0.75	4.091
0.800	1.0338	0.190	0.6503	0.6843	4.976
0.750	1.0276	0.236	0.5787	0.6132	5.620
0.700	1.0163	0.280	0.5126	0.5453	6.008
0.650	1.0000	0.3245	0.4514	0.4808	6.111
0.600	0.9788	0.3683	0.3949	0.4196	5.884
0.550	0.9527	0.4116	0.3429	0.3619	5.2596
0.500	0.9217	0.4547	0.2951	0.3078	4.1345
0.450	0.9355	0.4965	0.2524	0.2573	1.9086
0.400	0.9139	0.5373	0.2141	0.2106	1.6560
0.350	0.8851	0.5774	0.1798	0.1678	7.1103
0.300	0.8465	0.6168	0.1491	0.1292	15.4685
0.250	0.7954	0.6557	0.1219	0.0947	28.6490
0.200	0.7292	0.6943	0.0977	0.0648	50.7696
0.150	0.6440	0.7328	0.0765	0.0398	92.4246

Where:

$$\text{Error, \%} = \frac{\left[u^{0.7} r^{1.7} - (1 - 0.95\ \tau)^{\frac{2.05}{0.95}}\right]}{u^{0.7}\ r^{1.7}} \times 100$$

In solving equations (XII-10) and (XII-11), a very small value of $\Delta r = 0.001$ was used so that $d\tau/dr$ can be closely approximated by $\Delta\tau/\Delta r$. The results indicate that, as the drop becomes small due to vaporization of liquid, the correlation used in the program becomes insufficient to represent the theory. At the radius equal to 25% of the initial radius, the percent error introduced in the evaporation rate is nearly 30%. In view of this, it is suggested that the correlation

$$(1 - 0.95\,\tau)^{\frac{2.05}{0.95}}$$

be replaced by a better one.

LN0043 is $V = V_i(1 - 0.95\,\tau)^{\frac{3}{0.95}}$ does follow from

LN0042, $\dot{M}(t) = \dot{M}_i(1 - 0.95\,\tau)^{\frac{2.05}{0.95}}$

E. SUMMARY OF RESULTS

The model described in Chapter 12 of AMSHAH has been reviewed with the following conclusions.

1) There are several minor errors in the text involving numerical data and formulas. These have been cited and corrections indicated.

2) Except for the erroneous cases cited in (1) above, all formulas and calculations have been checked and found to be correct.

3) Several incorrect assumptions in the analysis and modeling have been noted. Among these, the most salient ones are:

a) If the time to reach the terminal settling velocity is not exceedingly small compared to the life of the drop, the model will not be applicable.

b) Incorrect value of the surface tension of the system liquid-air is being used for the interfacial tension of the liquid with water. Study of Table (XII,16) suggests that there is no relation between these two values.

4) The results obtained from this model could easily be off by a factor of 3 to 4 (or more).

F. *RECOMMENDATIONS*

1) The results obtained from this model will probably be far from the actual values, in view of the simplifying assumptions made. More work ought to be done, experimentally and otherwise, to obtain results that are realistic.

2) Very little data are available on the interfacial tension of various liquids. If the interfacial tension is not available for the liquid in question, the use of the model is highly questionable in view of the results cited in Table (XII,16). Experimental work to obtain interfacial tensions of the concerned liquids is necessary.

G. *TABLE OF SYMBOLS USED*

B = transfer factor defined by equation (12.14)

C_D = drag coefficient for a spherical drop

C_m = specific heat of the medium (water)

C_v = specific heat of the vapor of the chemical

d = diameter

g = gravitational acceleration

G = mass flux of medium = $\rho_m U$

$\dot{m}''$ = rate of evaporation per unit area of the drop

$\dot{m}$ = rate of evaporation per drop

$\dot{M}$ = total evaporation rate (for all drops)

Nu = Nusselt number

Pr = Prandtl number

r = R/R_i

R = radius of drop at any time

R_i = radius defined by equation (12.10)

Re_d = Reynolds number based on drop diameter

St = Stanton number

t = time

t' = time to reach terminal velocity

t_{ch} = characteristic time defined by equation (12.16)

T = boiling temperature of liquid at ambient temperature

T_m = temperature of medium

u = dimensionless velocity defined by U/V_i

U = terminal velocity of a deformable drop

v = dimensionless velocity defined by V/U_i

V = terminal velocity of a nondeformable drop

We = Weber number, $\rho_m U^2 R/\sigma$

We^* = Weber number, $\rho_m V^2 R/\sigma$

δ = defined by $\delta = 0.056\ We$

λ = heat of vaporization of liquid

ρ = density of liquid

σ = surface tension

σ_i = interfacial tension

$\sigma_{\ell a}$ = surface tension of chemical in air

$\sigma_{\ell w}$ = surface tension of chemical in water

τ = nondimensional time, t/t_{ch}

Subscripts

c = critical

i = initial

m = medium

1,2 = components 1 and 2, respectively

H. *LIST OF REFERENCES*

(1) Raj, P. P. K., and A. S. Kalelkar. Boiling rate model for heavy liquids with boiling temperatures less than ambient, ch. 12, pp.171-188. In *Assessment Models in Support of the Hazard Assessment Handbook (CG-446-3)*, Report No. CG-D-65-74. Prepared by Arthur D. Little, Inc. for the Department of Transportation, U.S. Coast Guard, NTIS AD 776617, January 1974.

(2) Levich, V. G. *Physicochemical Hydrodynamics*. Prentice-Hall, Englewood Cliffs, N.J., 1962.

(3) Boucher, D. F., and G. E. Alves. Fluid and particle mechanics, sec. 5, p. 44. In Perry, Chilton and Kirkpatrick (eds.), *Chemical Engineers Handbook*, 4th ed. McGraw-Hill Book Co., New York, 1963.

(4) Spalding, D. B. *Convective Mass Transfer*. Edward Arnold (Publishers) Ltd., London, 1963.

(5) McAdams, W. H. *Heat Transmission*. McGraw-Hill Book Co., New York, 1964.

(6) Bird, B. R., W. E. Stewart, and E. N. Lightfoot. *Transport Phenomenon*. John Wiley & Sons, Inc., New York, 1960.

(7) Weast, R. C. (ed.). *Handbook of Physics and Chemistry*, 55th ed., p. E35. Chemical Rubber Publishing Co., Cleveland, Ohio, 1974-75.

(8) Liley, P. E., Y. S. Touloukian, and W. R. Gambill. Physical and chemical data, sec. 3, p. 221. In Perry, Chilton and Kirkpatrick, *Chemical Engineers Handbook*, op. cit.

(9) Lange, N. A. (ed.). *Lange's Handbook of Chemistry*, 10th ed., pp. 1661, 1663, 1668. McGraw-Hill Book Co., New York, 1967.

Appendix A

THEORY OF LIQUID SPREAD ON WATER [A1]

SPREADING AND RETARDING FORCES

"Although the force of gravity acts downward, it causes a sidewise spreading motion of a floating oil film by creating an unbalanced pressure distribution in the pool of oil and the surrounding water. This force on an element of oil film acts in the direction of decreasing film thickness and is proportional to the thickness, its gradient, and the difference in density between oil and water. ... As the oil film spreads and becomes thinner, the gravity force diminishes.

"At the front edge of the expanding slick an imbalance exists between the surface tension at the water-air interface and the sum of surface tensions at the oil-air and oil-water interfaces. The net difference, called the spreading coefficient, is a force which acts at the edge of the film, pulling it outwards. This spreading force does not depend upon the film thickness as does the gravity force, and will not decrease as the oil film thins out (unless the chemical properties change through aging). Eventually the surface tension force will predominate as the spreading force.

"These spreading forces are counterbalanced by the inertia of the oil film and of the thin boundary layer of water below it which is dragged along by friction.... The inertia of an element of the oil layer decreases with its thickness as time progresses and the film spreads, but the inertia of the viscous layer of water below the oil increase with time as its thickness grows. Consequently, the viscous retardation will eventually outweigh the inertial resistance of the oil layer itself.

"It is also informative to consider these effects from the point of an energy balance. A pool of oil floating on water possesses a greater potential energy than the water it displaces, in proportion to its thickness. As it spreads and its thickness decreases, there is a loss of potential energy. Also, as air/water surface is replaced by an oil film, the surface energy per unit area (which has the same physical value as the interfacial tension) is reduced by an amount equal to the spreading coefficient.

[A1] Landau, L. D., and E. M. Lifshitz, *Fluid Mechanics*, p. 49, Pergamon Press, London, 1959.

Thus both surface energy and potential energy are decreased as the slick spreads. This energy is converted either into heat by viscous dissipation in the water beneath the slick or into the energy of gravity surface waves which propagate away from the expanding oil pool. In other words, each spreading force is associated with an energy-producing process and each retarding force with an energy-dissipating process.

"It is thus clear that the spread of an oil film will pass through several stages as time progresses, in each of which one spreading force will be balanced by one retarding force. Although there are four such possible combinations, for large scale slicks only three regimes are important: (i) the gravity-inertia regime (called "inertial spread"), (ii) the gravity-viscous regime (called "viscous spread"), and the surface tension-viscous regime (called "surface tension spread"). As time progresses, a large spill will pass through these three regimes in succession. A very small spill (a few liters, say) will almost from the start behave as a surface tension spread." ([A1], p. 49)

In what follows we will develop the equations of motion for spread and their solution in the three spreading regimes. We treat the radial case only.

EQUATIONS OF MOTION

The equations of motion in circular coordinates for radial symmetry (no dependence on θ, $V_\theta = 0$) and constant liquid density ($\partial\rho_L/\partial t = \nabla\rho_L = \nabla\cdot\vec{V} = 0$), valid in the gravity-inertia and gravity-viscous flow regimes are:

$$\frac{\partial V_r}{\partial r} + \frac{\partial V_z}{\partial z} + \frac{V_r}{r} = 0 \tag{A-1}$$

$$\frac{\partial V_r}{\partial t} + V_r \frac{\partial V_r}{\partial r} + V_z \frac{\partial V_r}{\partial z} = -\frac{1}{\rho_L}\left(\frac{\partial p}{\partial r}\right) + \frac{\mu}{\rho_L}\left(\frac{\partial^2 V_r}{\partial z^2}\right) \tag{A-2}$$

$$\frac{\partial V_z}{\partial t} + V_r \frac{\partial V_z}{\partial r} + V_z \frac{\partial V_z}{\partial z} = -\frac{1}{\rho_L}\left(\frac{\partial p}{\partial z}\right) - g \tag{A-3}$$

Here V_r and V_z are, respectively, the velocity in r- and z-directions; ρ_L is the liquid density; p the pressure; μ the dynamic viscosity; t the time; and g the acceleration of gravity. Equation (A-1) is the equation of continuity, while equations (A-2) and (A-3) are hydrodynamic expressions of Newton's law for the r and z components of velocity, respectively. In equation (A-2) a viscosity term, $\mu(\partial/\partial r)[(\partial V_r/\partial r) + (V_r/r)]$, has been neglected. The reason is as follows. It will be noticed from (A-1) that the term $[(\partial V_r/\partial r) + (V_r/r)]$ is equal to $-(\partial V_z/\partial z)$ which is very small since V_z is very small and constant compared to V_r, for all times except very near the beginning of the spill. Hence, $(\partial^2 V_z/\partial r \partial z)$ is small and can be neglected compared to $(\partial^2 V_r/\partial z^2)$.

If we integrate equation (A-2) through (A-3) with respect to z across δ (the thickness of the liquid spreading layer) from z_1 (the liquid-water interface) to z_2 (the liquid-air interface), we get the following. From (A-3), neglecting vertical acceleration, dV_z/dt, we get:

$$p_1 - p_2 = g\rho_L (z_2 - z_1) \tag{A-4}$$

From (A-2) we get, neglecting $V_z(\partial V_r/\partial z)$

$$\left(\frac{\partial V_r}{\partial t} + V_r \frac{\partial V_r}{\partial r}\right)\delta = -\left(\frac{g(\rho_w - \rho_L)\delta}{\rho_L}\right)\frac{\partial \delta}{\partial r} - \frac{\mu}{\rho_L}\left(\frac{\partial V_r}{\partial z}\right)\Bigg|_{z_1}^{z_2} \tag{A-5}$$

The normal velocity difference $(V_{z_2} - V_{z_1})$ is obtained from (A-1).

$$V_{z_2} - V_{z_1} = -\int_{z_1}^{z_2}\left(\frac{\partial V_r}{\partial r} + \frac{V_r}{r}\right)dz = -\delta\left(\frac{\partial V_r}{\partial r} + \frac{V_r}{r}\right) \tag{A-6}$$

From the definitions of V_{z_2}, V_{z_1}, and δ, we have, respectively,

$$V_{z_2} = \frac{\partial z_2}{\partial t} + V_r \frac{\partial z_2}{\partial r}$$

$$V_{z_1} = \frac{\partial z_1}{\partial t} + V_r \frac{\partial z_1}{\partial r}$$

$$\delta = z_2 + z_1$$

Then noting by a simple hydrostatic argument that $z_2 = \delta(\rho_w - \rho_L)/\rho_w$ and $z_1 = -\rho_L\delta/\rho_w$, we obtain

$$V_{z_2} = \left(\frac{\rho_w - \rho_L}{\rho_w}\right)\left(\frac{\partial \delta}{\partial t} + V_r \frac{\partial \delta}{\partial r}\right) \tag{A-7}$$

$$-V_{z_1} = \frac{\rho_L}{\rho_w}\left(\frac{\partial \delta}{\partial t} + V_r \frac{\partial \delta}{\partial r}\right) \tag{A-8}$$

Combining these with (A-6) gives finally

$$\frac{\partial \delta}{\partial t} + V_r \frac{\partial \delta}{\partial r} + \delta\left(\frac{\partial V_r}{\partial r} + \frac{V_r}{r}\right) = 0 \tag{A-9}$$

Making the identification, $G = g(\rho_w - \rho_L)/\rho_L$, and $\Lambda = \mu(\partial V_r/\partial z)$ in (A-5), we obtain

$$\left(\frac{\partial V_r}{\partial t} + V_r \frac{\partial V_r}{\partial r}\right)\delta + G\,\delta \frac{\partial \delta}{\partial r} = \frac{\Lambda}{\rho_L} \tag{A-10}$$

Equations (A-9) and (A-10) are the working equations of motion for δ and V_r for the spreading problem in the gravity-inertia and gravity-viscous regimes. Since no surface tension forces are present, they will not suffice for the viscous-surface tension regime of spread. Equations (A-9) and (A-10) are identical to equations (III-3a) and (III-3b) in Chapter 2 of this report.

Gravity-Inertia Regime

Here a solution to the equations of motion is given in terms of a similarity analysis. The similarity variable X in question is r/X_{LE} where r is the radial coordinate and X_{LE} the leading edge radius which is a function of time and is expressed as At^n. We drop the viscous term in this regime.

With this convention, equations (A-9) and (A-10) become, after letting $V_r = u$,

$$\frac{\partial \delta}{\partial t} + \left(\frac{u}{X_{LE}} - \frac{nX}{t}\right)\frac{\partial \delta}{\partial X} + \frac{\delta}{X_{LE}}\left(\frac{\partial u}{\partial X} + \frac{u}{X}\right) = 0 \tag{A-11}$$

$$\frac{\partial u}{\partial t} + \left(\frac{u}{X_{LE}} - \frac{nX}{t}\right)\frac{\partial u}{\partial X} + \frac{G}{X_{LE}}\left(\frac{\partial \delta}{\partial X}\right) = 0 \tag{A-12}$$

where

$$G = g\left(\frac{\rho_w - \rho_L}{\rho_L}\right)$$

Mass conservation requires that

$$2\pi \int_0^{X_{LE}} \delta r \, dr = L^3 \tag{A-13}$$

where L^3 is the initial volume of spill. This can only be satisfied if

$$\delta = D(X)/X_{LE}^2 \tag{A-14}$$

where D is a form factor. Then

$$2\pi \int_0^{X_{LE}} \frac{D r \, dr}{X_{LE}^2} = L^3 \tag{A-15}$$

In order to satisfy similarity conditions, the velocity, u, must have the form

$$u = \frac{U(X) X_{LE}}{t} \tag{A-16}$$

Now the continuity equation (A-11) can be written, substituting (A-16) for u and (A-14) for δ, as

$$\frac{d}{dX}\left[(U - nX) DX\right] = 0 \tag{A-17}$$

implying $(U - nX)DX$ is constant. The boundary condition is $U(X=0) = 0$. This is satisfied by

$$U = nX \tag{A-18}$$

which also satisfies (A-17). Substituting (A-14) and (A-16) into (A-12), integrating and imposing conservation of volume (A-15), we obtain for D

$$D = \frac{A^4 X^2}{4G} + \frac{L^3}{\pi} - \frac{A^4}{8G} \tag{A-19}$$

where A is an integration constant, $n = 1/2$, and $A = KG^{1/4} L^{3/4}$.

The value of K is determined by considering the rate of propagation of the leading edge of the slick. Dimensional arguments require that the leading edge velocity must be proportional to the characteristic wave speed, c, for a small disturbance. Since

$$c = (G \delta_{LE})^{1/2} \tag{A-20}$$

$$u_{LE} = k(G \delta_{LE})^{1/2} \tag{A-21}$$

Since the leading edge, δ_{LE}, is very thin at late times, $k = 1$. On the other hand [A2] at very early times, $t \to 0$, $u_{LE} = 2c$ giving $k = 2$. Obviously some value between 1 and 2 will suffice for k, the exact value being dependent on the exact nature of the air-water-liquid interface of the leading edge. Thus, the surface tension plays a role here too.

By substituting (A-21) into (A-14) and (A-19), we obtain for A

$$K = \left(\frac{16 k^2}{\pi (4 - k^2)} \right)^{1/4} \tag{A-22}$$

The range of K for $1 \leq k \leq 2$ is 1.14 to ∞. Taking $k = 1$ for the late time case and recalling from before $A = K G^{1/4} L^{3/4}$ we have

$$X_{LE} = A t^n = 1.14\ G^{1/4} L^{3/4} t^{1/2} \tag{A-23}$$

(A-23) will be seen to correspond to r in Table (III,2) for the gravity-inertia regime (Chapter 2 of this report) and also to Table 3.1 of Chapter 3 in AMSHAH [A3] in the same regime.

[A2] Fannelop, T. K., and G. D. Waldman, Dynamics of oil slicks, *AIAA Journal 10*(4):506-510, 1972.

[A3] Raj, P. P. K., and A. S. Kalelkar, *Assessment Models in Support of the Hazard Assessment Handbook* (AMSHAH), (CG-446-3), Report No. CG-D-65-74, prepared by Arthur D. Little, Inc. for the Department of Transportation, U.S. Coast Guard, NTIS AD-776617, January 1974.

Gravity-Viscous Regime

Before the equation of motion (A-2) can be solved to include the effect of viscosity through $\mu/\rho_L = \nu$, we must decide what type of drag law is to be used, since to solve (A-2) in a straightforward mathematical way is extremely difficult.

There are two principal ways to treat the edge effects of oil spread on water that are consistent with the equations of motion describing the spill. They are, respectively (1) without and (2) with the effect of inertial forces. The latter is the boundary layer approach and is derived in Appendix B of this report.

(1) The assumption that singularity at leading edge can be described as

$$\delta = \delta_0 (X_{LE} - r)^m \tag{A-24}$$

and inserting into (A-2) and neglecting inertial term

$$\left(\frac{\partial V_r}{\partial t} + V_r \frac{\partial V_r}{\partial r} + V_z \frac{\partial V_r}{\partial z} \right)$$

$$G \frac{\partial \delta}{\partial r} = \nu \frac{\partial^2 u}{\partial z^2} \tag{A-25}$$

with the additional assumptions that

$$\frac{\partial u}{\partial z} = \frac{u}{\delta} \tag{A-26}$$

$$\frac{\partial^2 u}{\partial z^2} = \frac{u}{\delta^2} \tag{A-27}$$

This means that no account of inertial effects is made, hence this is not a boundary layer theory.

As a result of the assumptions shown,

$$\frac{Gm}{\nu} \delta_0^3 (X_{LE} - r)^{3m-1} = u \tag{A-28}$$

Because u_{LE} cannot be zero at $r = X_{LE}$, i.e., the leading edge, the exponent $3m - 1$ must vanish; $m = 1/3$ as a result. Thus, δ is

$$\delta = \delta_0 (X_{LE} - r)^{1/3} \tag{A-29}$$

Now we assume $\delta_0 = At^n$ and require that the total volume of the spill be invariant with respect to time for a nonevaporation situation. This means that the total exponent on t must vanish thus giving the value of m for this set of assumptions.

$$L^3 = V = 2\pi \int_0^{X_{LE}} \delta r \, dr \tag{A-30}$$

$$V = 2\pi\delta_0 \int_0^{X_{LE}} r (X_{LE} - r)^{1/3} dr = 2\pi \left(\frac{9}{28}\right) \delta_0 \; X_{LE}^{7/3} \tag{A-31}$$

Since

$$u_{LE} = \dot{X}_{LE} = \frac{Gm}{\nu} \delta_0^3$$

or

$$\frac{G}{3\nu} A^3 t^{3n} = \dot{X}_{LE}$$

then

$$X_{LE} = \int \dot{X}_{LE} \, dt = \frac{GA^3}{3\nu} \; \frac{t^{3n+1}}{3n + 1}$$

Hence the volume V is

$$V = 2\pi \left(\frac{9}{28}\right) At^n \left(\frac{GA^3}{3\nu} \; \frac{t^{3n+1}}{3n+1}\right)^{7/3} \tag{A-32}$$

and

$$t^n \; t^{7n+7/3} = 1$$

$$8n + 7/3 = 0$$

$$n = -7/24, \quad X_{LE} \sim t^{3(-7/24)+1} = t^{1/8}$$

This is what was done in Chapter 8 of AMSHAH as seen in Table 8.1 for the gravity-viscous regime, radial case.

(2) Assumption that a viscous boundary layer holds and as a well-known standard result (see reference A1, p. 149), the vertical velocity gradient can be expressed as

$$\frac{\partial u}{\partial z} = .332 \sqrt{u^3/(\nu X_{LE})} \tag{A-33}$$

as derived in Appendix B of this report, equation (B-17). Here again we assume

$$\delta = \delta_0 (X_{LE} - r)^m \tag{A-34}$$

where

$$\delta_0 = At^n$$

and take the integrated form with respect to z of the momentum equation, i.e., (A-10).

$$\frac{G}{\nu} \delta \frac{\partial \delta}{\partial X} = \frac{\partial u}{\partial z} = \frac{.33}{\sqrt{\nu}} \frac{u^{3/2}}{X_{LE}^{1/2}} \tag{A-35}$$

$$\frac{Gm\delta_0^2}{\nu} (X_{LE} - r)^{2m-1} = \frac{.33}{\sqrt{\nu}} \frac{u^{3/2}}{X_{LE}^{1/2}} \tag{A-36}$$

It should also be noted that the boundary layer approach takes into account inertial effects, whereas the approach in (1) above does not. This is an important distinction.

Since u_{LE} must not vanish at the leading edge, $m = 1/2$. Conservation of volume gives

$$V = 2\pi \left(\frac{4}{15}\right) \delta_0 X_{LE}^{5/2} = 2\pi \left(\frac{4}{15}\right) At^n X_{LE}^{5/2} \tag{A-37}$$

Now

$$u_{LE} = \dot{X}_{LE} = \left(\frac{3\, Gm\, \delta_0^2 X_{LE}^{1/2}}{\sqrt{\nu}}\right)^{2/3} \tag{A-38}$$

$$\dot{X}_{LE} \sim \delta_0^{4/3} X_{LE}^{1/3}$$

$$\int dX_{LE}\, X_{LE}^{-1/3} \sim \int \delta_0^{4/3}\, dt$$

$$\frac{3}{2} X_{LE}^{2/3} \sim \frac{t^{(4n+3)/3}}{(4n+3)/3}$$

$$X_{LE} \sim t^{2n+(3/2)}$$

$$X_{LE}^{5/2} \sim t^{5n+(15/4)}$$

$$\delta_0 X_{LE}^{5/2} \sim t^{6n+(15/4)}$$

$$6n + 15/4 = 0$$

$$n = -15/24 = -5/8$$

$$X_{LE} \sim t^{2n+(3/2)} = t^{1/4} \qquad \text{(A-39)}$$

This is in accord with the result of Fannelop and Waldman. It is also the result in Table 3.1 of AMSHAH for the gravity-viscous case.

Thus, both the thickness profile $\delta = \delta_0 (X_{LE} - r)^m$ and the time rate of change of the leading edge differ from case (1) above.

Surface Tension-Viscous Regime

At very late times or for very thin slicks, the dominant spreading force is the net difference of three pairwise surface tensions, air-liquid, water-liquid, air-water. This difference is known by the spreading coefficient, σ, which pulls the edge of the liquid outward and is thus the spreading force. This force is resisted by viscous drag. The determination of σ must be measured by experiment, since it is a net value predicated on the rate of the spreading process. It is never simply the surface tension of one of the three pairs just mentioned. Schematically, the situation is shown below:

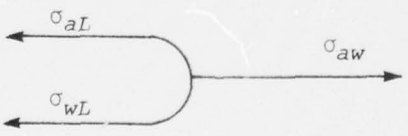

where $\sigma \sim (\sigma_{aw} - \sigma_{aL} - \sigma_{wL})$

An exact analysis of the flow problem is very difficult and has never been done. Following Fannelop and Waldman, we will present an engineering approximation. We note first that the rate of spread in this regime is independent of volume, as shown by Fay [A4]. This results in the one- and two-dimensional cases giving very similar results with regard to time behavior of X_{LE}.

The force balance for this regime is:

$$2\pi X_{LE}\sigma = \int_0^{X_{LE}} 2\pi r \, \Lambda \, dr \tag{A-40}$$

An equation for the unknown position of the leading edge, X_{LE}, is obtained by substituting for Λ the results of the boundary layer theory. Then, as usual, letting $X_{LE} = At^n$, it is found through dimensional consistency that $n = 3/4$ in agreement with experiment. If we further let

$$u = u_{LE} \ (r/X_{LE}) \tag{A-41}$$

which is consistent with the solutions of the first two regimes, and substitute in (A-40), we find for the radial case for a high-viscosity liquid

$$X_{LE} = 1.6 \left[\sigma^{1/2} / (\rho_w \mu_w)^{1/4}\right] t^{3/4} \tag{A-42}$$

It is the result given in Table 3.1 of AMSHAH.

TERMINATION OF SPREAD

All of the preceding deals with the movement of slick but not with its termination. Here we treat the matter briefly by recording comments and work by Fay [A4], since no reliable experimental evidence exists in this area.

It has been noticed by many that after some time slicks cease to spread. In almost all cases the final film thickness is much greater than that of a monomolecular layer, being about 10^{-3} cm in the case of oil spreading.

Fay proposed a theory with which to account for this. He claimed that the spreading coefficient is reduced by an increase in the water-

---

[A4] Fay, J. A., Physical processes in the spread of oil on a water surface, p. 463, *Prevention and Control of Oil Spills*, API, Washington, D.C., 1970.

oil surface tension, brought about by the dissolving of oil fraction in the water layer underneath the oil film. The volume of oil which can be dissolved in this layer per unit area would thus be proportional to $t^{1/2}$ or as a consequence of this the maximum area of the spill peak at an area proportional to volume to the .75 power. However, since both surface solubility and the surface tension of the water-oil interface are not well known, much work remains to be done experimentally before such a result can be accepted universally.

Appendix B

BOUNDARY LAYER THEORY

In the treatment of the liquid spreading problem in the gravity-viscous regime, use is made of the fact that a boundary layer exists and accounts most correctly for the existence of the drag force in that particular regime of spread. There are two good reasons for this. The first is that a serious attempt is made to account for the actual velocity gradient with the result that the proper viscous forces are quantified, which arises in the first place because of velocity gradients (shearing forces). Alternative treatements regard the velocity gradient as simply the x-component of velocity divided by liquid the layer thickness. The second reason is that the boundary layer as given here [B1] does *not neglect* the inertial terms ($\vec{V}\cdot\nabla\vec{V}$ for steady flow) in the equation of motion known as the Navier-Stokes equation. By inclusion of this force, the always diminishing but present inertial resistance is retained, a desirable representation of physical reality.

The result of all these considerations is that, for the velocity gradient, $\partial V_x/\partial z$, within the boundary layer, the well-known formula for laminar flow holds.

$$\frac{\partial V_x}{\partial z} = .332 \sqrt{\frac{\rho U^3}{\eta x}} \Bigg|_{z=0} \qquad \text{(B-1)}$$

Here V_x is the x-component of velocity in the boundary layer, ρ the density, and η the dynamic viscosity. U is the main stream velocity. The rationale leading to (B-1) will now be given.

It is a well-known fact that for large Reynolds numbers, Re, fluid flow may be considered as ideal. This is because for large Re the viscosity η is generally small. When a boundary such as a wall is present, however, the tangential component of velocity must vanish for a real fluid due to its finite viscosity. From these two facts, we conclude that the region of appreciable velocity gradient, $\partial V_x/\partial z$, occurs only over a thin layer adjacent to the wall. This layer is called the boundary layer. The flow in the boundary layer can be either laminar or turbulent, but we will consider only the laminar theory since this is the most relevant to our needs regarding spreading.

The rapid decrease of the velocity in the boundary is due ultimately to the viscosity, which cannot be neglected even if Re is large. This

---

[B1] Landau, L. D., and E. M. Lifshitz, *Fluid Mechanics*, p. 145, Pergamon, London, 1959.

is manifested by large velocity gradients in the boundary layer. As a result, the viscosity terms in the Navier-Stokes equation are large even if η is not.

Let us first consider the two-dimensional equations of motion for flow along a plane portion of the surface. We take this plane as the x,y-plane with the x-axis in the direction of flow. The velocity distribution is independent of y, and the velocity has no y-component.

The exact Navier-Stokes equation and the equation of continuity are thus

$$V_x \frac{\partial V_x}{\partial x} + V_z \frac{\partial V_x}{\partial z} = - \frac{1}{\rho} \frac{\partial p}{\partial x} + \nu \left(\frac{\partial V_x^2}{\partial x^2} + \frac{\partial V_x^2}{\partial z^2} \right) \tag{B-2}$$

$$V_x \frac{\partial V_z}{\partial x} + V_z \frac{\partial V_z}{\partial z} = - \frac{1}{\rho} \frac{\partial p}{\partial z} + \nu \left(\frac{\partial V_z^2}{\partial x^2} + \frac{\partial V_z^2}{\partial z^2} \right) \tag{B-3}$$

$$\frac{\partial V_x}{\partial x} + \frac{\partial V_z}{\partial z} = 0 \tag{B-4}$$

The flow is steady and V_x is the x-component of velocity, ρ the density, p the pressure, and ν the kinematic viscosity.

Since the boundary layer is thin, it is clear that the flow in it takes place parallel to the surface, i.e., V_z is small compared to V_x. This can be seen from (B-4). The velocity, V_x, varies rapidly along the z-axis, an appreciable change in it occurring at distances of the order, δ, the thickness of the boundary layer. Along the x-axis, on the other hand, the velocity varies slowly, an appreciable change in it occurring only over distances of the order of a length, ℓ, characteristic of the problem such as the dimension of the body in question. Hence, the z-derivatives of the velocity are large compared to the x-derivatives. It follows that, in equation (B-2), $\partial V_x^2 / \partial x^2$ may be neglected in comparison with $\partial V_x^2 / \partial z^2$; comparing (B-2) with (B-3), we see that $\partial p / \partial z$ is small compared to $\partial p / \partial x$. In these three approximations we can put $\partial p / \partial z = 0$. In other words, the pressure in the boundary layer is equal to the pressure in the main stream, $p(x)$, and is a function of x for the purpose of solving the boundary layer problem. In equation (B-2) we can write, rather than $\partial p / \partial x$, dp/dx; this in turn can be expressed in terms of the velocity $V(x)$ of the main stream. Since we have potential flow outside the boundary layer, Bernoulli's equation ($p + \frac{1}{2} \rho U^2 = \text{constant}$) holds, when $\left[(1/\rho)(dp/dx) = - U(dU/dx) \right]$.

Thus, we obtain the equations of motion in the laminar boundary layer in the form:

$$V_x \frac{\partial V_x}{\partial x} + V_z \frac{\partial V_x}{\partial z} - \nu \frac{\partial^2 V_x}{\partial z^2} = -\frac{1}{\rho}\frac{dp}{dx} = U\frac{dU}{dx} \tag{B-5}$$

$$\frac{\partial V_x}{\partial x} + \frac{\partial V_z}{\partial z} = 0 \tag{B-6}$$

Let U_0 be a velocity characteristic of the problem, such as the velocity of the mainstream at infinity. Instead of coordinates x,y and velocities V_x, V_z we introduce the dimensionless variables $x'z'$, V_x' V_z' :

$$x' = \frac{x}{\ell} \qquad z' = \frac{z}{\ell}\sqrt{R} \tag{B-7}$$

$$V_x' = \frac{V_x}{U_0} \qquad V_z' = \frac{V_z}{U_0}\sqrt{R} \tag{B-8}$$

$$U' = \frac{U}{U_0} \qquad R = U_0\frac{\ell}{\nu} \tag{B-9}$$

Then equations (B-5) and (B-6) become

$$V_x' \frac{\partial V_x'}{\partial x'} + V_z' \frac{\partial V_x'}{\partial z'} - \frac{\partial^2 V_x'}{\partial z'^2} = U' \frac{dU'}{dx'} \tag{B-10}$$

$$\frac{\partial V_x'}{\partial x'} + \frac{\partial V_z'}{\partial z'} = 0 \tag{B-11}$$

Since these equations and the boundary conditions on them do not involve the viscosity, their solutions are independent of the Reynolds number. Hence, when the Reynolds number is changed, the whole flow pattern in the boundary layer simply undergoes a similarity transformation. This means, in this case, that distances and velocities in the x-direction remain invariant, while distances and velocities in the z-direction vary as $1/\sqrt{R}$. Thus, if ν were to become vanishingly small, the boundary layer would collapse since R would become very large.

Next, we can say that the dimensionless velocities V_x' V_z' obtained from solving (B-10) and (B-11) are of the order unity, again because they do not depend on R . Since this is true, we must have from (B-8)

$$V_z \sim U_0/\sqrt{R} \tag{B-12}$$

Also, from $z = \ell\, z'/\sqrt{R}$ we have

$$\delta \sim \ell/\sqrt{R} \tag{B-13}$$

Since some interesting hydrodynamics are entailed in the application of the formalism to an infinite length flat plate, $\ell \to \infty$, we proceed to do so remembering that $x=0$ constitutes the leading edge. Because the stream is of infinite length, $dU/dx = 0$, and we have simply

$$V_x \frac{\partial V_x}{\partial x} + V_z \frac{\partial V_x}{\partial z} = \nu \frac{\partial V_x^2}{\partial z^2} \tag{B-14}$$

$$\frac{\partial V_x}{\partial x} + \frac{\partial V_z}{\partial z} = 0 \tag{B-15}$$

For boundary conditions at the surface of the plate, we have $V_x=V_z=0$ for $z=0$, $x\geq 0$. As we move away from the plate, the velocity must approach asymptotically the velocity U of the incident flow, i.e., $V_x = U$ for $z \to \infty$. As discussed previously, V_x' and V_z' can only be functions of x' and z' and not ν . Thus, V_x/U can only be a function of x' and z' such that ℓ does not appear, since in this case it is infinite. The combination $z'/\sqrt{x'} = z\sqrt{U/\nu x}$ satisfies this requirement, and we seek solutions of the form

$$V_x = U\, f_1\left[z\sqrt{U/\nu x}\right] \qquad V_z = \sqrt{U\nu/x}\, f_2\left[z\sqrt{U/\nu x}\right] \tag{B-16}$$

where f_1 and f_2 are two dimensionless functions. Using the continuity equation, we can express f_2 in terms of f_1 . The problem then reduces to determining a single function, f_1, of a single variable, $\zeta = z\sqrt{U/\nu x}$.

Since we are only interested in the variation of V_x, V_z being small anyway, we can draw an important conclusion from (B-16) without having to determine f_1. The velocity, V_x, increases from zero at the plate surface to a definite fraction of U for a given value of the argument f, i.e., for $z\sqrt{U/\nu x}$ = any given constant. Hence, we can conclude that the thickness of the boundary layer in flow along a plate is given in order of magnitude by

$$\delta \sim \sqrt{\nu x/U} \tag{B-17}$$

Thus as we move away from the edge of the plate, δ increases as the square root of the distance from the edge.

The function f can be determined by numerical integration and by considering the drag force on a unit area of the surface of the plate, say $\sigma xz = \eta(\partial V_x/\partial z)\Big|_{z=0}$. This yields

$$\eta\left(\partial V_x/\partial z\right)\Big|_{z=0} = .332\sqrt{\eta\rho/x}\; U^{3/2} \qquad \text{(B-18)}$$

which is essentially a differential version of the well-known result due to N. Blasius in 1908. We note that it was obtained by taking into account both inertial $V_z(\partial V_x/\partial z)$ etc. terms as well as the viscous term, $\nu(\partial V_x{}^2/\partial z^2)$. Thus, it forms a more realistic drag picture for surface spreading than simple counting of only the viscous term in the equations of motion in the viscous regimes. While $V_x(\partial V_x/\partial z)$ and $V_z(\partial V_x/\partial z)$ are not in general large because $\partial V_x/\partial z$ and V_z are small, they are finite and should not be neglected unless Re becomes very large, implying that the boundary thickness, δ, becomes very small compared to the thickness of the spreading fluid.

Appendix C

METHOD OF CHARACTERISTICS FOR SPREADING POOL

In this appendix we briefly comment on the usage of characteristics in the solution to the spreading problem of one liquid on another. For a detailed discussion of the origins and uses of the method of characteristics see Courant and Friedrichs [C1].

The equations of motion that we are interested in to determine δ and u for the spreading slick are for the radial case.

$$\frac{\partial \delta}{\partial t} + u \frac{\partial \delta}{\partial r} + \frac{\delta}{r} \frac{\partial}{\partial r}(ru) = 0 \tag{C-1}$$

$$\frac{\partial u}{\partial t} + u \frac{\partial u}{\partial r} + G \frac{\partial \delta}{\partial r} = \frac{\nu}{\delta} \frac{\partial u}{\partial z}\Bigg|_{z_1}^{z_2} \tag{C-2}$$

Here δ is the slick thickness, u the velocity in r direction, $G = [(\rho_W - \rho_L)/\rho_L]\, g$ (ρ_L the density of liquid, etc.). The variables z_2 and z_1 are the coordinates of the air-liquid and liquid-water interfaces, respectively, while ν is the kinematic viscosity of the liquid spreading.

If we now assume that, in the gravity-inertia stage of spreading, solutions of δ and u have the functional form

$$\delta = \delta(r - \Lambda t)$$

$$u = u(r - \Lambda t)$$

and letting

$$\xi = r - \Lambda t$$

we can rewrite (C-1) and (C-2) in the following form and obtain ordinary differential equations that are coupled

$$(u - \Lambda) \frac{d\delta}{d\xi} + \delta \frac{du}{d\xi} = \frac{-\delta u}{r} \tag{C-3}$$

$$G \frac{d\delta}{d\xi} + (u - \Lambda) \frac{du}{d\xi} = \frac{\nu}{\delta} \frac{\partial u}{\partial z}\Bigg|_{z_1}^{z_2} \tag{C-4}$$

[C1] Courant, R., and K. Friedrichs, *Supersonic Flow and Shockwaves*, p. 37, Interscience, New York, 1948.

Here the new variable, ξ, plays the role of phase parameter with Λ acting as a velocity of propagation of the disturbance attendant to the spreading slick. This will become clear in the discussion that follows.

The system of coupled equations has solutions of the form

$$\frac{d\delta}{d\xi} = \begin{vmatrix} \frac{-\delta u}{r} & \delta \\ \frac{\nu}{\delta}\frac{\partial u}{\partial z}\Big|_{z_1}^{z_2} & (u-\Lambda) \end{vmatrix} /\Delta \qquad \text{(C-5)}$$

$$\frac{du}{d\xi} = \begin{vmatrix} u-\Lambda & \frac{-\delta u}{r} \\ G & \frac{\nu}{\delta}\frac{\partial u}{\partial z}\Big|_{z_1}^{z_2} \end{vmatrix} /\Delta \qquad \text{(C-6)}$$

where

$$\Delta = \begin{vmatrix} u-\Lambda & \delta \\ G & u-\Lambda \end{vmatrix}$$

If one now attempts to integrate (C-5) and (C-6), one has to write the solution as an expansion around the poles of $d\delta/d\xi$ and $du/d\xi$. This is accomplished by setting the determinant Δ equal to zero, resulting in

$$u^2 - 2u\Lambda + \Lambda^2 - \delta G = 0$$

Solving for Λ, i.e., the eigenvalues of the matrix of the determinant Δ, we obtain

$$\Lambda_1 = u + c \qquad \Lambda_2 = u - c \qquad \text{(C-7)}$$

where $c = \sqrt{G\delta}$ as might have been guessed. We see that c has the dimension of velocity and is the characteristic velocity of a disturbance or small wave, i.e., a singularity of flow.

Now Λ_1 and Λ_2 are the eigenvalues to the set of coupled equations (C-3) and (C-4) and as such are associated with eigenvectors which we now seek.

The eigenvectors are determined from the secular equations (C-3), (C-4) for the homogeneous case, i.e., the right-hand sides are set equal to zero. This results in

$$du = \frac{c}{\delta}\, d\delta \quad \text{for } \Lambda_1 \tag{C-8}$$

and

$$du = \frac{-c}{\delta}\, d\delta \quad \text{for } \Lambda_2 \tag{C-9}$$

To integrate (C-8), recalling that $c = \sqrt{G\delta}$, we have

$$du = G^{1/2}\, \delta^{-1/2}\, d\delta \tag{C-10}$$

$$u = 2\, G^{1/2}\, \delta^{1/2} + \text{constant} \tag{C-11}$$

or

$$u - 2c = \text{constant} \tag{C-12}$$

These are known as P invariants and are constants of the motion for a point moving through the liquid with velocity $u + c$. Alternatively, we may state that for a point whose motion is characterized by the differential equation

$$\frac{dr}{dt} = u + c \tag{C-13}$$

$u - 2c$ is a constant. The solution of (C-13) yields one of the two sets of characteristic curves, C_1, associated with the problem. Thus if one travels a characteristic curve in the (r,t) plane whose equation is $dr/dt = u + c$, he will observe no change in the quanity $u - 2c$. Obviously the slope of C_1 is $u + c$ or Λ_1, a quantity which will in itself in general vary along C_1. This is shown in Figure C-1.

Integrating (C-9) gives the eigenvector associated with Λ_2 or $u - c$

$$u + 2c = \text{constant} \tag{C-14}$$

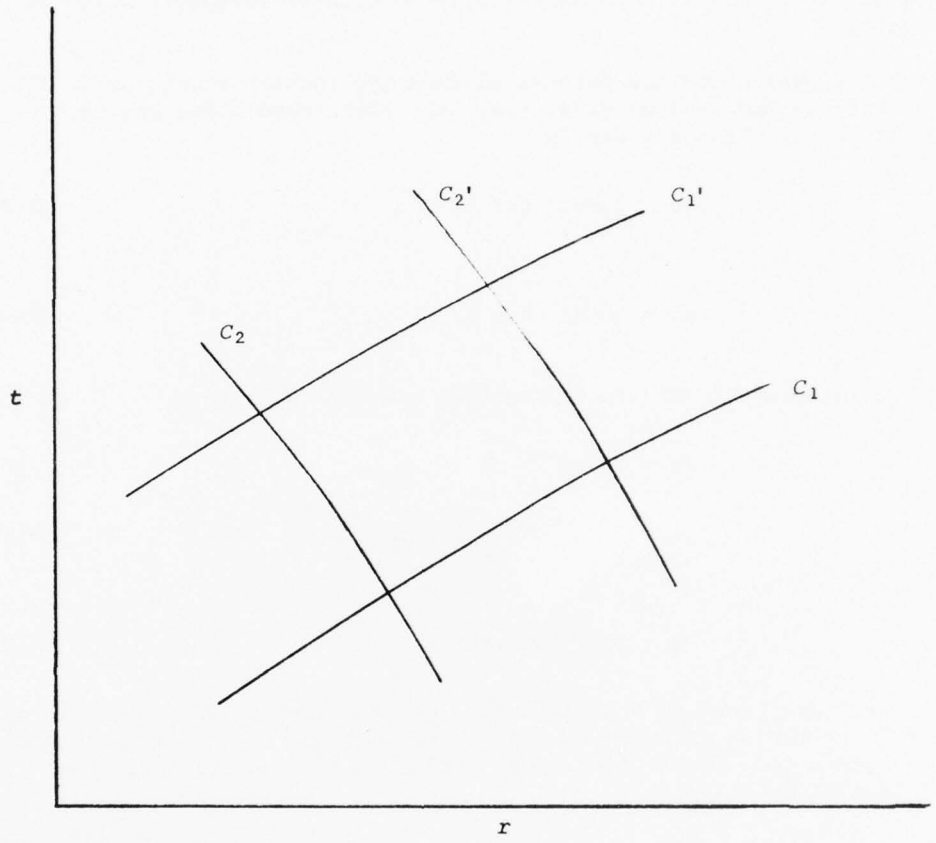

FIGURE C-1. Characteristic Curves

This is known as a Q invariant, and again $u + 2c$ is a constant of the motion for a point moving with velocity $u - c$. The family of curves generated by the differential equation

$$\frac{dr}{dt} = u - c \tag{C-15}$$

becomes the other set of characteristic curves known as C_2 and is depicted in Figure C-1. All considerations regarding C_1 hold analogously for C_2.

To summarize, we have assumed solutions to (C-1) and (C-2) in the form (C-3) and (C-4) by claiming a wavelike phase variable ξ exists, such that $\xi = r - \Lambda t$ where Λ turns out to be a characteristic or phase velocity. In determining the solutions of (C-3) and (C-4), one is naturally led to a simultaneous linear equation whose solution is determined through the extraction of the eigenvalues Λ of the matrix

$$\begin{pmatrix} u & \delta \\ G & u \end{pmatrix}$$

This is seen to be equivalent to expansion of $d\delta/d\xi$ and $du/d\xi$ around their poles through the vanishing of the determinant

$$\Delta = \begin{vmatrix} u - \Lambda & \delta \\ G & u - \Lambda \end{vmatrix} = 0$$

Solving for the two eigenvalues Λ_1 and Λ_2 in terms of G, δ, and u, we determine the two characteristic velocities $\Lambda_1 = u + c$ and $\Lambda_2 = u - c$, along with their associated eigenvectors that integrate to $u - 2c$ = constant and $u + 2c$ = constant, respectively. These are known as the Riemann P and Q invariants and are constants of the motion along characteristic curves C_1 determined from $dr/dt = \Lambda_1$ and C_2 determined from $dr/dt = \Lambda_2$.

For application of the foregoing to spreading in the gravity-inertia regime, we invoke the conditions of local continuity, namely

$$r\,u\,\delta = \text{constant} \tag{C-16}$$

or

$$u\,\delta\,dr + r\,\delta\,du + ru\,d\,\delta = 0 \tag{C-17}$$

We seek a solution to (C-17) in the neighborhood of a singularity, at a fixed value of r. Thus we have

$$d\delta = -\frac{\delta}{u}\,du \tag{C-18}$$

Utilizing (C-8) for du and inserting in (C-18)

$$d\delta = -\frac{\delta}{u}\,\frac{c}{\delta}\,d\delta = -\frac{c}{u}\,d\delta \tag{C-19}$$

In order to satisfy (C-19) $u = -c$, or the propagation of the singularity, proceeeds backwards at the characteristic speed $c = \sqrt{G\delta}$. Along with this singularity, we associate the eigenvalue $\Lambda_1 = u + c$ and the eigenvector $u - 2c$ or the P invariant. Thus in our case $\Lambda_1 = 0$ and the P invariant is $-3c$ is a constant. The slope of the characteristic curve for the disturbance Λ_1 is of course zero.

On the other hand, if we utilize (C-9) for du in (C-18) we get

$$d\delta = -\frac{\delta}{u}\,du = +\frac{\delta}{u}\,\frac{c}{\delta}\,d\delta = \frac{c}{u}\,d\delta \tag{C-20}$$

Now $u = c$ and the singularity propagates forward with characteristic speed c. Along with this singularity we associate Λ_2 or $u - c$ and the Q invariant $u + 2c$. Here $\Lambda_2 = 0$, $Q = 3c$.

In other words, in the vicinity of the singularity, motion will occur at characteristic velocities. As one proceeds to expand solutions for u and δ around the singularities as in (C-5) and (C-6), one obtains the retardation effects resulting from viscous drag. These are small in the initial flow or gravity-inertia regime but become more important in the gravity-viscous regime, rendering the method of characteristics less convenient and insightful.

As a final note, Fannelop and Waldman [C2] use the derviation given by Stoker [C3] where they define P and Q invariants

$$P = 2c + u \tag{C-21}$$

$$Q = 2c - u \tag{C-22}$$

[C2] Fannelop, T. K., and G. D. Waldman, Dynamics of oil slicks, *AIAA Journal 10*(4):506-510, 1972.

[C3] Stoker, J., *Water Waves*, p. 308, Interscience, New York, 1957.

AD-A044 198 ENVIRO CONTROL INC ROCKVILLE MD F/G 13/2
A CRITICAL TECHNICAL REVIEW OF SIX ADDITIONAL HAZARD ASSESSMENT--ETC(U)
MAR 77 A H RAUSCH, R M. /KUMAR, C J LYNCH DOT-CG-33377-A
UNCLASSIFIED USCG-D-54-77 NL

3 OF 3
AD
A044198

END
DATE
FILMED
10-77
DDC

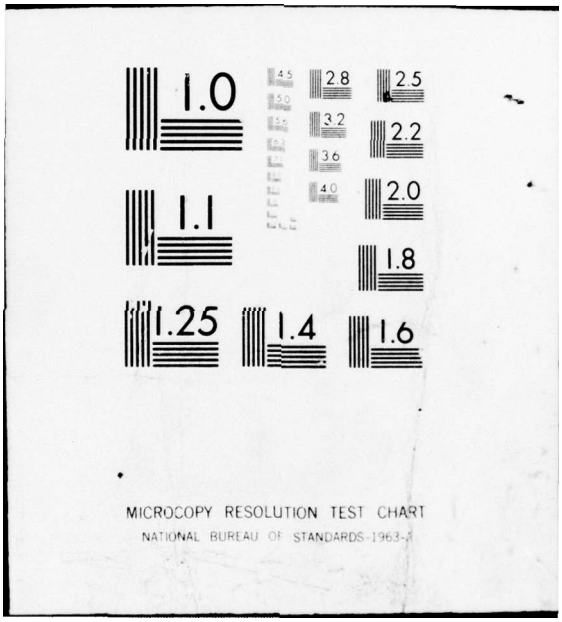
1.0
1.1
1.25
1.4
1.6
1.8
2.0
2.2
2.5
2.8
3.2
3.6
4.0
4.5
5.0
5.6
MICROCOPY RESOLUTION TEST CHART
NATIONAL BUREAU OF STANDARDS-1963-A

These satisfy

$$\frac{\partial P}{\partial t} + (u + c)\frac{\partial P}{\partial x} = 0 \qquad \text{(C-23)}$$

$$\frac{\partial Q}{\partial t} + (u - c)\frac{\partial Q}{\partial x} = 0 \qquad \text{(C-24)}$$

It is easily seen, by reversing the signs in (C-21) and (C-22), that these invariants correspond to Λ_2 and Λ_1, respectively, or are reversed from our case.

To evaluate these invariants according to Fannelop and Waldman one must realize that u is a relative velocity with respect to particle motion of the leading edge. For their P invariant $u = 0$ or the leading edge travels at characteristic speed c. Thus $P = 2c$. In our case, $Q = 3c$ since u is an absolute velocity and equals c. On the other hand, their Q invariant or backward wave corresponds to a relative velocity of $c - (-c)$ or $2c$. Their Q is thus equal to $2c - 2c$ or 0, whereas our Q corresponding to this is for $u = -c$, just $u - 2c$ or $-3c$.

Appendix D

SOLUTION OF DIFFUSION EQUATIONS USING TIME-DEPENDENT GREEN'S FUNCTION

INTRODUCTION

In this appendix we develop the theory attendant to the proper understanding of the method of solution of differential equations, known as the Green's function method. We then discuss this method's application to the vapor dispersion diffusion equation, which includes the effects of both wind- and time-varying vapor sources from a finite area.

INHOMOGENEOUS PROBLEMS, GREEN'S FUNCTIONS

A partial or ordinary differential equation may be inhomogeneous due either to boundary conditions or to the presence of sources [D1]. The simple idea behind the use of Green's functions is to invert the differential operator producing a certain result and, by so doing, to solve for the unknown function in question. Since the operator being inverted is a differential operator, its inverse might well be intuited to be an integral operator--and so it is, as will be seen shortly. The kernal of this integral operator is called the Green's function associated with the differential operator it is inverting. Thus, the Green's function technique is analogous to Sylvester's rule for inverting linear equations to solve for unknowns.

First let us consider the inhomogeneous differential equation where L is a differential operator and f is a source term.

$$L\,\mu\,(\vec{x}) = f\,(\vec{x}) \tag{D-1}$$

Here μ is an unknown function whose argument is $\vec{x}$, a function of several independent variables in general, L is a hermitian operator, which implies that its eigenvalues are real and whose domain of definition is Ω. $\mu\,(\vec{x})$ is subject to the usual type of boundary conditions, Dirichlet, Neumann, or Cauchy.

Since we want to solve for $\mu(\vec{x})$, if we can only determine L^{-1}, the inverse of L, we can apply it to both sides of (D-1) to obtain

$$L^{-1}\,L\,\mu\,(\vec{x}) = L^{-1}\,f\,(\vec{x}) \tag{D-2}$$

[D1] Courant, R., and D. Hilbert, *Methods of Mathematical Physics*, vol. 1, p. 351, Interscience, New York, 1953.

Since by definition $L^{-1} L$ is the unity appropriate to our system, we have

$$\mu(\vec{x}) = L^{-1} f(\vec{x}) \tag{D-3}$$

provided L^{-1} exists and has well-behaved properties in Ω. It must also allow the boundary conditions imposed on $\mu(\vec{x})$ to be satisfied. It will be seen that this is guaranteed by correctly choosing the eigenfunctions of L in which to expand both f and μ.

We now expand both μ and f in eigenfunctions of L, say $\mu_n(\vec{x})$

$$\mu(\vec{x}) = \sum_{n=0}^{\infty} c_n \mu_n(\vec{x}) \tag{D-4}$$

$$f(\vec{x}) = \sum_{n=0}^{\infty} d_n \mu_n(\vec{x}) \tag{D-5}$$

where c_n and d_n are Fourier coefficients. Since $L\mu_n = \lambda_n \mu_n$ where λ_n is the nth eigenvalue of L we write (D-1) as

$$\sum_n c_n \lambda_n \mu_n(\vec{x}) = \sum_n d_n \mu_n(\vec{x}) \tag{D-6}$$

Because the eigenfunctions, μ_n, are orthogonal and therefore linearly independent, we can express c_n as

$$c_n = d_n/\lambda_n \tag{D-7}$$

Now for d_n we have

$$d_n = \int_{\Omega} \mu_n(\vec{x}') f(\vec{x}') dx'^3 = (\mu_n \cdot f) \tag{D-8}$$

or simply the inner product of f with μ. From all this, we then have

$$\mu(\vec{x}) = \sum_n \frac{\mu_n (\mu_n \cdot f)}{\lambda_n} \tag{D-9}$$

Thus it is evident that L^{-1} is

$$L^{-1} = \sum_n \frac{\mu_n (\mu_n^{\bullet}}{\lambda_n} \tag{D-10}$$

or $G(\vec{x},\vec{x}')$, the Green's function associated with L and Ω, is precisely

$$G(\vec{x},\vec{x}') = \sum_n \frac{\mu_n(\vec{x})\,\mu_n(\vec{x}')}{\lambda_n} \tag{D-11}$$

and exists providing no $\lambda_n = 0$.

The solution to our problem can now be expressed as

$$\mu(\vec{x}) = \int_\Omega G(\vec{x},\vec{x}')\, f(x')\, dx'^3 \tag{D-12}$$

Symbolically, L^{-1} is

$$L^{-1} = \int_\Omega G\, dx'^3 \tag{D-13}$$

It is useful to note that because L^{-1} is the inverse of L we have

$$L\,L^{-1} = 1 = \int_\Omega L\,G\, dx'^3 \tag{D-14}$$

For this to be true, the product LG, or more precisely the differential operator L operating on G must produce the Dirac delta function

$$L\,G(\vec{x},\vec{x}') = \delta(\vec{x}-\vec{x}') \tag{D-15}$$

The integral

$$\int_\Omega \delta(\vec{x}-\vec{x}')\, dx'^3 = 1 \tag{D-16}$$

over the domain of Ω is equal to unity if $\vec{x}$ is included within it. This follows from the properties of the delta function

$$\begin{aligned} \delta(\vec{x}-\vec{x}') &= 0 \qquad \vec{x} \neq \vec{x}' \\ \delta(\vec{x}-\vec{x}') &= \infty \qquad \vec{x} = \vec{x}' \end{aligned} \tag{D-17}$$

This procedure formally solves, in a very general manner, a *linear* ordinary or partial *nonhomogeneous* differential equation.

We now proceed to determine a means of handling boundary conditions pertaining to a given differential equation. It turns out that since (D-12) is a particular integral for the inhomogeneous equation

$$L\,\mu(\vec{x}) = f(\vec{x}) \tag{D-18}$$

we can add to (D-12) a solution $\phi(\vec{x})$ to the *homogeneous* equation

$$L\phi(\vec{x}) = 0 \tag{D-19}$$

If $\phi(\vec{x})$ also satisfies the given set of *inhomogenous boundary conditions* while $\mu(\vec{x})$ satisfies *homogeneous boundary conditions*, then the general solution is simply

$$\mu(\vec{x}) + \phi(\vec{x}) \tag{D-20}$$

or

$$L[\mu(\vec{x}) + \phi(\vec{x})] = L\mu(\vec{x}) + L\phi(\vec{x}) = f(\vec{x}) + 0 \tag{D-21}$$

To obtain $\phi(\vec{x})$ via $G(\vec{x},\vec{x}')$ we must make use of Green's theorem and specify L and the boundary conditions imposed on a particular problem. Since we are interested in solving the diffusion equation for concentration of airborne vapor, we must solve

$$\frac{\partial C(\vec{r},t)}{\partial t} + \vec{v}\cdot\nabla C(\vec{r},t) = \nabla\cdot\vec{\vec{D}}\cdot\nabla\vec{C}(\vec{r},t) \tag{D-22}$$

where $\vec{v}$ is the wind velocity and $\vec{\vec{D}}$ the diffusion tensor.

The boundary condition is that over the region of the spreading pool the flux of $C(\vec{r},t)$ is $\vec{J}$ or

$$J = -\vec{n}\cdot\vec{\vec{D}}\cdot\nabla C \tag{D-23}$$

and that C itself is a priori indeterminate since, for a parabolic differential equation like (D-22) in an open system, either ∇C or C can be given but not both. $\vec{J}$ is of course determined from the heat transfer solution of a boiling liquid on another host liquid and, in general, is a function of time. This will be shown in another appendix. It will be recalled that the type of boundary condition denoted by (D-23) is known as a Neumann condition. It should be noticed that (D-22) is a homogeneous differential equation since

$$L = -\nabla\cdot\vec{\vec{D}}\cdot\nabla + \frac{\partial}{\partial t} + \vec{v}\cdot\nabla \tag{D-24}$$

The boundary condition is nonhomogeneous because of (D-23).

The Green's function is determined from L or the condition $LG = \delta(\vec{r}-\vec{r}', -\vec{v}(t-t'))$

$$-\nabla\cdot\vec{\vec{D}}\cdot\nabla G(\vec{r}-\vec{r}',t-t') + \frac{\partial}{\partial t}G(\vec{r}-\vec{r}',t-t') + \vec{v}\cdot\nabla G = \delta(\vec{r}-\vec{r}'-\vec{v}(t-t')) \tag{D-25}$$

We will return to consideration of (D-25) later. For now, we consider how to determine $C(\vec{r},t)$ from $G(\vec{r}-\vec{r}',t-t')$ and $J = \vec{n}\cdot\vec{\vec{D}}\cdot\nabla C$ the Neumann boundary conditions [D2].

Green's theorem states that

$$\int_{t_0}^{t_1} dt' \int_V dx'^3 (\phi\nabla'^2\psi - \psi\nabla'^2\phi) = \int_{t_0}^{t_1} dt' \int_A \left(\phi \frac{\partial\psi}{\partial n'} - \psi \frac{\partial\phi}{\partial n'}\right) da' \qquad \text{(D-26)}$$

The integral over time t' proceeds from t_0 to t_1 while the volume integral of the scale functions ϕ,∇^2,ψ, etc. is equivalent to the surface integral over the boundary of the system at time t' of ϕ,ψ, and the normal derivatives of ψ and ϕ. This result follows from the divergence theorem of vector analysis. Primes refer to source points.

Letting $\phi = G$ and $\psi = C$, we obtain

$$\int_{t_0}^{t_1} dt' \int_V dx'^3 (G\nabla'^2 C - C\nabla'^2 G) = \int_{t_0}^{t_1} dt' \int_A \left(G \frac{\partial C}{\partial n'} - C \frac{\partial G}{\partial n'}\right) da' \qquad \text{(D-27)}$$

In our case we must replace $\nabla'^2 C$ by $\nabla'\cdot\vec{\vec{D}}\cdot\nabla' C$ and similarly for $\nabla'^2 G$. This results in, using (D-22) and (D-25)

$$\int_{t_0}^{t_1} dt' \int_V dx'^3 \left[G\left(\frac{\partial C}{\partial t'} + \vec{v}\cdot\nabla C\right) - C\left(\frac{\partial G}{\partial t'} + \vec{v}\cdot\nabla G - \delta\left(\vec{r}-\vec{r}'-\vec{v}(t-t')\right)\right)\right]$$

$$= \int_{t_0}^{t_1} dt' \int_A (G\vec{n}'\cdot\vec{\vec{D}}\cdot\nabla' C - C\vec{n}'\cdot\vec{\vec{D}}\cdot\nabla G)\, da' \qquad \text{(D-28)}$$

The integral, $\int_{t_0}^{t_1} \int_V C(r',t')\,\delta\left(\vec{r}-\vec{r}'-\vec{v}(t-t')\right) dt'dx'^3$ is simply

---

[D2] Jackson, J. D., *Classical Electrodynamics*, p. 186, John Wiley, New York, 1966.

$C(\vec{r},t)$. We next note that the antisymmetry in t, t', and $\vec{r}$ and $\vec{r}'$ with regard to derivatives of $G(\vec{r}-\vec{r}',t-t')$, such that $\nabla' G = -\nabla G$ and $(\partial G)/(\partial t') = -(\partial G)/(\partial t)$, enables us to transform (D-28) into the following form

$$C(\vec{r},t) = \int_{t_0}^{t_1} dt' \int_V dx'^3 \; G\left(\frac{\partial C}{\partial t'} + \vec{v}\cdot\nabla C\right) + C\left(\frac{\partial G}{\partial t'} + \vec{v}\cdot\nabla G\right)$$

$$- \int_{t_0}^{t_1} dt' \int_A (G\vec{n}'\cdot\vec{\vec{D}}\cdot\nabla' C - C\vec{n}'\cdot\vec{\vec{D}}\cdot\nabla G)\, da' \qquad \text{(D-29)}$$

$$C(\vec{r},t) = \int_V dx'^3 \int_{t_0}^{t_1} dt' \; \frac{\partial}{\partial t'}(GC) + \int_{t_0}^{t_1} dt' \int_V [\vec{v}\cdot\nabla(GC)]\, dx'^3$$

$$- \int_{t_0}^{t_1} dt' \int_A \vec{n}'\cdot(G\vec{\vec{D}}\cdot\nabla' C - C\vec{\vec{D}}\cdot\nabla G)\, da' \qquad \text{(D-30)}$$

The principle of causality requires that $G = 0$ for times t' equal to or greater than t_1, hence the first term of (D-30) is simply

$$\int_V dx'^3 \, GC\Big|_{t'=t_0}$$

As for the second term, if we take $\vec{v}$ as a constant, which it is for the wind convection in a given problem, we can convert the volume integral using the theorem of Gauss to

$$\vec{v}\cdot\int_{t_0}^{t_1} dt' \int_A GC\, da'$$

Collecting all terms, we have finally for $C(\vec{r},t)$

$$C(\vec{r},t) = \int_V G(\vec{r}-\vec{r}',\ t-t')C(\vec{r}',t')\Big|_{t'=t_0} dx'^3$$

$$+ \vec{v}\cdot\int_{t_0}^{t_1} dt' \int_A G(\vec{r}-\vec{r}',t-t')C(\vec{r}',t')da'$$

$$- \int_{t_0}^{t_1} dt' \int_A \vec{n}'\cdot(G\vec{\vec{D}}\cdot\nabla'C - C\vec{\vec{D}}\cdot\nabla G)da' \qquad \text{(D-31)}$$

Equation (D-31) is an integral equation because, while $\nabla'C$ is given and is proportional to the mass flux $\vec{J}$ on the boundaries, C itself is not given a priori on the boundary and must satisfy (D-31).

GREEN'S FUNCTION SOLUTION TO TRANSIENT DISPERSION PROBLEM NEAR SOURCE

The equation governing the dispersion of airborne cargo concentration, C, as a function of time and space is,

$$\frac{\partial C}{\partial t} + \vec{v}\cdot\nabla C = \nabla\cdot\vec{\vec{D}}\cdot\nabla C \qquad \text{(D-32)}$$

where

$\vec{v}$ = velocity vector of convection, approximately that of wind

$\vec{\vec{D}}$ = diffusion tensor

By definition, the Green's function, G, required to solve (D-32) must satisfy

$$\frac{\partial G}{\partial t} + \vec{v}\cdot\nabla G - \nabla\cdot\vec{\vec{D}}\cdot\nabla G = \delta(\vec{\rho} - \vec{v}\tau) \qquad \text{(D-33)}$$

where

$\vec{\rho} = \vec{r} - \vec{r}'$

$\tau = t - t'$

$\delta \to \infty \quad \vec{\rho} = \vec{v}\tau$

$\delta = 0 \quad \vec{\rho} \neq \vec{v}\tau$

and primed quantities refer to source points and unprimed quantities to field points. The quantity denoted as $\delta(\vec{\rho} - \vec{v}\tau)$ is a Dirac delta function. Thus we see that G is the solution to equation (D-32) for a unit source in space and time. Using this fact, the solution to equation (D-32) may be stated in the form of an integral equation (D-31) which we repeat here in explicit functional form.

$$C(\vec{r},t) = \int_{V'} G(\vec{r}-\vec{r}',t-t')C(\vec{r}',t')\Big|_{t'=t_0} dx'^3$$

$$+ \vec{v} \cdot \int_{t_0}^{t'} dt' \int_{A'} \vec{n}' G(\vec{r}-\vec{r}',t-t')C(\vec{r}',t')da'$$

$$+ \int_{t}^{t} dt' \int_{A'} \vec{n}' \cdot \vec{\vec{D}} \cdot (\nabla' G(\vec{r}-\vec{r}',t-t'))C(\vec{r}',t')da'$$

$$- \int_{t_0}^{t} dt' \int_{A'} \vec{n}' \cdot \vec{\vec{D}} (\nabla' C(\vec{r}',t'))G(\vec{r}-\vec{r}',t-t')da' \qquad \text{(D-34)}$$

Again, $\vec{n}'$ is the unit normal vector to the spill surface, da' the differential source area, and t_0 the time of spill. Equation (D-34) is the exact solution to the dispersion problem, (D-32), and thus no approximations have been employed in its construction. Consequently, as is the case for many integral equations, (D-34) is difficult in general to solve in closed form.

It turns out, however, that our physical system is such that the initial concentration is zero, and the product $\vec{v} \cdot \vec{n}'$ vanishes since the wind blows parallel to the water and hence to the spill's surface. Thus the first two terms of (D-34) are zero. In addition, the last term on the right-hand side of (D-34) can be transformed by invoking Ficks' law for the flux of C, $\vec{J}(\vec{r},t)$,

$$\vec{J} = -\vec{\vec{D}} \cdot \nabla C$$

Assuming $t_0 = 0$, we now write (D-34) as

$$C(\vec{r},t) = \int_0^t dt' \int_{A'} da'\ \vec{n}'\cdot[\vec{\vec{D}}\cdot(\nabla' G)C + \vec{J}G] \qquad \text{(D-35)}$$

It is useful at this point to reflect on the meaning of the bracketed terms in the integral equation (D-35). What in effect is being said is that the concentration, $C(\vec{r},t)$, at a *field* point away from the source, depends on two *source* terms, which are integrated over the source area and all time. The first term

$$\vec{\vec{D}}\cdot(\nabla' G)C(\vec{r}',t')$$

represents the contribution to $C(\vec{r},t)$ of a varying boundary source strength indicated by

$$\vec{n}'\cdot(\vec{\vec{D}}\cdot\nabla' G)C$$

whereas the second term gives the contribution due to the mass flux which is normal at the surface of the spill. Again, however, it must be remembered that the

$$\vec{\vec{D}}\cdot(\nabla' G)C$$

term is not an independent boundary condition and because of its presence makes (D-35) an integral equation rather than an explicit solution to a boundary value problem.

EXPLICIT FORM OF GREEN'S FUNCTION FOR TIME-INDEPENDENT SOURCE

Success in obtaining proper results conveniently depends on the choice of the Green's function. If we assume that there is little or no accumulation of concentration, C, at the source, only the second term is retained in equation (D-35). For an unbounded domain, the solution to (D-33) for G is

$$G(\vec{r}-\vec{r}',t-t') = \frac{1}{(4\pi\tau)^{3/2}\,|\vec{\vec{D}}|^{1/2}}\ e^{-\left[\left((\vec{\rho}-\vec{v}\tau)\cdot\vec{\vec{D}}^{-1/2}\right)^2/4\tau\right]} \qquad \text{(D-36)}$$

Using the second term of (D-35) with a constant uniform mass flux from a point source and recalling for a continuous source that $x - x' = v(t - t')$, we find on integration that

$$C = \frac{Q}{8\pi x(D_y D_z)^{1/2}}\ e^{-\left[(v/4x)\ (y^2/D_y + z^2/D_z)\right]} \qquad \text{(D-37)}$$

Here diffusion due to shear effects has been neglected, $D_{xy} = 0$, etc. and $Q = \int \vec{J} \cdot \vec{n}\, da$, the flux source strength. If we make the identification, $D_y = v\sigma_y^2/2x$, $D_z = v\sigma_z^2/2x$, $D_x = v\sigma_x^2/2x$, $\sigma_x = 2x$

$$C(y,z) = \frac{Q}{4\pi v \sigma_y \sigma_z} \; e^{-(y^2/2\sigma_y^2 + z^2/2\sigma_z^2)} \tag{D-38}$$

the usual expression for a *constant point source* Gaussian plume model. Thus it is seen that the Green's function method reduces to the well-known standard form for time-independent point sources.

It is to be noted that this expression for a constant point source Gaussian plume model is not the answer to our transient problem and is only valid provided we can simplify (D-35) to read

$$C = \int_0^t dt' \int_{A'} (\vec{n}' \cdot \vec{J}) G \, da' \tag{D-39}$$

This will, however, be inconsistent with the choice (D-36) since the gradient of the Green's function *will not vanish* at the boundary and one will have to incorporate the first term of (D-35) which is difficult to handle.

The problem is normally resolved by simulating a proper boundary condition through a judicious choice of the Green's function. Thus, if the source is at a height, H, we avoid the need of integrating over the *entire* domain at $z = 0$ by using

$$G = \frac{1}{2} \; (G_+ + G_-) \tag{D-40}$$

where $G^{\pm}$ is the function (D-37) and z is replaced by $z \pm H$. Then with this modification, (D-38) becomes

$$C = \frac{Q}{4\pi v \sigma_y \sigma_z} \; e^{-H^2/2\sigma_z^2} \tag{D-41}$$

for the ground level concentration in the windward direction at the plume centerline. However, this does not resolve the problems of the realistic calculation of (D-35), except in the point source limit or in the case where the concentration of contaminant at the source is negligible. Again we note that (D-41) is a well-known and familiar form.

SOLUTION FOR INSTANTANEOUS SOURCE

Should the source of the vapor dispersion be instantaneous, the expression for J becomes

$$J = M\delta(t') \qquad t' = 0 \tag{D-42}$$

where M is the mass of the source. Inserting (D-42) in (D-35) and using as before (D-36) for G, we obtain after a short calculation

$$C = \frac{M}{(2\pi)^{3/2}\sigma_x\sigma_y\sigma_z}\, e^{-\left[(x-vt)^2/2\sigma_x^2 + y^2/2\sigma_y^2 + z^2/2\sigma_z^2\right]} \tag{D-43}$$

In obtaining (D-43) we used the fact that $D_x = v\sigma_x^2/2x$, $D_y = v\sigma_y^2/2x$, $D_z = v\sigma_z^2/2x$ and that axial dispersion (in x-direction) is explicitly present, hence $\sigma_x \neq 2x$. Again, equation (D-43) is the well-known form for the puff model.

It is well known that this model can lead to unphysical concentrations near the source. This is largely due to two factors. The first is that it is unphysical to expect an instantaneous release of vapor to take place. The second is that, even if such a large instantaneous release were possible, the diffusion equation of motion would not be capable of correctly describing the resulting time evolution of the concentration. The correct descriptive equation would be a nonlinear differential equation.

SOLUTION FOR TRANSIENT CASE, NEAR IN REGION

For the problem at hand, in an unbounded domain, we utilize the following two equations to solve for $C(\vec{r},t)$.

$$\frac{\partial G}{\partial t}(\vec{\rho},\tau) + \vec{v}\cdot\nabla G(\vec{\rho},\tau) - \nabla\cdot\vec{\vec{D}}\cdot\nabla G(\vec{\rho},\tau) = \delta(\vec{\rho} - \vec{v}\tau) \tag{D-44}$$

$$C(\vec{r},t) = \int_0^t dt' \int_{A'} \vec{n}'\cdot\vec{\vec{D}}\cdot\nabla' G(\vec{\rho},\tau) C(\vec{r}',t')\, da'$$

$$+ \int_0^t dt' \int \vec{n}'\cdot\vec{J}(\vec{r}',t') G(\vec{\rho},\tau)\, da' \tag{D-45}$$

For the solution of (D-44) we have as before for $G(\vec{\rho},\tau)$

$$G(\vec{\rho},\tau) = \frac{1}{(4\pi)^{3/2}\,|\vec{\vec{D}}|^{1/2}\,\tau^{3/2}}\; e^{-\left[\left((\vec{\rho}-\vec{v}\tau)\cdot\vec{\vec{D}}^{-1/2}\right)^2/4\tau\right]} \qquad \text{(D-46)}$$

We [D3] retain the first term of (D-45) and employ for $\vec{J}$

$$\vec{J} = \vec{k}\,\frac{h\Delta T}{\rho}\,erfc(\beta t^{1/2})\,e^{\beta t} \qquad \text{(D-47)}$$

where

h	=	surface heat transfer coefficient
ΔT	=	temperature difference between water and boiling liquid cargo
ℓ	=	latent heat of boiling cargo
β	=	$\alpha h/\kappa$
κ	=	conduction heat transfer coefficient
α	=	thermal diffusivity
c_v	=	specific heat at constant volume
ρ	=	density

One finds in the limit as $t \to 0$, $J \to h\Delta T$ or the mass flux is convection-controlled. On the other hand, as $t \to \infty$, $J \to \kappa/\alpha\sqrt{\pi t}$ which implies that the mass flux is conduction-limited. Both behaviors are in well-known agreement with experimental facts. To simplify the solution indicated by (D-45), the following form may well be a sufficient approximation.

$$\vec{J} = \frac{\vec{k}h\Delta T}{\ell}\left(1+\frac{h\alpha}{\kappa}\sqrt{\pi t}\right) \qquad \text{(D-48)}$$

[D3] Churchill, R. V., *Operational Mathematics*, p. 199, McGraw-Hill, New York, 1958.

* U.S. GOVERNMENT PRINTING OFFICE : 1977 O-728-949/13111